

**Investigation on the Application of Active Algal-bacterial Granular Sludge  
for Hexavalent Chromium Removal from Wastewater**

**January 2021**

**Xiaojing YANG**

# **Investigation on the Application of Active Algal-bacterial Granular Sludge for Hexavalent Chromium Removal from Wastewater**

A Dissertation Submitted to  
the Graduate School of Life and Environmental Sciences,  
the University of Tsukuba  
in Partial Fulfillment of the Requirements  
for the Degree of Doctor of Philosophy in Environmental Studies  
(Doctoral Program in Sustainable Environmental Studies)

**Xiaojing YANG**

## Abstract

Heavy metals (HMs) are regarded as a great challenge to wastewater treatment plants (WWTPs) due to their toxic effects on aquatic organisms and human beings. As one of the typical HMs, hexavalent chromium (Cr(VI)) has significant carcinogenic and mutagenic effects to humans. Among the various methods for HMs removal, biosorption is considered as a cost-effective and environmentally friendly process. Conventional bacterial aerobic granular sludge (AGS) system has been considered as a promising biotechnology for wastewater treatment, which is now frequently attempted for HMs removal tests. As a novel biotechnology, algal-bacterial AGS is expected to largely reduce operation costs due to much less consumption of carbon source and energy in comparison to the bacterial AGS process. However, to the best of our knowledge, still, very little information is available on the application of algal-bacterial AGS biomass as a biosorbent for Cr(VI) removal or recovery from wastewater. Moreover, in most of the previous studies for concerning HMs removal by AGS, microbial activity of AGS during the adsorption process was ignored, which is, however, critical to the reuse and recycles of HM loaded AGS and the interpretation of the underlying mechanisms.

In this study, mature bacterial or algal-bacterial granules were used for Cr(VI) removal from synthetic wastewater, in terms of both total Cr removal and Cr(VI) reduction. The algal-bacterial AGS was cultivated from mature bacterial AGS, and compared with the bacterial AGS in terms of Cr(VI) removal capacity, granular stability and metal content. Besides, the influences of environmental factors on Cr(VI) removal and the responses of algal-bacterial AGS were evaluated. Moreover, the underlying mechanisms were also studied by the means of chemical fractionation and microcharacterization. Major results can be summarized as follows.

(1) Batch tests revealed that Cr(VI) biosorption onto algal-bacterial AGS was highly pH dependent and the maximum Cr(VI) biosorption capacity of 51.0 mg g<sup>-1</sup> occurred at pH 2. Compared to the conventional bacterial AGS, algal-bacterial AGS demonstrated higher biosorption capacity (9.60 mg/g vs. 8.49 mg/g under the same test conditions;  $p=0.0014$ ) and better granular stability, implying that algal-bacterial AGS can be more potentially utilized as a Cr(VI) removal and recovery biomaterial for the treatment of Cr(VI)-containing wastewater.

(2) Microbial activity and granular stability of algal-bacterial AGS were maintained after 6 h biosorption at an initial Cr(VI) concentration of 5 mg/L. The highest Cr(VI) reduction (99.3%) and total Cr removal (89.1%) were achieved within 6 h at pH 2 and 6, respectively. Metal cations enhanced Cr(VI) reduction but suppressed total Cr removal. In addition, the test

natural organics promoted Cr(VI) removal, especially on Cr(VI) reduction; while salinity > 5 g/L severely inhibited both Cr(VI) reduction and total Cr removal.

(3) 85.1% of total Cr was removed by active algal-bacterial AGS after 6 h under pH 6 at an initial Cr(VI) concentration of 5 mg/L, which decreased dramatically to 29.6% when sterilized algal-bacterial AGS was used. Glucose promoted Cr(VI) removal by active AGS while no effect on sterilized one. Besides, total Cr removal via bacterial AGS was inhibited by 11.2% but maintained in the case of algal-bacterial AGS when antibiotic levofloxacin added. Extracellular polymeric substances (EPS) analysis showed that more soluble microbial products (SMP) and loosely bound EPS were secreted by algal-bacterial AGS under Cr(VI) exposure. Moreover, results from Cr distribution and fractionation revealed that around 17.3% of the loaded Cr was EPS bounded and 69.2% was intracellularly accumulated, 61.7% of loaded Cr was organic bound fraction, and totally around 90.5% of Cr was in an immobile form, indicating the safety of using algal-bacterial AGS for hazardous heavy metals removal.

Results from this research are expected to facilitate the utilization of algal-bacterial AGS with high efficiency for heavy metal remediation in the real world of wastewater treatment.

**Key words:** Algal-bacterial aerobic granular sludge; Bacterial aerobic granular sludge; Environmental factor; Chemical fractionation; Hexavalent chromium

## Contents

<b>Abstract .....</b>	<b>i</b>
<b>Contents.....</b>	<b>iii</b>
<b>List of tables .....</b>	<b>v</b>
<b>List of figures .....</b>	<b>vi</b>
<b>Abbreviations.....</b>	<b>viii</b>
<b>Chapter 1 Introduction .....</b>	<b>1</b>
1.1 Heavy metal issue and hexavalent chromium.....	1
1.2 Conventional methods for chromium remediation .....	1
1.3 Biosorption and biosorbents.....	2
1.4 Algal-bacterial AGS .....	3
1.5 Factors affecting Cr(VI) bioremediation.....	4
1.6 Mechanisms of Cr(VI) biosorption .....	5
1.7 Research objectives and originality .....	6
1.8 Structure of the thesis.....	6
<b>Chapter 2 Feasibility of Cr(VI) removal from synthetic wastewater using algal-bacterial     AGS in comparison with bacterial AGS .....</b>	<b>8</b>
2.1 Background .....	8
2.2 Materials and methods .....	8
2.2.1 Preparation of algal-bacterial AGS and bacterial AGS .....	8
2.2.2 Batch Cr(VI) biosorption tests .....	9
2.2.3 Analytical methods.....	10
2.3 Results and discussion .....	11
2.3.1 Cr(VI) biosorption by algal-bacterial AGS .....	11
2.3.2 Comparison between algal-bacterial AGS and bacterial AGS .....	13
2.3.3 Mechanisms .....	15
2.4 Summary .....	15
<b>Chapter 3 Effects of environmental conditions on the performance of Cr(VI) removal by     algal-bacterial AGS.....</b>	<b>29</b>
3.1 Background .....	29

3.2 Materials and methods .....	29
3.2.1 Cultivation and characterization of algal-bacterial AGS .....	29
3.2.2 Optimization of Cr(VI) biosorption .....	30
3.3 Results and discussion .....	30
3.3.1 Characterization of algal-bacterial AGS for Cr(VI) removal.....	30
3.3.2 Optimization of parameters for Cr(VI) biosorption .....	31
3.3.3 Effects of environmental factors .....	34
3.4 Summary .....	37
<b>Chapter 4 Mechanisms of Cr(VI) removal by algal-bacterial AGS .....</b>	<b>43</b>
4.1 Background .....	43
4.2 Materials and methods .....	44
4.2.1 Cultivation of bacterial AGS and algal-bacterial AGS .....	44
4.2.2 Cr(VI) biosorption and desorption experiments .....	44
4.2.3 EPS extraction and chemical fractionation .....	45
4.2.4 Statistical analysis .....	47
4.3 Results and discussion .....	47
4.3.1 Effect of cell viability and additional electron donor on Cr(VI) removal.....	47
4.3.2 Variations in EPS during Cr(VI) removal process .....	50
4.3.3 Desorption of Cr from Cr-loaded algal-bacterial AGS .....	51
4.3.4 Distribution and chemical fractionation of Cr in Cr-loaded algal-bacterial AGS..	52
4.3.4 Mechanisms hypothesis .....	53
4.4 Summary .....	55
<b>Chapter 5 Conclusions and future research perspectives.....</b>	<b>63</b>
5.1 Conclusions .....	63
5.2 Future research perspectives .....	66
<b>References.....</b>	<b>67</b>
<b>Acknowledgements .....</b>	<b>77</b>
<b>Publications .....</b>	<b>78</b>

## **List of tables**

Table 2-1 Fitting results of biosorption data of Cr(VI) onto algal-bacterial AGS to the kinetic models.....	17
Table 2-2 Concentrations of released metal ions from algal-bacterial AGS during biosorption from Cr(VI)-containing wastewater for 24 h over the test pH range of 1.0-12.0....	18
Table 2-3 Comparison of maximum Cr(VI) biosorption capacities between algal-bacterial AGS and previously reported biosorbents.....	19
Table 2-4 Average contents of dominant metals in the algal-bacterial AGS and conventional bacterial AGS .....	20
Table 3-1 Experimental design and test conditions for Cr(VI) biosorption by algal-bacterial AGS .....	38

## List of figures

Figure 1-1 Research framework of Cr(VI) removal by algal-bacterial AGS .....	7
Figure 2-1 Cr(VI) biosorption at an initial Cr(VI) of 50 mg/L with algal-bacterial AGS dosage of 2 g/L: (a) effect of pH during 24 h contact, and (b) effect of contact time at pH 2 .....	21
Figure 2-2 Plot for determination of pH at zero point charge (pH <sub>zpc</sub> ) of algal-bacterial AGS: zeta potential of granules as a function of solution pH .....	22
Figure 2-3 FTIR spectra of initial (a) bacterial AGS, (b) algal-bacterial AGS and (c) Cr-loaded algal-bacterial AGS after 24 h biosorption (at an initial Cr(VI) of 50.0 mg/L, biosorbent dosage of 2 g/L and pH 2). .....	23
Figure 2-4 Plots of isotherms of Cr(VI) biosorption onto algal-bacterial granules: (a) Freundlich isotherm, and (b) Langmuir isotherm (at an initial Cr(VI) concentration of 12.5, 25.0, 50.0, 100.0, 150.0, or 300.0 mg/L, algal-bacterial AGS dosage of 2 g/L and pH 2 for 24 h contact) .....	24
Figure 2-5 Comparison of Cr(VI) biosorption capacity and granular integrity between conventional bacterial AGS and algal-bacterial AGS (at initial Cr(VI) of 50.0 mg/L, biosorbent dosage of 2 g/L and pH 2). .....	25
Figure 2-6 Changes in algal-bacterial AGS diameter and granular size distribution before and after biosorption (at initial Cr(VI) of 50.0 mg/L, biosorbent dosage of 2 g/L and pH 2) .....	26
Figure 2-7 Images of the conventional bacterial AGS and algal-bacterial AGS. Digital photos of test granules (A and B), and SEM observation of granules from surface (C-F) or cross section (G and H), respectively .....	27
Figure 2-8 Concentrations of three main metal ions (Mg <sup>2+</sup> , Ca <sup>2+</sup> and Fe <sup>2+/3+</sup> ) released into the aqueous solution from AGS after 24 h contact with Cr(VI) solution (Cr(VI), 50.0 mg/L) or deionized water (DW) at pH 2 .....	28
Figure 3-1 Images of algal-bacterial AGS from surface (a) or cross section (b and c), respectively .....	39



Figure 3-2 Granular SOUR and stability of algal-bacterial AGS after biosorption (contact time, 6 h; initial pH, 6; granule dosage, 5 g-TS/L, Cr(VI), 5 mg/L) .....	40
Figure 3-3 Effects of different operation parameters including (a) initial pH, (b) contact time, (c) granule dosage, and (d) initial Cr(VI) concentration on Cr distribution in solution and algal-bacterial AGS.....	41
Figure 3-4 Effects of environmental conditions on Cr distribution in solution and algal-bacterial AGS: (a) coexisting anions, (b) coexisting cations, (c) humic acid, (d) tannic acid, (e) salinity, and (f) different carbon sources.....	42
Figure 4-1 Schematic diagram of experiments for EPS extraction and Cr distribution in Cr-loaded algal-bacterial AGS.....	57
Figure 4-2 Effect of cell viability and electron donors on Cr distribution in solution and AG-AGS: (a) active algal-bacterial AGS; (b) heat inactivated algal-bacterial AGS; (c) active bacterial-AGS.....	58
Figure 4-3 Changes of EPS contents and components in algal-bacterial AGS during Cr(VI) removal: (a) soluble EPS (S-EPS); (b) loosely bound EPS (LB-EPS); (c) tightly bound EPS (TB-EPS); (d) total EPS.....	59
Figure 4-4 Desorption ratio of Cr from Cr-loaded algal-bacterial AGS: (a) effect of different desorption solution; (b) effect of different concentration of H <sub>2</sub> SO <sub>4</sub> . Condition for Cr(VI) removal experiment prior to desorption: contact time, 16 h; initial pH, 6; granule dosage, 5 g-TS/L, Cr(VI), 5 mg/L. Desorption time, 12 h.....	60
Figure 4-5 The distribution and content of different metal extracted from Cr-loaded algal-bacterial AGS: (a) EPS distribution; (b) intra/extra cellular distribution; (c) chemical fractionation .....	61
Figure 4-6 Conceptual diagram of Cr(VI) removal mechanism by microbial and microalgae cells in algal-bacterial AGS .....	62
Figure 5-1 Graphical conclusion of Chapter 2 .....	63
Figure 5-2 Graphical conclusion of Chapter 3 .....	64
Figure 5-3 Graphical conclusion of Chapter 4 .....	65

## Abbreviations

AGS	Aerobic granular sludge
Chl- <i>a</i>	Chlorophyll <i>a</i>
COD	Chemical oxygen demand
Cr(III)	Trivalent chromium
Cr(VI)	Hexavalent chromium
DO	Dissolved oxygen
DOC	Dissolved organic carbon
DW	Deionized water
EPA	Environmental protection agency
EPS	Extracellular polymeric substances
FTIR	Fourier-transform infrared spectroscopy
HMs	Heavy metals
IS	Ionic strength
LB-EPS	Loosely bound extracellular polymeric substances
LVX	Levofloxacin
MCL	Maximum contaminant level
MF	Mobility factor
MLSS	Mixed liquor suspended solids
MLVSS	Mixed liquor volatile suspended solids
MSM	Mineral salt medium
NOMs	Natural organic matters
PN	Proteins
PS	Polysaccharides
SBRs	Sequencing batch reactors
SD	Standard deviation
SEM	Scanning electron microscope
SOUR	Specific oxygen utilization rate
SVI	Sludge volume index
TB-EPS	Tightly bound extracellular polymeric substances
TS	Total solids
VS	Volatile solids

WAS

Waste activated sludge

WWTPs

Wastewater treatment plants

# Chapter 1 Introduction

## 1.1 Heavy metal issue and hexavalent chromium

Heavy metals (HMs) mainly from industrial discharge pose a great threat to human health and the environment due to their toxic effects of long-term environmental contamination and pollution (Huang et al., 2019a; Zhang et al., 2017). The most common HMs found in wastewater like arsenic, cadmium, lead, mercury and chromium (Cr) are well known for their toxicity, non-biodegradability, persistence in the environment and bioaccumulative nature (Jobby et al., 2018; Rahman and Singh, 2019). Among these HMs, the presence of Cr in industrial effluents has become a serious problem since its compounds have a wide range of applications in various industrial processes like electroplating, printing, dyeing, tanning, textile manufacturing and metallurgy (Mitra et al., 2017; Shahid et al., 2017). Cr mainly exists as trivalent Cr(III) and hexavalent Cr(VI) in aqueous environment (Rozada et al., 2008; Zou et al., 2020). Cr(III) can be readily precipitated with hydroxides at neutral or higher pH conditions and is generally considered lowly toxic because of the inability to pass through the bacterial membrane (Ma et al., 2012; Lai et al., 2016; Viti et al., 2014). In contrast, highly water-soluble Cr(VI) can easily cross the membrane of cells, causing 100 times more toxic than Cr(III), thus leading to severe effects on organisms (Jang et al., 2020; Ma et al., 2019).

## 1.2 Conventional methods for chromium remediation

With the rapid industrialization process, voluminous pollution of Cr in the environment has been found due to the direct discharge of chromium-containing wastes or the leakage from improper handling. The Cr concentration in industrial effluents varies from several to thousands of mg per liter (Xia et al., 2019). More seriously, Cr(VI) was frequently detected in soil, surface water or groundwater around factories or mining areas with the Cr(VI) concentration of 0.01-2900 mg/L (Das and Mishra, 2010; Němeček et al., 2014; Hausladen et al., 2018), making Cr contamination in the environment become a major concern.

According to the US Environmental Protection Agency (USEPA) regulation, the maximum contaminant level (MCL) of total chromium in drinking water is 0.1 mg/L (US EPA, 2009), which is 0.05 mg/L as recommended by the European Commission (Lilli et al., 2015). To meet the increasingly stringent effluent discharge limit, many techniques have been employed to remove Cr(VI) from wastewater. Conventional methods for the removal of Cr(VI) from wastewater including chemical precipitation, electrochemical technologies, ion exchange,

membrane technologies, oxidation, adsorption on activated carbon etc, have some obvious disadvantages such as low treatment efficiency, sensitive operating conditions, or high costs (Abbas et al., 2016; Fu and Wang, 2011; Peng and Guo, 2020; Wang and Chen, 2009).

### **1.3 Biosorption and biosorbents**

Biosorption is the process where metal or metalloid species, compounds and particulates are concentrated on the surface of the biological materials from solution (Saravanan et al., 2017). Compared to conventional technologies, biosorption process for Cr(VI)-containing wastewater has become a promising technology due to its high efficiency, low operating costs, abundant resources, eco-friendliness, and so on (Fomina and Gadd, 2014; Jobby et al., 2018). A number of biomaterials such as algae (Pradhan et al., 2019), fungi (Shi et al., 2019), bacteria (Ma et al., 2018), activated sludge (Wu et al., 2010), aerobic granular sludge (AGS) (Sun et al., 2010) and agricultural wastes (Ding et al., 2016; Olguin et al., 2013) have been exploited as biosorbents.

As by-products of wastewater treatment plants (WWTPs), waste activated sludge (WAS) is cost effective and has been proven to be efficient in heavy metal removal (Wu et al., 2010; Zhou et al., 2016). Utilization of WAS for heavy metal treatment could reduce the disposal issues and remove the hazardous pollutants simultaneously. The main components in waste WAS are polysaccharides, proteins and lipids with various functional groups for the binding of metal ions (Zhou et al., 2016). However, biomass of WAS is in the form of suspended flocs with poor settling ability, results in high energy requirement in the post-separation process when applied for heavy metal removal (Nancharaiah and Reddy, 2018). Moreover, freely suspended microbial cells in WAS can easily be disintegrated under high pressures and loss its efficiency, thus limit its industrial applications (Saravanan et al., 2017).

Fortunately, a new technology of aerobic granular sludge (AGS) can overcome some of the limitations of WAS, due to the many superior properties possessed by AGS like porous microbial structure, excellent settleability, rich binding sites for metals and the ability to withstand shock and toxicant loadings (Franca et al., 2018; Wang et al., 2018). The advantages of using the bacterial AGS as biosorbents can be summarized as follows: (i) The compact structure and excellent settleability of AGS can facilitate the post-separation process (Franca et al., 2018); (ii) The aggregation of different microbial populations generates a porous structure of granules, ensuring relatively large surface area and providing plenty of vacant surface sorption sites for sorbates (Liu et al., 2003); (iii) The overgrowth of microorganisms on the granules may bring abundant surface functional groups for sorbates complexation or other

biological interactions (Sun et al., 2010); (iv) The negatively charged surface of AGS has an affinity for HM ions (Sun et al., 2011a; Sun et al., 2011b). Up to now, original or surface modified AGS has been proven to be highly effective towards various HMs including Cr(VI). However, the drawbacks of AGS process, like the relatively low structural stability during prolonged operations, and the slow growth of AGS biomass, limit the biosorbent development from the conventional bacterial AGS process.

#### **1.4 Algal-bacterial AGS**

Most recently, a new type of AGS, algal-bacterial AGS is intensively studied. As reported, algae can naturally grow on AGS and entangle with bacteria biomass rapidly when exposed to artificial sunlight (Zhang et al., 2018; Zhang et al., 2020). This kind of granular consortium of algae and bacteria can be quickly established due to the fast growth of algal biomass, which also exhibited an excellent and stable nutrients removal performance, i.e. 90-99% of organics, 60-70% of total N and 65-90% of total P removal, and a low sludge volume index (SVI) value ( $SVI_{30}=28-45$  mL/g) after maturation (Zhang et al., 2018; Zhang et al., 2020). A recent work found that algal-bacterial AGS can adapt to low carbon environment (chemical oxygen demand (COD)/N = 1) and maintain excellent granular stability (Zhao et al., 2018). Moreover, the algal-bacterial AGS can function well in shaking photoreactors without conventional air bubbling (aeration) that is usually applied for AGS cultivation and maintenance (Zhao et al., 2018). Therefore, the algal-bacterial AGS system is expected to have great potentials for reducing energy consumption and operation cost in the WWTPs.

On the other hand, algae with fast biomass growth have been reported to be able to effectively adsorb HMs from wastewater due to its large surface to volume ratio (Kumar et al., 2019) and high selectivity of specific HMs binding (Micheletti, et al., 2008; Son et al., 2018). Even though the poor settleability of algae makes its field application for HMs removal impractical, the combination of AGS with algae, namely algal-bacterial AGS may possess their merits and overcome the drawbacks simultaneously. When applied as adsorbent for HMs, e.g. Cr(VI) removal from wastewater, it is hypothesized that algal-bacterial AGS could be a more suitable biosorbent which can couple the high HMs adsorption capacity of algae with the porous and compact structure of bacterial AGS. Considering its rapid growth rate in wastewater and easy separation from the treated wastewater after biosorption, algal-bacterial AGS would be more promising for Cr(VI) removal in practical applications.

## 1.5 Factors affecting Cr(VI) bioremediation

The biosorption capacity of Cr(VI) ions from liquid solution by biosorbents depends upon various factors such as solution pH, contact time, temperature, initial metallic concentration, biosorbent dosage (Saravanan et al., 2017). Among them, solution pH is the most important parameter that significantly affects both surface chemical properties of granules and solution chemistry of chromium in aqueous solution (Zhuo et al., 2017; Feng et al., 2018). Cr(VI) ions are more easily removed through electrostatic interaction at lower pH value (1-3) due to the positively charged surface of the biosorbents (Akram et al., 2017; Cherdchoo et al., 2019). Besides, initial metallic concentration is also a crucial factor for biosorption capacity, and the maximum biosorption capacity would increase according to the elevation of initial metal concentration, due to the fact that more metals are available while the number of active sites on biosorbents surface are limited (Saravanan et al., 2017).

Moreover, when evaluating the Cr(VI) removal efficiency of biosorbents, effects of different background circumstances should be also taken into consideration due to the complexity of contaminated surface water and actual industrial wastewater. These environmental factors include co-existing anions/cations, natural organic matters (NOMs), ionic strength (IS), and carbon sources, etc.

Some oxyanions such as  $\text{NO}_3^-$ ,  $\text{H}_2\text{PO}_4^-$ ,  $\text{HPO}_4^{2-}$ ,  $\text{SO}_4^{2-}$ ,  $\text{CO}_3^{2-}$  and  $\text{HCO}_3^-$ , etc. that are widely found in natural waters, can act as electron acceptors and compete for the surface adsorption sites with Cr ions, thus, suppressing or preventing the Cr(VI) removal (Tan et al., 2020). On the other hand, Cr-containing industrial wastewater usually contains other HMs, like Cu, Co, Ni, Mn and Zn, thus their co-existing may also have competitive effect or even influence microorganism' functions (Ma et al., 2019). Natural organic matters (NOMs) are ubiquitous in the aquatic environment. As the complex mixture of polyfunctional organic acids, NOMs play an important role in HMs adsorption/immobilization through altering their speciation, solubility, mobility and bioavailability, or competing for the active surface sites of adsorbents (Zhao et al., 2016). IS is one of the crucial factors that affect the equilibrium uptake of HMs by adsorbents and the IS of aqueous solution varies with salt concentration proportionally (Zhang et al., 2019). As reported, the competition between anions of salt ( $\text{Cl}^-$ ) with chromate anions (mainly existed as  $\text{HCrO}_4^-$ ) to the active sites of algae and bacteria would inhibit the Cr(VI) removal efficiency (Aksu and Balibek, 2007). Carbon sources are not only indispensable for the growth of heterotrophic microorganisms but also paramount as electron donors contributing towards Cr(VI) bioreduction (Tan et al., 2020).

## 1.6 Mechanisms of Cr(VI) biosorption

The mechanisms of biosorption process can be classified into (1) metabolism dependent and (2) non-metabolism dependent mechanisms according to the usage of active or inactive biomass, respectively (Saravanan et al., 2017). When inactive biomass, which consists of dead or inactive cells, is used for Cr(VI) removal, the process could be described as non-metabolism dependent, and physio-chemical interaction happens between the solid part of biosorbent and metal ions in the liquid part (Wang et al., 2018). These physio-chemical interactions are principally dependent on the organic substrates present on cell surface and could be concluded as ion exchange, surface complexation, electrostatic extraction, chelation and precipitation (Wang et al., 2018). EPS secreted by microorganisms are principally responsible for extracellularly uptake of metal ions, and the main components are polysaccharides, proteins and lipids which possess various anionic functional groups for the binding of metal ions (Zhou et al., 2016). Besides, metal ions could also be complexed effectively with the negatively charged components of cell wall, like chitin of fungi cell wall (Wang et al., 2008). Moreover, the uptake of metal by non-metabolisms is a passive process and takes place immediately then reaches the equilibrium in a short time of 30–40 min (Saravanan et al., 2017).

Metabolism dependent biosorption process is resulted from active metabolic process of the living cells and strongly supported by microbial viability (Wang et al., 2018). On the one hand, the physio-chemical interactions still happen when microorganisms are alive, and metal ions could be adhered on the surface of the cells due to the existing of various functional groups. On the other hand, Cr(VI) ions could be further reduced to Cr(III) or accumulated in cells through a metabolically active process which is operated by respiration energy in living organisms (Jobby et al., 2018). These processes may occur in both extra and intra cells. Extracellular Cr(VI) reduction is primarily mediated by the metal respiratory (Mtr) pathway, which mainly consists of five primary protein components: OmcA, MtrC, MtrA, MtrB, and CymA (Coursolle et al., 2017). Then the produced Cr(III) may be precipitated on cell surface or existing in the form of soluble organo-Cr(III) complex (Huang et al., 2019b). In addition, the intracellular reduction or accumulation occurs when the Cr(VI) ions are actively transported across cell membranes via the sulfate transport protein (Tan et al., 2020). Cr(VI) can be reduced to Cr(III) by either intracellular or membrane-associated reductase, then localized in the cytoplasm or cell membrane, respectively (Thatoi et al., 2014; Baldiris et al., 2018 ).



## **1.7 Research objectives and originality**

As described above, algal-bacterial AGS could be a promising biomaterial for efficient Cr(VI) removal from wastewater. However, up to now, little information is available on the application of algal-bacterial AGS biomass as a biosorbent for Cr(VI) removal and recovery from wastewater, not to mention the potential of practice application in real wastewater treatment. Therefore, the objectives of this study were: (1) to assess the feasibility and performance of using algal-bacterial AGS for handling Cr(VI)-containing wastewater; (2) to compare the Cr(VI) biosorption capacity of algal-bacterial AGS with the conventional bacterial AGS; (3) to assess the effect of environmental factors on Cr(VI) removal performance. In addition, this work also analyzed the underlying mechanisms involved in the Cr(VI) bioremediation processes by algal-bacterial AGS. Results from this study are expected to provide important and scientific data for the application of algal-bacterial AGS in efficient Cr(VI) containing wastewater remediation in practice.

## **1.8 Structure of the thesis**

The thesis structure with the main contents in each chapter is introduced in the research framework as shown in Figure 1-1.

Chapter 1 gave an overview on the Cr(VI) removal strategies and the application potential of algal-bacterial AGS for heavy metal removal. Moreover, the mechanisms involved in Cr(VI) removal by active or in active biomass were addressed. Finally, the objectives of this research and structure of thesis were arrived in this chapter.

Chapter 2 examined the feasibility of Cr(VI) removal from synthetic wastewater using algal-bacterial AGS in comparison with bacterial AGS, together with the evaluation on granular morphology, granular stability, surface functional groups, metal ion contents and Cr(VI) biosorption capacity.

Chapter 3 investigated the effects of different environmental conditions on the performance of Cr(VI) removal by algal-bacterial AGS, including co-existing anions/cations, NOMs, salinity and carbon sources were studied with respect to both Cr(VI) reduction and total Cr immobilization.

Chapter 4 explored the underlying mechanism for Cr(VI) removal by algal-bacterial AGS with cell viability, EPS variation, Cr localization and chemical fractionation.

At last, Chapter 5 summarized the main findings in this research. For better application of algal-bacterial AGS for Cr(VI) removal, future studies were also prospected.

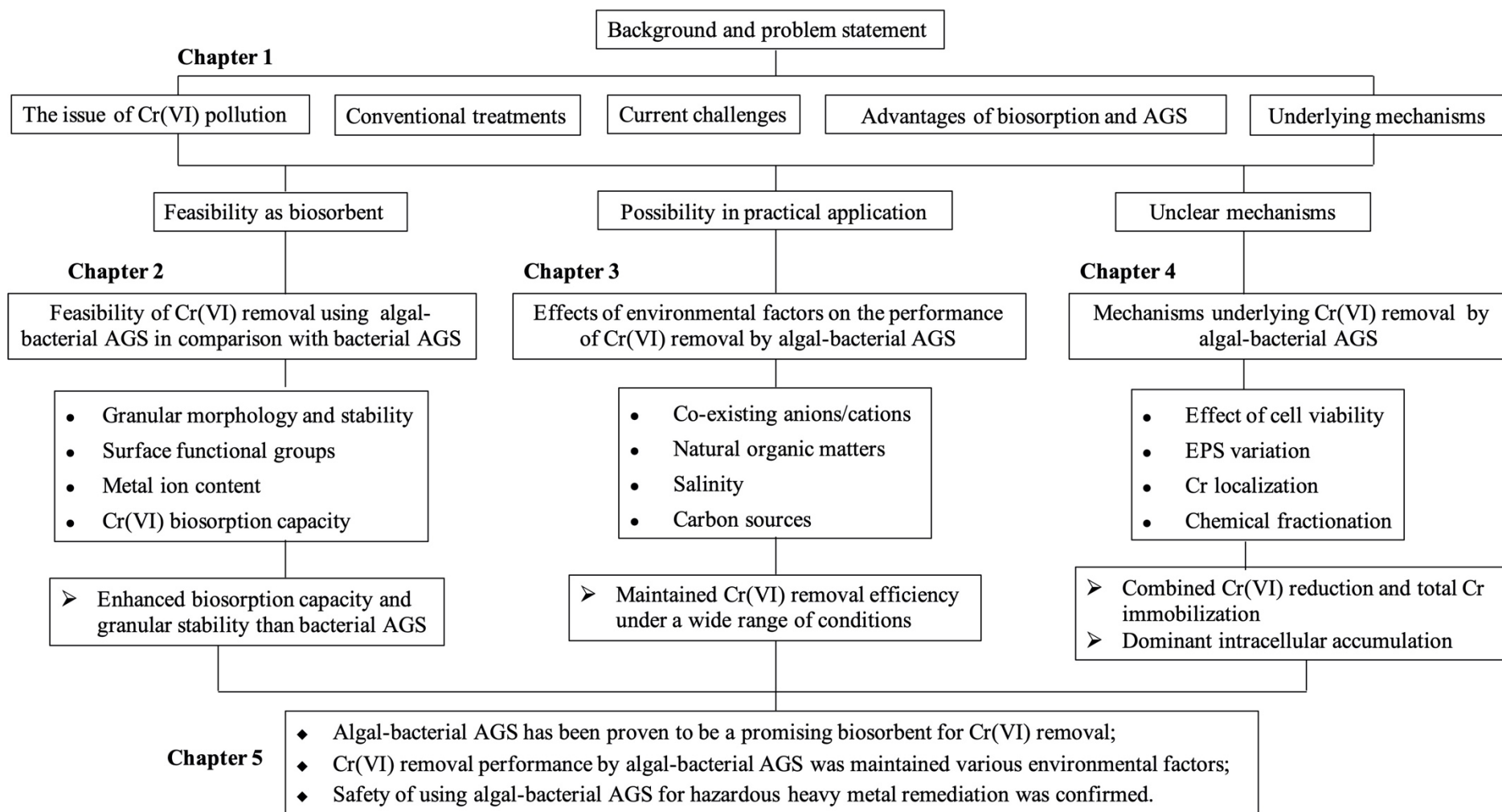


Figure 1-1 Research framework of Cr(VI) removal by algal-bacterial AGS.

## **Chapter 2 Feasibility of Cr(VI) removal from synthetic wastewater using algal-bacterial AGS in comparison with bacterial AGS**

### **2.1 Background**

HMs as one of the most worldwide concerned environmental issues, are regarded as a great challenge to WWTPs due to their toxic effects on aquatic organisms and human beings. Chromium, mainly in the form of Cr(VI) and Cr(III), is one of the typical HMs that have carcinogenic and mutagenic effects to humans. Biosorption is considered as a cost-effective and environmentally friendly Cr(VI) removal process from wastewater. AGS is considered as a promising biotechnology for wastewater treatment, when applied as biosorbent, it has many superior properties like porous microbial structure, excellent settleability, rich binding sites for metals and the ability to withstand shock and toxicant loadings (Franca et al., 2018; Wang et al., 2018). Most recently, a new type of AGS, algal-bacterial AGS which is granular consortium of both algae and bacteria, has been established successfully (Zhang et al., 2018; Zhang et al., 2020). It is hypothesized that algal-bacterial AGS could be a more suitable biosorbent which can couple the high HMs adsorption capacity of algae with the porous and compact structure of bacterial AGS (Kumar et al., 2015; Franca et al., 2018; Wang et al., 2018). Considering its rapid growth rate in wastewater and easy separation from the treated wastewater after biosorption, algal-bacterial AGS would be more promising for Cr(VI) removal in practical applications.

Up to now, still, little information is available on the application of algal-bacterial AGS biomass as a biosorbent for Cr(VI) removal from wastewater. Therefore, the objectives of this chapter are: (1) to assess the feasibility and performance of using algal-bacterial AGS for handling Cr(VI)-containing wastewater; (2) to compare the Cr(VI) biosorption capacity of algal-bacterial AGS with the conventional bacterial AGS. Results from this chapter are expected to provide useful information for the reuse of algal-bacterial AGS as biosorbent for the cost-effective treatment of Cr(VI)-containing wastewater.

### **2.2 Materials and methods**

#### **2.2.1 Preparation of algal-bacterial AGS and bacterial AGS**

Mature algal-bacterial AGS and bacterial AGS were respectively cultivated in two lab-scale sequencing batch reactors (SBRs) made of acrylic transparent plastic (with a working volume of 14.4 L and exchange ratio of 49.3% each). The main components in the synthetic

wastewater were: 300 mg COD/L (sodium acetate), 50 mg NH<sub>4</sub>-N/L (NH<sub>4</sub>Cl), 5 mg PO<sub>4</sub>-P/L (KH<sub>2</sub>PO<sub>4</sub>), 10 mg Ca<sup>2+</sup>/L (CaCl<sub>2</sub>·2H<sub>2</sub>O), 5 mg Fe/L (FeSO<sub>4</sub>·H<sub>2</sub>O), and 5 mg Mg/L (MgSO<sub>4</sub>·7H<sub>2</sub>O). The reactors were operated at room temperature (25±2 °C) with each cycle of 6 h consisting of feeding (3 min), an anaerobic phase (120 min), an aerobic phase (230 min), settling (3 min), and decanting (4 min). The sludge retention time was controlled at approximately 35 days through quantitative sludge discharge. Air was introduced into the reactors by air pumps (KOSHIN Co., Ltd, Japan), and the superficial uplift air velocity was controlled at 0.48 cm/s by an air flowmeter. Artificial light (at an illumination intensity of 1450 lux for 12 hours per day) was provided for the growth of algae and no light for conventional AGS throughout the cultivation. *Leptolyngbya* was the dominant algae species (65-75%) in the algal-bacterial AGS in this study. The amount of chlorophyll *a* (Chl-*a*) in the algal-bacterial AGS was around 5.1-5.3 mg per gram mixed liquor volatile suspended solids (MLVSS).

Excellent organics and nutrients removals were achieved by each reactor, such as dissolved organic carbon (DOC) removal > 96%, NH<sub>4</sub><sup>+</sup>-N removal > 99%, total nitrogen removal > 66%, and total phosphorus removal > 89%. Before the biosorption experiments, the granules were collected from the SBRs at the end of aeration step, and then washed with deionized water for three times. The granules with size between 0.5-2.5 mm were used in this study.

### 2.2.2 Batch Cr(VI) biosorption tests

A 1000 mg/L Cr(VI) stock solution was prepared with potassium dichromate (K<sub>2</sub>Cr<sub>2</sub>O<sub>7</sub>), which was firstly dried at 105 °C for 24 h and then dissolved in deionized water. Right before the adsorption experiments, the stock solution was diluted to the designated concentrations according to the experimental design. Solution pH was adjusted by adding 1 M HCl or NaOH and measured with a pH meter (Mettler Toledo FE20, Switzerland).

The biosorption kinetic experiments were carried out in 300 mL conical flasks loaded with 40 mL suspended granules (with granule mass (dry weight) concentration of around 10 g/L) and 160 mL Cr(VI) solution. The initial Cr(VI) concentration was 50 mg/L in this kinetics study. The resultant mixture was shaken at 125 rpm and then the samples were collected at different time intervals. The isotherm experiments were conducted in 50 mL plastic centrifuge tubes with 5 mL suspended granules and 20 mL Cr(VI) solution. The Cr(VI) concentration in the mixture ranged from 12.5 to 300 mg/L. The initial solution pH in kinetic and isotherm experiments was adjusted to about 2.0. During the evaluation of the effect of solution pH (varied from 1.0 to 12.0) on Cr(VI) biosorption, the experiments were conducted at an initial Cr(VI) concentration

of 50 mg/L with a mixture volume of 25 mL containing 5 mL suspended granules. All the absorption experiments were conducted in duplicate at room temperature ( $25 \pm 2$  °C).

### 2.2.3 Analytical methods

After tests, the supernatant was sampled from each flask or tube, and then filtered through 0.22  $\mu$ m membrane. Metal concentration in filtrates was quantified with the methods as described elsewhere (Chen et al., 2018). In brief, Cr(VI) concentration in filtrates was quantified by a UV spectrophotometer at 540 nm (UV 1800, Shimadzu, Japan) after complexation with 1,5-diphenyl-carbazide in acidic medium; total Cr, Ca, Mg, and Fe ions in the filtrates were determined using ICPS-8100 (Shimadzu ICPS-8100, Japan) after the sample being completely digested with HNO<sub>3</sub> and H<sub>2</sub>O<sub>2</sub> at 100 °C. Cr(III) concentration was obtained by subtracting Cr(VI) concentration from the total Cr concentration. All samples were prepared in triplicate and determined.

The quantification and characterization of granular biomass including mixed liquor (volatile) suspended solids (ML(V)SS), morphology of granules and granular size were performed according to the same procedures described previously (Zhao et al., 2018). For example, Leica M205 C Microscope (Leica Microsystems, Switzerland) and scanning electron microscope (SEM) (JSM6330f, Japan) were used to record the morphological characteristics of the granules before and after Cr(VI) adsorption. In this study, microbial activity of organisms in the algal-bacterial AGS and granular stability were also measured, which was indicated by specific oxygen uptake rate (SOUR) as described in a previous study (Chen et al., 2018). In brief, for SOUR test, 3 g-wet weight (0.04 g-VS/g) granules were added into a 100 mL glass flask containing 90 mL synthetic wastewater (for algal-bacterial AGS cultivation), then an aerator and a dissolved oxygen (DO) meter (DO-31P, TOA-DKK, Japan) were inserted. The granular mixture was agitated with a magnetic stirrer at 300 rpm to ensure the suspension of granules when no aeration supplied. The mixture was firstly aerated till a relatively stable DO level achieved (over 5 mg-DO/L), then the aeration was stopped and at the same time the flask was sealed with a DO meter inside. Due to the consumption of DO by microorganisms, the DO level decreased immediately and was recorded timely as DO<sub>t</sub>. Then a DO versus time curve was made and only the linear portion was used for SOUR (mg-DO/(g-VS·h)) calculation with the equation:  $SOUR = (DO_{t1} - DO_{t2}) / (t \cdot VS)$ , in which DO<sub>t1</sub> and DO<sub>t2</sub> represented the DO value before and after the time interval (t), respectively. As for the testing of granular stability, 1 g-wet weight granules were added into a 50 mL plastic tube containing 40 mL DW. The mixture

was firstly shaken at 200 rpm on a shaker for 5 min and then settled down for 1 min, the ratio of TS in the supernatant (30 mL) to the TS of total granules was recorded as integrity coefficient.

Zeta potentials of algal-bacterial AGS were measured by a Zetasizer Nano ZS (Malvern Instruments, UK) at 20 °C. Fresh granules were fully grinded in deionized water firstly, then the suspensions with small fragments from the granules in it were measured. Fourier Transform Infrared Spectroscopy (FTIR; JASCO FTIR-300, Japan) was also applied to identify the functional groups in the granules, and the spectra were obtained in the range of 400-4000 cm<sup>-1</sup>.

Biosorption capacity ( $q$ , mg-Cr(VI) g-MLSS<sup>-1</sup>) and desorption ratio (%) were calculated using the same equations as described previously (Chen et al., 2018).

Both Freundlich and Langmuir isotherms (Eqs. (1) and (2)) were adopted to fit the adsorption isotherm data.

$$\text{Langmuir isotherm: } \frac{C_e}{q_e} = \frac{1}{k_L q_m} + \frac{C_e}{q_m} \quad (1)$$

$$\text{Freundlich isotherm: } \ln q_e = \ln k_F + \frac{1}{n} \ln C_e \quad (2)$$

where  $q_e$  and  $q_m$  represent the amount of Cr(VI) adsorbed on granules at equilibrium and the predicted maximum biosorption amount (mg/g), respectively.  $C_e$  is the equilibrium concentration of Cr(VI) (mg/L). Constant  $k_L$  is related to the biosorption energy (L/ mg). The two constants  $k_F$  and  $n$  represent the biosorption capacity intensity, and larger values of them denote better biosorption capacity.

All the experiments were carried out in duplicate, and the analysis of samples was performed in triplicate with the results being expressed as mean or mean  $\pm$  standard deviation (SD). For data analysis, one-way analysis of variance (ANOVA) was used to compare the difference among the tested scenarios by using Microsoft Excel 2010. Statistical significance was assumed if  $p < 0.05$ .

## 2.3 Results and discussion

### 2.3.1 Cr(VI) biosorption by algal-bacterial AGS

#### (1) Effect of initial solution pH

Solution pH is one of the most important parameters that significantly affect both surface chemical properties of granules and solution chemistry of chromium in aqueous solution (Zhuo et al., 2017; Feng et al., 2018). The changes of Cr species and Cr(VI) biosorption capacity of algal-bacterial granules at different initial pHs (from pH 1.0 to 12.0) are depicted in Figure 2-1a. As seen, the Cr(VI) biosorption capacity of algal-bacterial AGS is highly pH dependent,

and the relatively higher biosorption capacity is reached at pH 1.5-2. When the solution pH is greater than 2, the biosorption capacity of Cr(VI) onto the algal-bacterial AGS decreases significantly along with the increase of solution pH. This observation is correlating with the optimum pH at 1-3 noted for Cr(VI) biosorbed onto conventional bacterial AGS or microalgae (Han et al., 2007; Chen et al., 2018; Pradhan et al., 2019). The pH of wastewaters containing Cr(VI) from various industries is around 2 (Machado et al., 2010; Moussavi et al., 2010), thus the present algal-bacterial AGS is promising to be applied as biosorbents for Cr(VI) removal from the industrial wastewaters.

It's worth noting that when the solution pH continues to decrease from pH 2, partial Cr(VI) was bio-reduced to Cr(III) (Figure 2-1a), which is in agreement with the statement made by Sun et al. (Sun et al., 2010) that Cr(VI) tends to be reduced to Cr(III) at a low pH (around 2) when biosorbents are present. Considering that  $\text{HCrO}_4^-$  is the major species of Cr(VI) in the pH range of 1.0 - 4.0 (Han et al., 2007), the enhanced migration of Cr(VI) anions to the AGS at  $\text{pH} < 2$  is probably attributable to the increased electrostatic attraction, as the granules were positively charged when pH was lower than 2.2 (indicated by  $\text{pH}_{\text{zpc}}$  in Figure 2-2, the pH of zero point charge).

This deduction was further confirmed by the FTIR spectra of algal-bacterial AGS before and after Cr(VI) biosorption for 24 h (Figure 2-3). Slight shifts were observed for the peaks at around  $3300\text{ cm}^{-1}$  ( $-\text{OH}$  and/or  $-\text{NH}$  stretching of hydroxyl and amine groups) and  $1398\text{ cm}^{-1}$  ( $-\text{COO}$  stretching of carboxylic groups) before and after Cr(VI) biosorption (Karthik et al., 2017; Cid et al., 2018; OChemOnline, 2020). As reported, amino groups (in amine and protein) can be protonated at pH 2 and electrostatically attract chromate anions, e.g.  $\text{HCrO}_4^-$ , thus responsible for Cr(VI) biosorption (Bai et al., 2002). On the other hand, the major species of Cr(III) in the same pH range is  $\text{Cr}^{3+}$ , which is difficult to be attracted onto granular surface due to the electric repulsion. However, it can be complexed with carboxylic groups on the granule (Han et al., 2007) and then adsorbed onto algal-bacterial AGS.

To further reveal the underlying mechanisms involved in the pH dependence of Cr(VI) biosorption by algal-bacterial AGS, the concentrations of the released metal ions from granules into the aqueous solution were measured under different pH conditions after 24 h biosorption (Table 2-2). Results show that under the strongly acidic and alkaline conditions, more released metal ions were detected, especially  $\text{Mg}^{2+}$  and  $\text{Ca}^{2+}$ , implying that ion exchange might also be attributable to the biosorption of Cr(VI) onto the algal-bacterial AGS.

## **(2) Biosorption kinetics**

The effect of contact time on biosorption capacity of Cr(VI) is presented in Figure 2-1b. The Cr(VI) concentration was decreased rapidly from 50.2 mg/L to 39.7 mg/L in the first 0.5 h, which should be owing to the presence of sufficient vacant surface sorption sites. After 0.5 h, the Cr(VI) biosorption process slowed down and reached equilibrium at 48 h. The concentration of Cr(III) in the aqueous solution was noticed to gradually increase after 24 h. As the granule surface was positively charged at pH 2, Cr(III) cations were difficult to be adsorbed onto granules due to the electric repulsion, which may complex with specific surface functional groups like carboxylic groups (Han et al., 2007). With the consumption of these functional groups and insufficient binding sites for Cr(III), it would be released into the solution.

To reveal the transport mechanisms involved in the biosorption process, the pseudo-first-order model and pseudo-second-order model were applied in this study. From Table 2-1, the pseudo-second-order model ( $R^2 = 0.992$ ) better fits the experiment data than the pseudo-first-order model ( $R^2 = 0.707$ ). This result indicates that the biosorption of Cr(VI) onto algal-bacterial AGS can be described by chemical sorption, with which new chemical species may be generated at the sorbent surface (Suksabye et al., 2009). Besides, by using the pseudo-second order model, the best fit  $q_e$  value of 9.73 mg/g for the Cr(VI) biosorption is very close to the experimental value (9.71 mg/g).

Freundlich and Langmuir isotherms were also adopted to fit the isotherm data. Results in Figure 2-4 clearly reveal that both isotherms are able to describe the biosorption process well with high correlation coefficients ( $R^2 > 0.925$ ), while Freundlich isotherm shows a better fit ( $R^2 = 0.997$ ). Empirically, the Cr(VI) biosorption can be regarded more likely with the formation of multilayers of ions on the algal-bacterial AGS. The maximum biosorption capacity of  $q_m$  (51.0 mg/g) calculated from the Langmuir isotherm is comparable with previous studies using raw or treated AGS, microalgae or other biosorbents (Table 2-3). Considering its rapid biomass growth rate in wastewater and easy separation from the treated wastewater after biosorption, the repeated reuse of the disposed algal-bacterial AGS as biosorbent can be a promising option for Cr(VI) removal and recovery from wastewater.

### **2.3.2 Comparison between algal-bacterial AGS and bacterial AGS**

Conventional bacterial AGS has been applied as biosorbent for HMs removal in various research, which is proven to be applicable (Wang et al., 2018). However, the drawbacks of AGS process, the relatively low structural stability during prolonged operation, would lower down



the treatment efficiency in the subsequent solid/liquid separation after adsorption process. More importantly, the biomass growth of bacterial AGS is relatively slow, which makes it not practical to frequently take granules out of the AGS system for other special purposes like adsorption. On the other hand, in addition to much faster biomass growth and more stable granular structure (Zhang et al., 2018; Zhang et al., 2020), algal-bacterial AGS possesses many superiorities with respect to reduction in energy consumption and operation cost on aeration when compared to conventional bacterial AGS (Zhao et al., 2018; Zhao et al., 2019). However, up to the present, little information is available on the comparison of their performance as biosorbent. As shown in this study, with significantly higher Cr(VI) biosorption capacity (9.60 mg/g vs. 8.49 mg/g under the same test conditions;  $p=0.0014$ ), algal-bacterial AGS also demonstrated better granular stability before and after adsorption (Figure 2-5). Moreover, even after 24 h contact at pH 2, algal-bacterial AGS could maintain better granular morphology, which was indicated by its lower integrity coefficient (Figure 2-5), i.e., the ratio of solids in the supernatant to the weight of total granules after being subjected to a certain degree of agitation (Ghangrekar et al., 2005). The excellent stability of algal-bacterial AGS during biosorption was also confirmed by the very slight change of its average diameter and size distribution before and after biosorption for 24 h (Figure 2-6). Results indicate that the growth of algae on AGS would be responsible for the enhanced biosorption capacity and granular stability of algal-bacterial AGS. Therefore, we further compared the conventional bacterial AGS and algal-bacterial AGS from different aspects including surface characteristics and metal ion exchange efficiency.

Seen from the images in Figure 2-7, the algal-bacterial AGS were green in most parts of the granules, with algae growing on the surface as well as in the core of the granules. It's the twining of microalgae and filaments instead of filaments alone that forms the granular skeleton of algal-bacterial AGS (Figure 2-7G and H), which would be beneficial for structural stability of the granules. Moreover, the two AGS were examined by FTIR with no distinguished wavelength variance in functional groups being observed (Figure 2-3), suggesting that organic matters and surface functional groups might have limited contribution to the enhanced biosorption capacity of algal-bacterial AGS.

Ion exchange has been proven to involve in Cr(VI) biosorption by both conventional bacterial AGS (Chen et al., 2018) and algal-bacterial AGS (section 3.1.1), and both granules contain a significant amount of metal ions (Table 2-4). Seen from Figure 2-8, more metal ions were detected to release from algal-bacterial AGS than conventional bacterial AGS, especially

the release of  $\text{Ca}^{2+}$  after 24 h biosorption. More specifically, it's the light metal ions ( $\text{Ca}^{2+}$  and  $\text{Mg}^{2+}$ ) that were released more when contact with Cr(VI), not the heavy metal ions like  $\text{Fe}^{2+/3+}$ . These observations are consistent with the previous studies that light metal ions tend to be released during HMs adsorption (Xu and Liu, 2008; Wang et al., 2010). These results directly confirm the involvement of ion exchange in Cr(VI) adsorption and its contribution to the enhanced biosorption capacity of algal-bacterial AGS.

### 2.3.3 Mechanisms

Based on the above results, it's concluded that algal-bacterial AGS is a promising biosorbent for Cr(VI) removal and has superiorities than conventional bacterial AGS in both biosorption capacity and granular stability. Cr(VI) removal by algal-bacterial AGS is accomplished by both biosorption and bioreduction reactions, and four mechanisms are involved in this complex process. (1) Electrostatic interactions: the granule surface is positively charged at pH 2 and Cr(VI) anions can be adsorbed on the protonated sites. (2) Bioreduction: during this process Cr(VI) is reduced to Cr(III) with the organic matters of granules function as reductants at a low pH. (3) Surface complexation: Cr(III) cations are difficult to be adsorbed onto the granules due to electric repulsion, which may complex with specific surface functional groups like carboxylic groups. (4) Ion exchange: the light metal ions like  $\text{Ca}^{2+}$  and  $\text{Mg}^{2+}$  are released from the granules and heavy metal Cr ions are adsorbed onto the granules during the biosorption process. In addition, intracellular accumulation is also assumed to be involved. In summary, as a biosorbent consisting of alive microbes, due to its exceptional capability to maintain microbial activity and granular stability, algal-bacterial AGS possesses great potential for being re-utilized in wastewater treatment for heavy metal removal/recovery.

## 2.4 Summary

Cr(VI) biosorption onto algal-bacterial AGS is highly pH dependent and follows the pseudo-second-order model, with the maximum biosorption capacity of 51.0 mg/g at pH 2 estimated from Langmuir model, although the isotherm data better fit the Freundlich equation. Desorption tests evidenced the bioreduction of Cr(VI) to Cr(III). Compared to conventional bacterial AGS, algal-bacterial AGS shows advantages in both biosorption capacity and granular stability. The Cr(VI) biosorption process using algal-bacterial AGS mainly involves electrostatic interactions, ion exchange, surface complexation and bioreduction. algal-bacterial AGS is promising to be developed as an efficient biosorbent for Cr removal/recovery from

wastewater due to its excellent stability and settleability during the biosorption/desorption processes.

Table 2-1 Fitting results of biosorption data of Cr(VI) onto algal-bacterial AGS to the kinetic models.

Model	Parameters			
	$R^2$	$k_1$ (h <sup>-1</sup> )	$k_2$ (g/mg·h)	Theoretical $q_e$ (mg/g)
pseudo-first order <sup>a</sup>	0.707	0.54	-	51.72
pseudo-second order <sup>b</sup>	0.992	-	0.16	9.73

<sup>a</sup>  $\log(q_e - q_t) = \log q_e - k_1 t / 2.303$ , <sup>b</sup>  $t/q_t = 1/(k_2 q_e^2) + t/q_e$ ;  $k_1$  is the pseudo-first-order rate constant (h<sup>-1</sup>),  $k_2$  is the pseudo-second-order rate constant (g/mg·h),  $q_t$  and  $q_e$  represent the amount of Cr(VI) adsorbed on granules at time  $t$  and equilibrium time (mg/g), respectively.

Table 2-2 Concentrations of released metal ions from algal-bacterial AGS during biosorption from Cr(VI)-containing wastewater for 24 h over the test pH range of 1.0-12.0.

pH	Concentration of dissolved metal ions (mg/L)		
	Mg <sup>2+</sup>	Ca <sup>2+</sup>	Fe <sup>2+/3+</sup>
1.0	12.86	20.66	3.94
2.0	8.10	21.10	3.22
3.0	2.60	14.18	0.63
6.8	0.43	5.59	0.51
12.0	3.56	18.72	2.37

Table 2-3 Comparison of maximum Cr(VI) biosorption capacities between algal-bacterial AGS and previously reported biosorbents.

Biosorbents	Treatment	pH	Temperature (°C)	Sorbent conc. (g/L)	Contact time (h)	q <sub>m</sub> (mg/g)	References
Algal-bacterial AGS		2	25	2	24	51.0	This study
Bacterial AGS		2	25	NA	1	16.8	Chen et al., 2018
Bacterial AGS	PEI <sup>a</sup>	5.5	25	0.5	24	401.5	Sun et al., 2010
Rice husk	Hydrothermal	2	25	10	47	31.1	Ding et al., 2016
<i>Bacillus megaterium</i> (bacteria)		4	28	2	1	30.7	Srinath et al., 2002
<i>Rhizopus nigricans</i> (fungi)		2	30	0.2% (w/v)	0.5	38.8	Bai et al., 2002
<i>Rhizopus nigricans</i> (fungi)	APTS <sup>b</sup>	2	30	0.2% (w/v)	0.5	51.2	Bai et al., 2002
<i>C. reinhardtii</i> (green algae)		2	25	0.6	2	18.2	Arıca et al., 2005
<i>C. reinhardtii</i> (green algae)	HCl	2	25	0.6	2	21.2	Arıca et al., 2005
<i>C. reinhardtii</i> (green algae)	Heat	2	25	0.6	2	25.6	Arıca et al., 2005
<i>Scenedesmus sp.</i> (microalgae)		1	30	10% (w/v)	2	0.3	Pradhan et al., 2019

<sup>a</sup> Polyethylenimine; <sup>b</sup> Amino Propyl Trimethoxy Silane.

Table 2-4 Average contents of dominant metals in the algal-bacterial AGS and conventional bacterial AGS.

Granule	Metal ions (mg/g-MLSS)				
	Na <sup>+</sup>	K <sup>+</sup>	Mg <sup>2+</sup>	Ca <sup>2+</sup>	Fe <sup>2+/3+</sup>
Conventional bacterial AGS	19.61	13.00	10.45	8.80	12.56
Algal-bacterial AGS	8.14	9.21	7.14	10.81	13.04

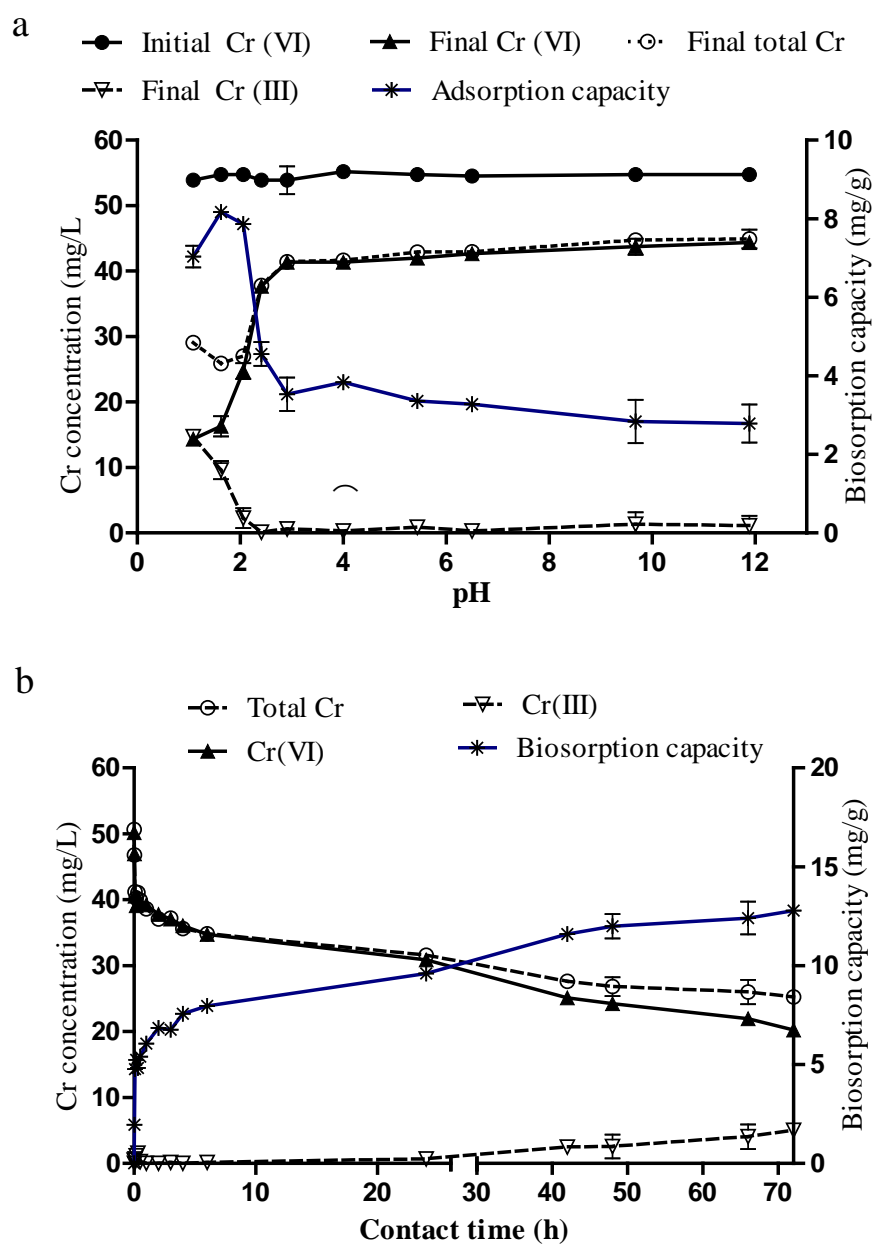


Figure 2-1 Cr(VI) biosorption at an initial Cr(VI) of 50 mg/L with algal-bacterial AGS dosage of 2 g/L: (a) effect of pH during 24 h contact, and (b) effect of contact time at pH 2.



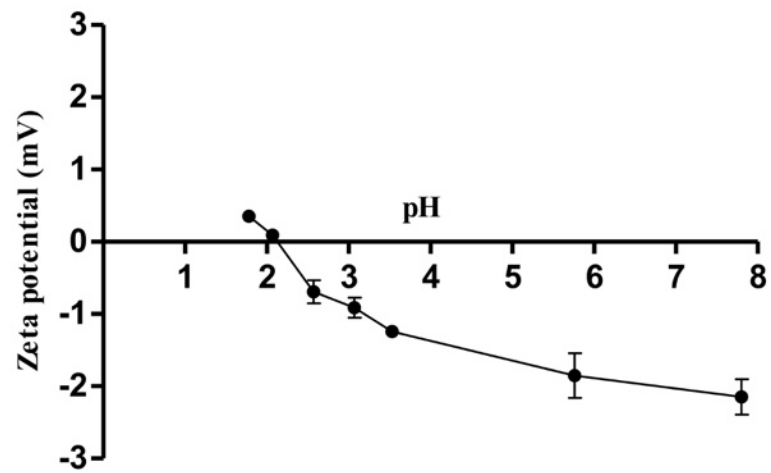


Figure 2-2 Plot for determination of pH at zero point charge (pHzpc) of algal-bacterial AGS: zeta potential of granules as a function of solution pH.

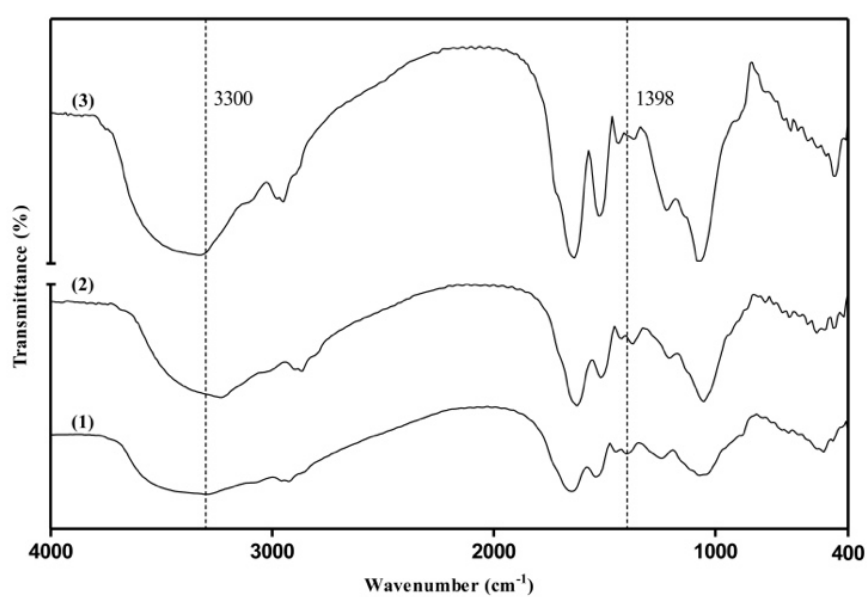


Figure 2-3 FTIR spectra of initial (a) bacterial AGS, (b) algal-bacterial AGS and (c) Cr-loaded algal-bacterial AGS after 24 h biosorption (at an initial Cr(VI) of 50.0 mg/L, biosorbent dosage of 2 g/L and pH 2).

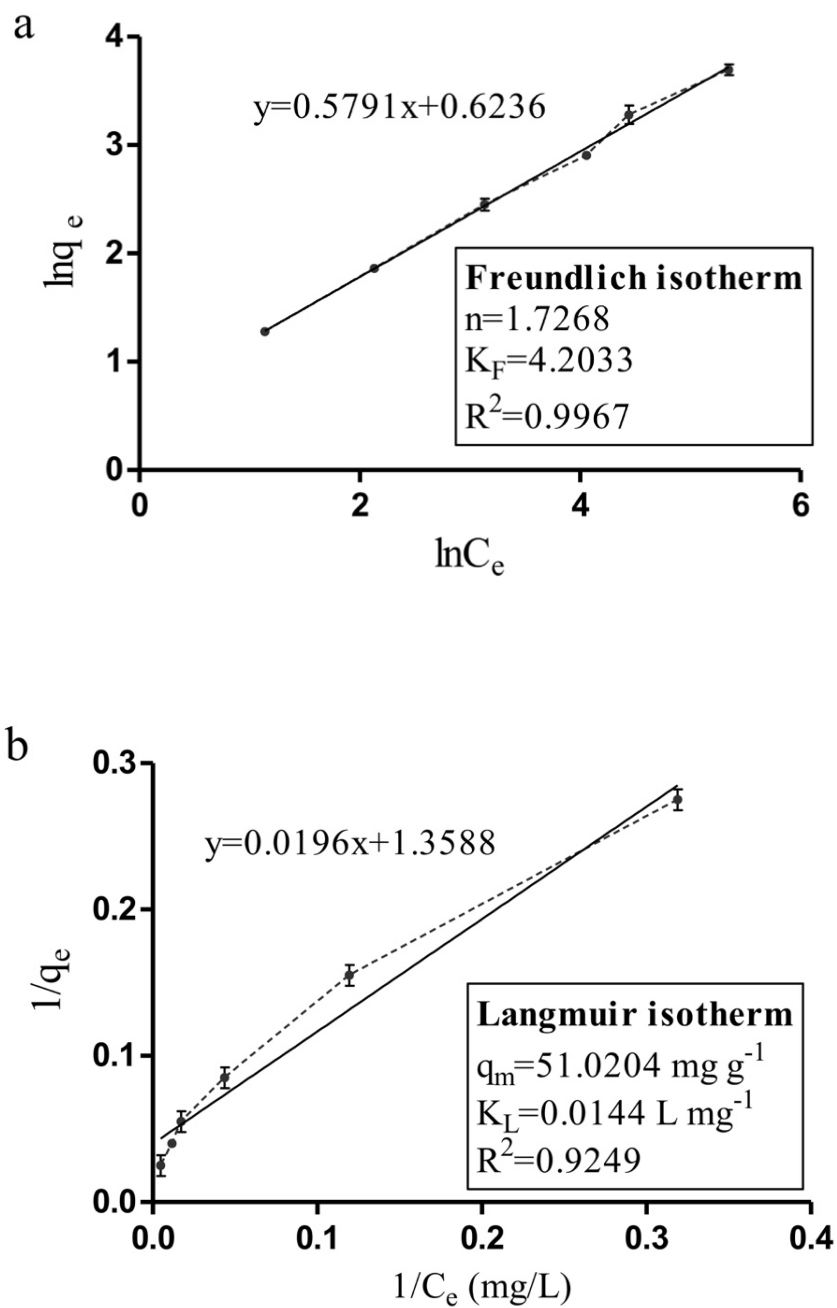


Figure 2-4 Plots of isotherms of Cr(VI) biosorption onto algal-bacterial granules: (a) Freundlich isotherm, and (b) Langmuir isotherm (at an initial Cr(VI) concentration of 12.5, 25.0, 50.0, 100.0, 150.0, or 300.0 mg/L, algal-bacterial AGS dosage of 2 g/L and pH 2 for 24 h contact).

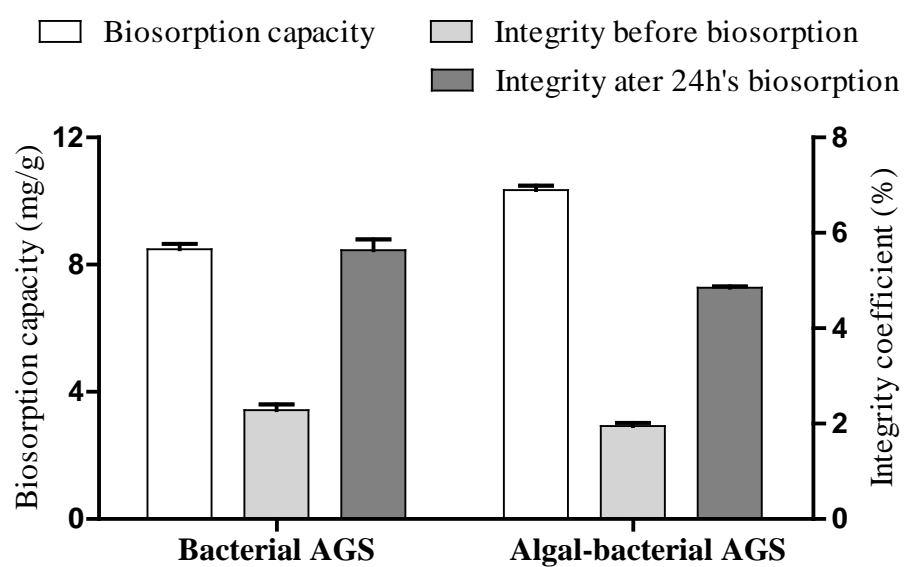


Figure 2-5 Comparison of Cr(VI) biosorption capacity and granular integrity between conventional bacterial AGS and algal-bacterial AGS (at initial Cr(VI) of 50.0 mg/L, biosorbent dosage of 2 g/L and pH 2).

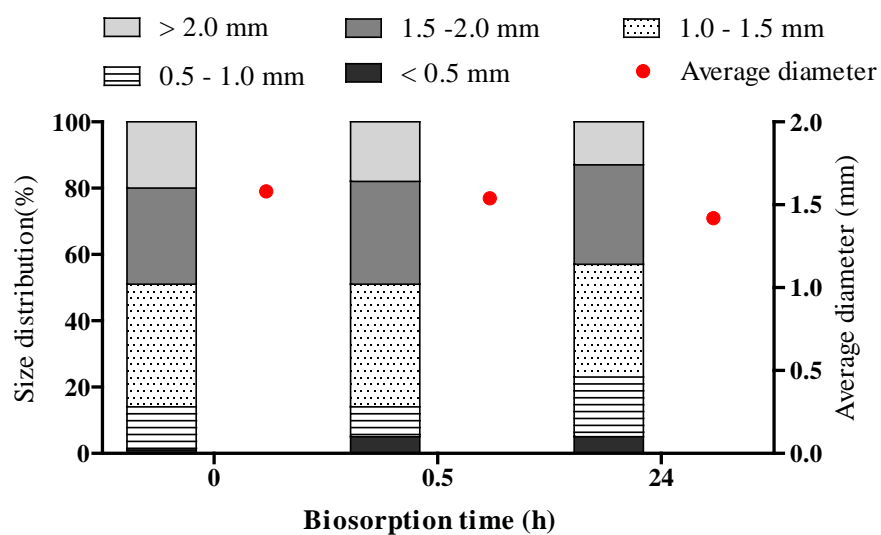
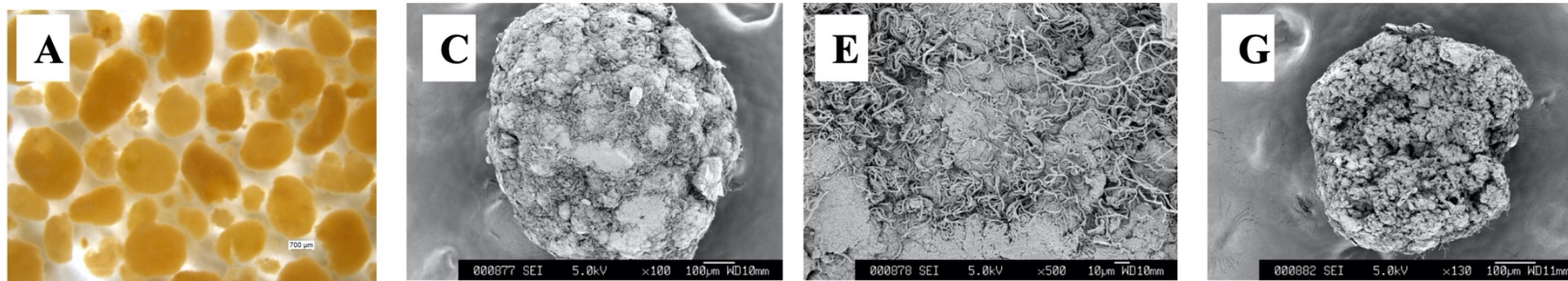


Figure 2-6 Changes in algal-bacterial AGS diameter and granular size distribution before and after biosorption (at initial Cr(VI) of 50.0 mg/L, biosorbent dosage of 2 g/L and pH 2).

## Bacterial AGS



## Algal-bacterial AGS

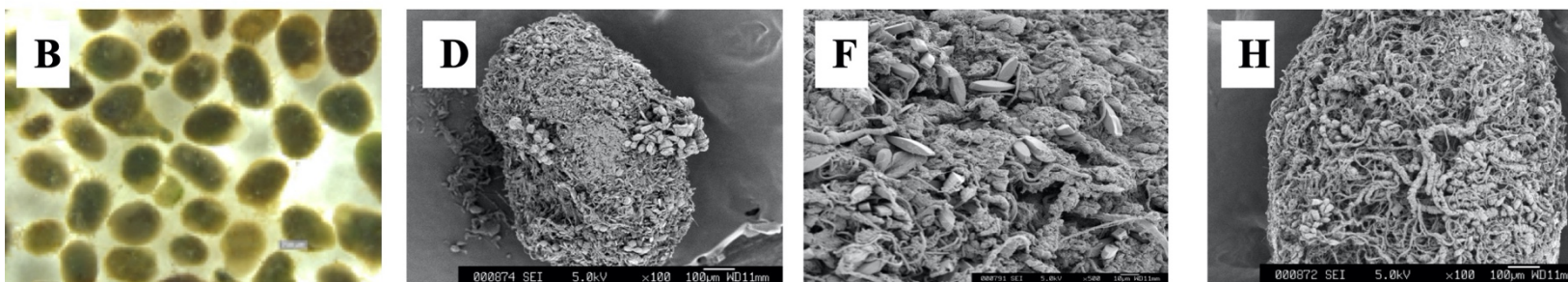


Figure 2-7 Images of the conventional bacterial AGS and algal-bacterial AGS. Digital photos of test granules (A and B), and SEM observation of granules from surface (C-F) or cross section (G and H), respectively.

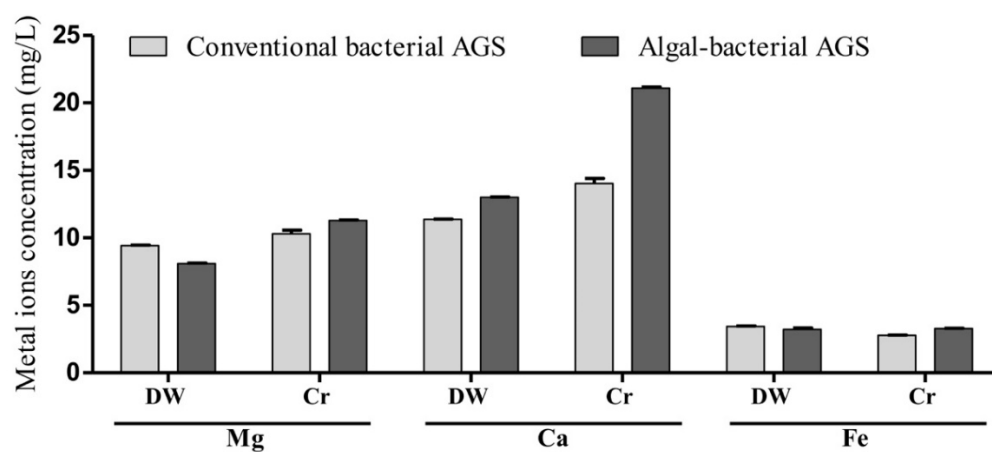


Figure 2-8 Concentrations of three main metal ions ( $\text{Mg}^{2+}$ ,  $\text{Ca}^{2+}$  and  $\text{Fe}^{2+/3+}$ ) released into the aqueous solution from AGS after 24 h contact with Cr(VI) solution (Cr(VI), 50.0 mg/L) or deionized water (DW) at pH 2.

## **Chapter 3 Effects of environmental conditions on the performance of Cr(VI) removal by algal-bacterial AGS**

### **3.1 Background**

Results from Chapter 2 demonstrated that compare to the conventional bacterial AGS, algal-bacterial AGS demonstrated higher biosorption capacity and better granular stability, implying that algal-bacterial AGS can be more potentially utilized as a Cr(VI) removal and recovery biomaterial for the treatment of Cr(VI)-containing wastewater. However, when applied in real world, the effects of different background circumstances should be also taken into consideration due to the complexity of contaminated surface water and actual industrial wastewater. These environmental factors include co-existing anions/cations, natural organic matters (NOMs), ionic strength (IS), and carbon sources, etc. On the other hand, Cr(VI) could be reduced to Cr(III) when biomaterials were utilized specially at low pH values (Sun et al., 2010). Even though Cr(III) is less toxic and mobile than Cr(VI), it can still cause allergic skin reactions and cancer at excessive levels (Kotaś and Stasicka, 2000). Thus, its necessary to distinguish Cr(VI) reduction and total Cr immobilization during the Cr(VI) removal processes, and total Cr should be substantially removed from the wastewater. Therefore, Chapter 3 aimed to evaluate Cr(VI) removal performance under different conditions and interference factors. Cr(VI) removal was determined in both aspects of Cr(VI) reduction and total Cr immobilization. Results of this study are expected to provide relative data support of this new approach and further insight into the practical application of algal-bacterial AGS in treating Cr(VI)-contaminated wastewater.

### **3.2 Materials and methods**

#### **3.2.1 Cultivation and characterization of algal-bacterial AGS**

The algal-bacterial AGS used in this study were cultivated in a lab-scale sequencing batch reactor (SBR) made of acrylic transparent plastic with a working volume of 1.16 L (H = 50 cm, D = 6 cm) and exchange ratio of 50%. The reactor was inoculated with the mature bacterial AGS and fed with synthetic domestic wastewater (mg/L): sodium acetate (392 or COD of 300 );  $\text{NH}_4\text{Cl}$  (115),  $\text{KH}_2\text{PO}_4$  (13.2),  $\text{NaHCO}_3$  (150),  $\text{CaCl}_2 \cdot 2\text{H}_2\text{O}$  (40),  $\text{MgSO}_4 \cdot 2\text{H}_2\text{O}$  (51) and  $\text{FeSO}_4 \cdot 7\text{H}_2\text{O}$  (25). The reactor was operated at a typical cycle of 4 h under room temperature ( $25 \pm 2$  °C): 1 min feeding, 60 min non-aeration, 176 min aeration, 2 min settling, and 1 min effluent withdrawal, resulting in a hydraulic retention time (HRT) of 8 h. During the whole



cultivation, an artificial light with an illumination intensity of 3000 lux (12 h/day) was set above the reactor to maintain the growth of algae. Mature algal-bacterial AGS was obtained after 30 days' cultivation and Chl-a content was around 3.8 mg/g of volatile solids (VS).

Morphological characteristics of mature algal-bacterial AGS were recorded by both microscope (Leica M205 C, Switzerland) and scanning electron microscope (JSM6330f, Japan). Microbial activity and granular stability (indicated by (SOUR) and integrity coefficient, respectively) were measured as described in Chapter 2.

### **3.2.2 Optimization of Cr(VI) biosorption**

Biosorption of Cr(VI) by algal-bacterial AGS was carried out in a mineral salt medium (MSM, g/L):  $K_2HPO_4$  3.5,  $KH_2PO_4$  1.5,  $NH_4Cl$  1.0,  $MgSO_4$  0.3,  $NaCl$  0.5 (Němeček et al., 2014). Before each test, algal-bacterial AGS with size of 1.0 - 2.0 mm were collected from the reactor at the end of aeration phase and rinsed twice with deionized water (DW). All the tests were conducted in 50 mL glass flasks containing 1 g wet weight (0.05 g-total solids (TS)/g) granules and 10 mL MSM, or 500 mL glass flasks containing 10 g wet weight granules and 100 mL MSM. To optimize the operation parameters for Cr(VI) biosorption by algal-bacterial AGS, the influences of pH, contact time, initial Cr(VI) concentration and granule dosage were investigated. Then the effects of different environmental conditions including coexisting anions or cations, natural organic matters (NOM), salinity and carbon source (as electron donor) on biosorption process were further explored. The detailed experimental design and test conditions are shown in Table 3-1.

## **3.3 Results and discussion**

### **3.3.1 Changes in bioactivity and stability of algal-bacterial AGS after Cr(VI) biosorption**

Mature algal-bacterial AGS granules were fluffy and gray green when observed from the outer surface, indicating the existence of filamentous bacteria (Figure 3-1a). However, seen from the cross section, it was dark green, and the filamentous algae entangled with each other to construct a compact irregular sphere (Figure 3-1b and c). The batch Cr(VI) adsorption tests demonstrated that algal-bacterial AGS was capable of removing Cr(VI) from aqueous solution. However, no apparent difference in morphology could be discerned. On the other hand, the viability of microorganisms in fresh algal-bacterial AGS should be concerned when taking other pollutants or nutrients removal capabilities into consideration. Thus, the variations in microbial activity and granular stability of algal-bacterial AGS were determined.

As shown in Figure 3-2, after biosorption for 6 h, only very slight change could be observed in microbial activity and granular stability indicated by SOUR (57-62 mg/g-VS•h) and integrity coefficient (2.2-2.8 %), in comparison with the control group (no Cr(VI) addition), about 57-60 mg/g-VS•h and 2.2-2.6%, respectively. This observation suggests the limited impact of Cr(VI) on the functions of algal-bacterial AGS under the test conditions, i.e. the relatively low Cr(VI) concentration (5 mg/L) and a short exposure time (6 h) at almost neutral pH. On the other hand, AGS itself also possesses excellent tolerance to toxic compounds, due to its layered and compact structure, hierarchical distribution of microorganisms and the embedding of protective extracellular polymeric matrix. As reported, AGS could maintain its stability and microbial activity at 5 or 10 mg/L Cu(II) (Jiang et al., 2020) or 5 mg/L silver nanoparticles (Quan et al., 2015) for more than 50 days. The above results imply the possibility of stable maintenance of algal-bacterial AGS system for Cr(VI)-containing wastewater treatment.

### 3.3.2 Optimization of operation factors for Cr(VI) biosorption

#### (1) Initial pH

Solution pH plays a critical role in the biosorption of Cr(VI), as it determines both the charge of sorbent surface and the interconversion of Cr species. In order to optimize solution pH for the maximum total Cr removal efficiency by algal-bacterial AGS, biosorption experiments were conducted under different initial pHs varied from 2 to 9 at an initial Cr(VI) concentration of 5 mg/L. The equilibrium solution pH after 6 h biosorption was also detected, about 0.2 - 0.5 unit change, showing a slight increase trend when initial solution pH < 7 but a decline trend when the initial solution pH = 7 or higher. Seen from Figure 3-3a, the decrease of initial pH value from 9 to 6 significantly enhanced Cr(VI) removal efficiency from 44.6% to 90.0% after 6 h biosorption by algal-bacterial AGS, with very limited or no Cr(III) being detected. However, when the initial solution pH continued to decline, an increase in Cr(VI) reduction was detectable, while a decreasing tendency was observed for total Cr removal due to the increase trend of Cr(III) concentration in the solution.

At pH 2, the surface charge density of the algal-bacterial AGS would be positive, according to the  $pH_{PZC}$  (pH of zero point charge) value of 2.2 (Chapter 2). Under this condition, Cr(VI), mainly as  $HCrO_4^-$  can be easily absorbed onto the positively charged granule surface due to their strong electrostatic attraction. However, the lowest total Cr removal rate was obtained at this pH value, as almost 46.5% of total Cr was still remained in the form of Cr(III)

in solution. As reported, Cr(VI) can be easily reduced to Cr(III) with electron donors' coexisting in solution under acidic conditions, and the formed Cr(III) is a soluble cation which can be mainly stabilized as aquo-oxo species in the form of  $\text{Cr}^{3+}$  or  $\text{Cr}(\text{OH})^{2+}$  (Reizabal et al., 2020). Thus the formed Cr(III) is difficult to be sorbed onto algal-bacterial AGS surface owing to their electrostatic repulsion. Moreover, protons ( $\text{H}^+$ ) would also compete with Cr(III) for the active sites on granule surface, further hindering the biosorption process (Wang et al., 2020b).

With the increase of solution pH from 4 to 6, more negatively charged functional groups such as hydroxyl, carboxyl and amine groups (Chapter 2) would be deprotonated and exposed as active sites, thus enhancing the reaction between biomass and Cr(III), with the highest total Cr removal efficiency achieved at pH 6 and only 2.9% Cr being remained as Cr(III) in the solution. The predominant interactions between granules and cationic Cr(III) species would be electrostatic attraction under this pH condition. Besides, almost no change in microbial activity and granular structure of algal-bacterial AGS at pH 6 (Figure 3-2) to some extent may also contribute to the highest total Cr removal efficiency, which will be further discussed.

However, at neutral or more alkaline pH,  $\text{OH}^-$  competition would inhibit the electrostatic force between algal-bacterial AGS and Cr(VI) anions (Akram et al., 2017). In addition, Cr(VI) reduction can be suppressed and Cr(III) solubility would become minimum at pH 7-10 (Markiewicz et al., 2015). This can explain the decrease in total Cr removal and almost no Cr(III) was detected under pH 7-9 after biosorption for 6 h.

Overall, algal-bacterial AGS can effectively reduce Cr(VI) in the pH range of 2–6 and pH 6 was noticed as the optimum pH with respect to total Cr removal. Interestingly, the biosorption capacity for Cr(VI) has been reported to be higher at pH 1-3 and then decrease with the increase of pH in previous studies (Akram et al., 2017; Chen et al., 2018); while pH 5-6 is more commonly considered as the optimum pH for Cr(III) biosorption (Ranasinghe et al., 2018; Yao et al., 2009). Thus it's deduced that under the test conditions Cr(VI) might be firstly reduced to Cr(III) and then adsorbed by algal-bacterial AGS, and this inference would be further confirmed in the following experiments.

## **(2) Biosorption duration**

The effect of contact time on Cr(VI) biosorption was investigated up to 12 h at pH 6 and initial Cr concentration of 5 mg/L (Figure 3-3b). The Cr(VI) removal rate increased linearly with the contact time, achieving 84.6% and 96.3% after 6 or 12 h biosorption, respectively. Cr(III) in the solution was kept at a low level (< 5% of the total Cr) during the whole sorption

process, suggesting a quick adsorption of the generated Cr(III) species onto granules. The adsorption of Cr onto algal-bacterial AGS was rapid at first, due to abundant available active sites on the granule surface, and then slowed down, attributable to the progressive exhaustion of the remaining vacant active sites by the adsorbed metal ions (Yao et al., 2009; Ranasinghe et al., 2018). Besides, the reduced concentration gradient between adsorbent and adsorbate with the consumption of metal ions would also contribute to this phenomenon (Akram et al., 2017).

### **(3) Granule dosage and initial Cr(VI) concentration**

The dependence of Cr(VI) removal and total Cr sorption capacity on granule dosage was studied at different ratios of algal-bacterial AGS to liquid volume varying from 1.25 to 10 g-TS/L. During 6 h biosorption, the Cr(VI) removal rate was increased with the increase in granule dosage, while the total Cr biosorption capacity peaked (1.15 mg/g) at the dosage of 2.5 g/L (Figure 3-3c), then declined to 0.49 mg/g at the dosage of 10 g/L. The increase of Cr(VI) removal efficiency was mainly due to the availability of more surface active sites for metal ions, provided by the larger amount of algal-bacterial AGS. However, at a fixed HM concentration and liquid volume, the increase in granule dosage would result in the reduction of adsorbate to adsorbent ratio, as well as the total effective adsorbent surface area, thus leading to a lower Cr biosorption capacity (Akram et al., 2017). It is worth noting that Cr biosorption capacity was lower at the dosage of 1.25 g/L than 2.5 g/L, which might be attributable to the possible reduction of Cr(VI) into Cr(III) firstly and then the subsequent adsorption of reduced Cr(III) to algal-bacterial AGS. Although a lower granule dosage may enable a higher concentration gradient between Cr(VI) ions and adsorbate, the concentration gradient between Cr(III) ions and adsorbate may not increase proportionally, due to the limited reduction of Cr(VI) to Cr(III) by the small amount of algal-bacterial AGS. This finding suggests that a proper dosage of granules is necessary for the efficient Cr(VI) reduction and total Cr removal.

Similarly, the effect of initial Cr(VI) concentration was also studied in the range of 2.5 to 150 mg/L (Figure 3-3d). The Cr(VI) removal rate was firstly detected to decline as the Cr(VI) concentration was increased to 50 mg/L, then maintained when the Cr(VI) concentration was continuously elevated to 150 mg/L. When the initial Cr(VI) concentration > 50 mg/L, the Cr(VI) removal rate was relatively low, and over 75% of the Cr(VI) ions were remained in solution after 6 h biosorption. This observation may be attributed by the saturation of surface adsorption sites, slowing down the increase in Cr biosorption capacity. However, the total Cr biosorption capacity increased from 0.50 to 5.78 mg/g after biosorption for 6 h with the increase of initial

Cr(VI) concentration accordingly. Considering the reduction of Cr(VI) to Cr(III) by algal-bacterial AGS during the biosorption process, a higher initial Cr(VI) concentration would also facilitate Cr(VI) reduction efficiency, as almost all the active sites for Cr(VI) reduction could interact with metal ions. Consequently, more cationic Cr(III) ions would be available for the binding to negatively charged surface sites and the number of collisions between adsorbate and adsorbent may be enhanced as well (Bardestani et al., 2019). Therefore, the increasing biosorption capacity with higher initial Cr(VI) concentration could be ascribed to the elevated driving force of the concentration gradient between Cr(III) ions and algal-bacterial AGS.

In general, the optimal working conditions for adsorbents can be determined by either adsorption capacity or removal efficiency, depending on the target applications. In this study, algal-bacterial granules were designed to remediate low Cr(VI) concentration wastewater, thus Cr removal efficiency is more crucial. At an initial Cr(VI) concentration of 5 mg/L, pH 6 and granule dosage of 5 g-TS/L, over 96% and 100% of total Cr can be removed after biosorption for 12 h and 16 h, respectively. These conditions could be further adjusted according to the actual requirements to meet different demands, such as shorter contact time or higher initial metal concentrations.

### **3.3.3 Some environmental factors**

Due to the complexity of contaminated water environment and actual industrial wastewater, the effects of different background circumstances should be taken into consideration regarding the efficiency of Cr adsorption by algal-bacterial AGS in practice. In this study, the environmental conditions considered include coexisting anions and cations, NOMs, salinity and carbon sources. To make the inhibition or promotion effects of these factors more comparable, these biosorption tests were conducted at initial solution pH 6, contact time of 6 h, granule dosage of 5 g/L and initial Cr(VI) concentration of 5 mg/L, which could achieve a total Cr removal efficiency of around 80% in the previous adsorption tests.

#### **(1) Co-existing anions and cations**

Some common oxyanions, such as  $\text{NO}_3^-$ ,  $\text{H}_2\text{PO}_4^-$ ,  $\text{HPO}_4^{2-}$ ,  $\text{SO}_4^{2-}$ ,  $\text{CO}_3^{2-}$  and  $\text{HCO}_3^-$ , etc. widely found in natural waters, can act as electron acceptors and compete for the surface adsorption sites with Cr ions. Thus, they may suppress or inhibit the Cr(VI) removal process (Tan et al., 2020). On the other hand, Cr-containing industrial wastewater usually contains other HMs, like Cu, Co, Ni, Mn and Zn, and their coexistence may also have competitive effect or

even influence microorganisms' functions (Ma et al., 2019a). In this study, during the biosorption experiments, the coexisting anions  $\text{H}_2\text{PO}_4^-/\text{HPO}_4^{2-}/\text{SO}_4^{2-}/\text{Cl}^-$  and cations  $\text{Mg}^{2+}/\text{Ca}^{2+}$  in the MSM didn't affect the Cr(VI) biosorption behaviors when compared with DW conditions (data not shown). So, the effects of coexisting anions (5 or 10 mg/L) including  $\text{NO}_3^-$ ,  $\text{CO}_3^{2-}$ , and  $\text{HCO}_3^-$ , and cations (5 mg/L) including  $\text{Co}^{2+}$ ,  $\text{Cu}^{2+}$ ,  $\text{Ni}^{2+}$ ,  $\text{Mn}^{2+}$  and  $\text{Zn}^{2+}$  were further studied.

As shown in Figure 3-4a, the presence of these anions at a low concentration of 5 -15 mg/L did not affect Cr(VI) reduction or total Cr removal, indicating that Cr(VI) is a better electron acceptor than these three anions under the test conditions. As for the cations, almost no suppressive effect was found on Cr(VI) reduction under the coexistence of these cations, while noticeable improvements were obtained in the tests with Cu, Zn and Mn addition, among which Cu exhibited the strongest promotion effect. These results are consistent with the previous reports that Cu(II) could promote Cr(VI) reduction by different microbes, as it's not only an important component of some antioxidases but also the shuttle for electrons (Han et al., 2017; Ma et al., 2019a; Mala et al., 2015). However, all these five metals inhibited the removal of total Cr to some extent, indicating the competition between the foreign metal ions with Cr(III) ion for the biosorption on algal-bacterial AGS, and their inhibition effect was in a descending order of  $\text{Zn}^{2+} < \text{Cu}^{2+} < \text{Mn}^{2+} < \text{Ni}^{2+} < \text{Co}^{2+}$ .

## **(2) Natural organic matters (NOMs)**

NOMs are ubiquitous in the aquatic environment. With the complex mixture of polyfunctional organic acids, NOMs play an important role in HMs adsorption or immobilization through altering their speciation, solubility, mobility and bioavailability, or competing for the active surface sites of adsorbents (Zhao et al., 2016). In this study, humic acid and tannic acid were chosen as the model NOMs and their effects on Cr(VI) removal are shown in Figure 3-4c and d. Results show that the presence of tannic acid enhanced total Cr removal obviously from 91.5% to 97.6% over the test range of 5 - 40 mg/L. In contrast, humic acid only exhibited some slight enhancement on Cr removal at humic acid < 10 mg/L, while a higher concentration of humic acid (20 - 40 mg/L) inhibited the total Cr removal. This observation is in agreement with previous studies relating to the effects of NOMs on HMs adsorption (Liu et al., 2016; Lv et al., 2013; Wang et al., 2019). Compared to humic acid, tannic acid with a smaller molecular size and lower molecular weight may access relatively easier to the inner pores of algal-bacterial AGS (Wang et al., 2019), which exhibited better promotion effect on Cr removal. In fact, the

concentrations of NOMs in typical groundwaters (around 0.5 mg/L) or surface water (around 20 mg/L or higher) are usually at a relatively narrow range (Liu et al., 2016), therefore, the coexistence of NOMs in algal-bacterial AGS biosorption system would not be problematic.

### **(3) Salinity**

Ionic strength (IS) is one of the crucial factors that affect the equilibrium uptake of HMs by adsorbents and the IS of aqueous solution varies with salt concentration proportionally (Zhang et al., 2019). In order to evaluate the impact of salinity on Cr(VI) biosorption by algal-bacterial AGS, batch experiments were performed at various NaCl concentrations as shown in Figure 3-4e. No significant difference in Cr (VI) removal efficiency (77.6-78.3%) was noticed when NaCl concentration varied from 0 to 1 g/L, which declined dramatically when NaCl was increased to 5 g/L or higher. This observation may be ascribed to the competition between the anion ( $\text{Cl}^-$ ) and chromate anions (mainly as  $\text{HCrO}_4^-$ ) to the active sites of algae and bacteria (Aksu and Balibek, 2007). Results from this study also indicate that algal-bacterial AGS system could tolerate a relatively low salinity < 5 g/L, and a higher salinity would significantly reduce Cr (VI) biosorption capacity of algal-bacterial AGS. Thus, more attention should be paid to salinity level when applying algal-bacterial AGS into the real HM-containing wastewater treatment.

### **(4) Carbon source**

Carbon sources are not only indispensable for the growth of heterotrophic microorganisms but also paramount as electron donors contributing towards Cr(VI) bioreduction (Tan et al., 2020). However, their effects on metal ions' transport in biosorbents haven't been addressed. In this study, 7 different organics, i.e. sodium acetate, sucrose, fructose, glucose, lactic acid, succinic acid and sodium citrate were adopted as sole carbon source for Cr(VI) biosorption by algal-bacterial AGS, respectively. As shown in Figure 3-4f, algal-bacterial granules were able to reduce and adsorb Cr(VI) ions under no carbon source condition (control group), achieving about 80.4% of total Cr removal. Compared to the control, the total Cr removal efficiency was obviously improved to some extent with the coexistence of all the test carbon sources. Among them, fructose was found most effective, achieving 91.3% of total Cr removal after biosorption for 6 h, followed by glucose (90.8%), succinic acid (88.9%), lactic acid (87.7%), sucrose (85.5%), sodium acetate (84.5%) and sodium citrate (81.7%), respectively. These observations are consistent with previous studies (Huang et al., 2019b; Mishra et al., 2012; Tan et al., 2020),

demonstrating that monosaccharides like glucose and fructose are most effective for Cr(VI) reduction by bacterial species. It's worth noting that the highest Cr(VI) removal rates were achieved in the coexistence of succinic acid and citrate, reaching 100% and 90.6%, respectively, even after 3 h contacting, of which 30.6% or 38.6% were in the form of Cr(III) in solution. The remaining Cr(III) in solution could be attributed to the formation of soluble organo-Cr(III) complex with succinic acid and citrate, which is inclined to exist predominantly in solution (Huang et al., 2019b). Therefore, the selection of proper carbon source for algal-bacterial AGS system is also important in practical applications, which can be determined by the different targets of algal-bacterial AGS system, i.e. Cr(VI) decontamination or total Cr removal.

### **3.4 Summary**

The present work demonstrated Cr(VI) removal by algal-bacterial AGS in both aspects of Cr(VI) reduction and total Cr immobilization, with the highest reduction rate of 99.3% achieved at the pH 2 after 6 h, but optimum pH for total Cr immobilization rate (89.1%) was pH 6. Co-existing oxyanions exhibited slight effects on Cr(VI) removal, while cations, NOMs and carbon sources all promoted the Cr(VI) reduction rate. However, the removal of total Cr was suppressed at different extents due to the existing of competitive cations or the formation of organo-Cr(III) complex between Cr(III) and organics. Changes of ionic strength exhibited significant inhibition to both Cr(VI) reduction and total Cr removal. Collectively, the results obtained provide useful information on Cr(VI) removal under a wide range of environmental conditions, which may find application on the remediation of Cr(VI) contaminated water and soil.



Table 3-1 Experimental design and test conditions for Cr(VI) biosorption by algal-bacterial AGS.

No.	Concerned parameters		Other operational conditions
	Concerned parameter	Test range and substance(s)	
1	Initial pH	2, 4, 5, 6, 7, 8, 9	<ul style="list-style-type: none"> <li>○ Contact time = 6 h,</li> <li>○ Granule dosage = 5 g-TS/L,</li> <li>○ Initial Cr(VI) = 5 mg/L</li> </ul> (if they were not the concerned parameters in the tests), and <ul style="list-style-type: none"> <li>○ MSM = 10 mL if it was not specified.</li> </ul>
2	Contact time	0.5, 1, 2, 3, 4, 6, 8, 10, 12 (h)*	
3	Granule dosage	1.25, 2.5, 5, 7.5, 10 (g-TS/L)	
4	Initial Cr(VI) concentration	2.5, 5, 10, 20, 50, 100, 150 (mg/L)	
5	Coexisting ions	Initial concentration of anion ( $\text{NO}_3^-$ , $\text{CO}_3^{2-}$ or $\text{HCO}_3^-$ ) = 5 and 15 mg/L Initial concentration of cation ( $\text{Co}^{2+}$ , $\text{Cu}^{2+}$ , $\text{Mn}^{2+}$ , $\text{Ni}^{2+}$ or $\text{Zn}^{2+}$ ) = 5 mg/L	
6	NOM	Initial humic acid or tannic acid = 0, 5, 10, 20 and 40 mg/L	
7	Salinity	NaCl: 0, 0.5, 1, 5, 10, 20 or 40 g/L	
8	Carbon sources	Glucose, sucrose, sodium acetate, sodium citrate, or carbon-free sources: 10 mM	

\* MSM =100 mL. NOM, natural organic matters; MSM, mineral salt medium; TS, total solids.

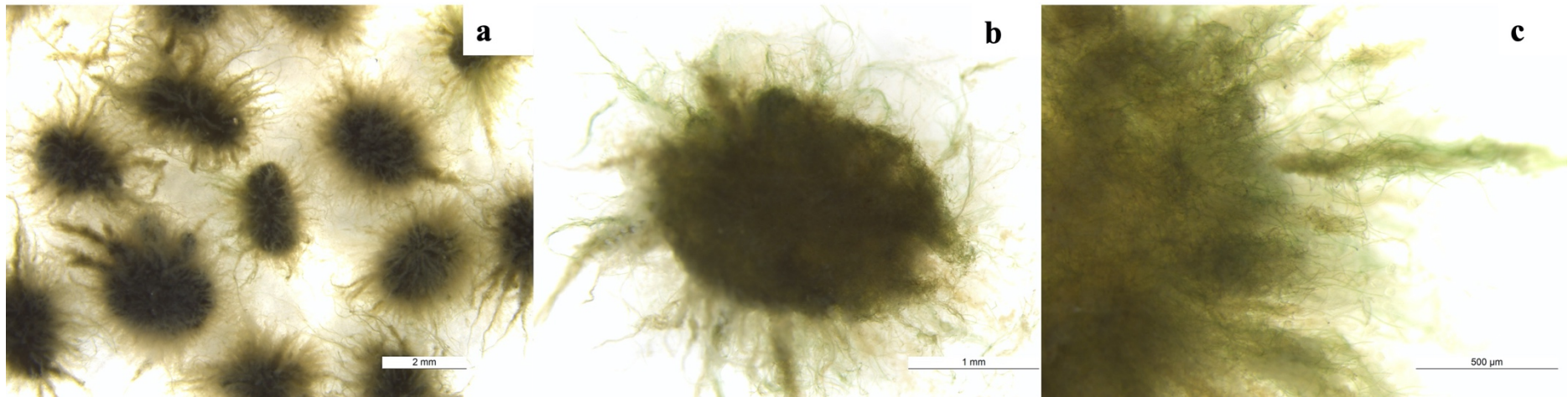


Figure 3-1 Images of algal-bacterial AGS from surface (a) or cross section (b and c), respectively.

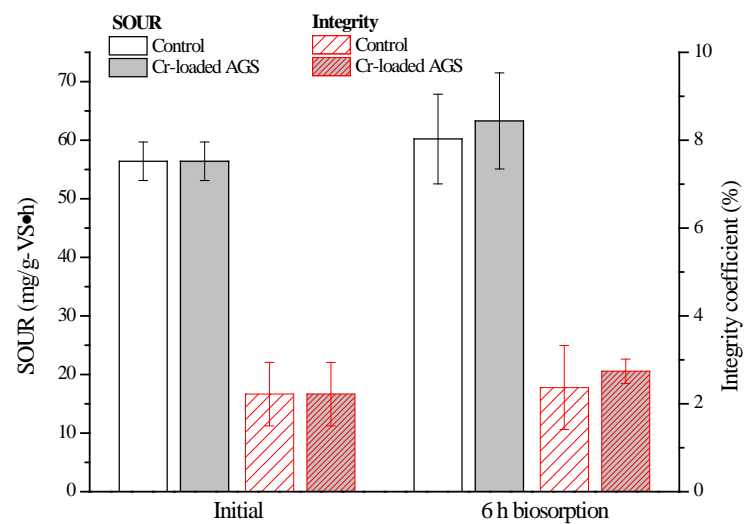


Figure 3-2 Granular SOUR and stability of algal-bacterial AGS after biosorption (contact time, 0, 3 or 6 h; initial pH, 6; granule dosage, 5 g-TS/L, Cr(VI), 5 mg/L)

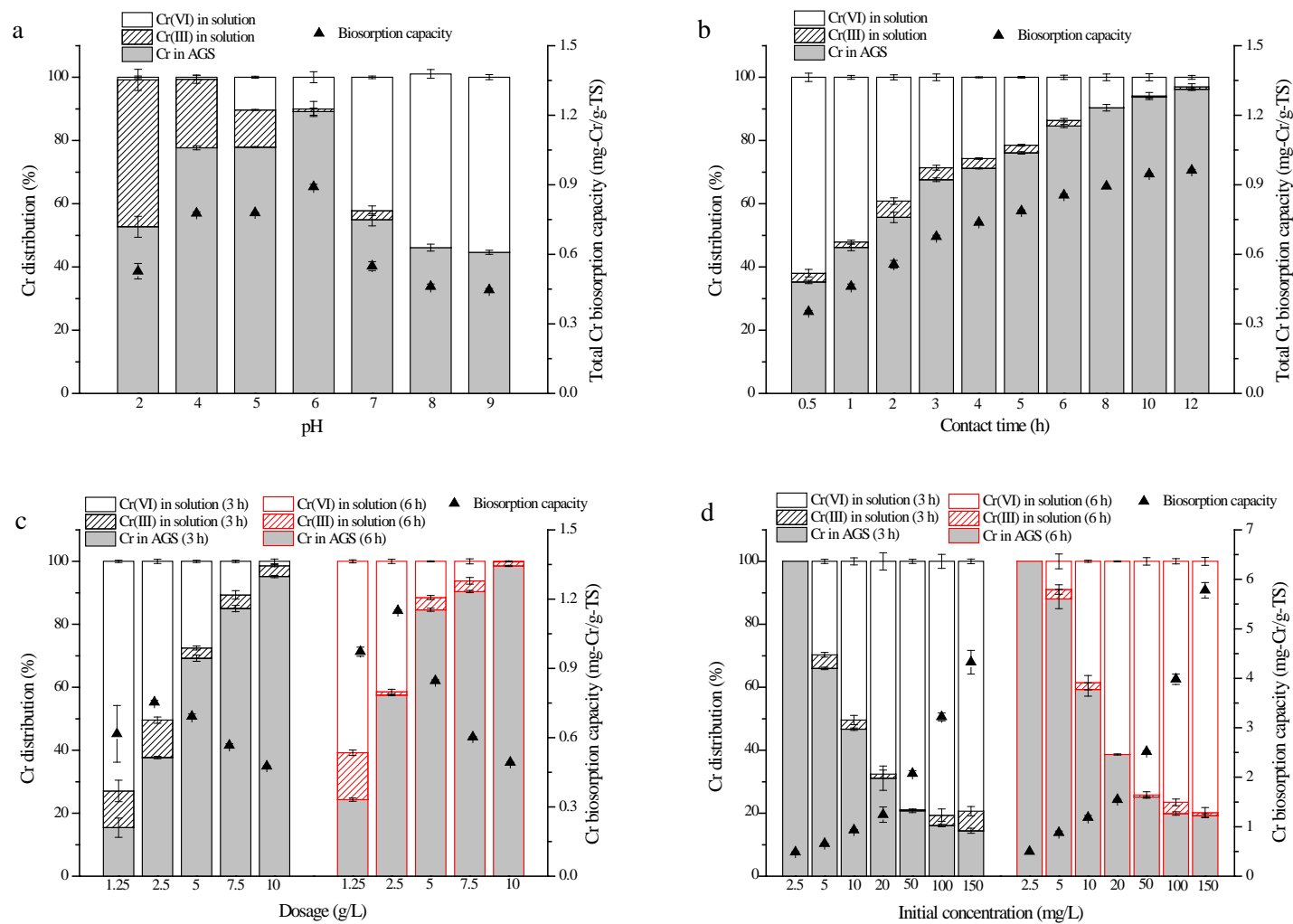


Figure 3-3 Effects of different operation parameters including (a) initial pH, (b) contact time, (c) granule dosage, and (d) initial Cr(VI) concentration on Cr distribution in solution and algal-bacterial AGS.

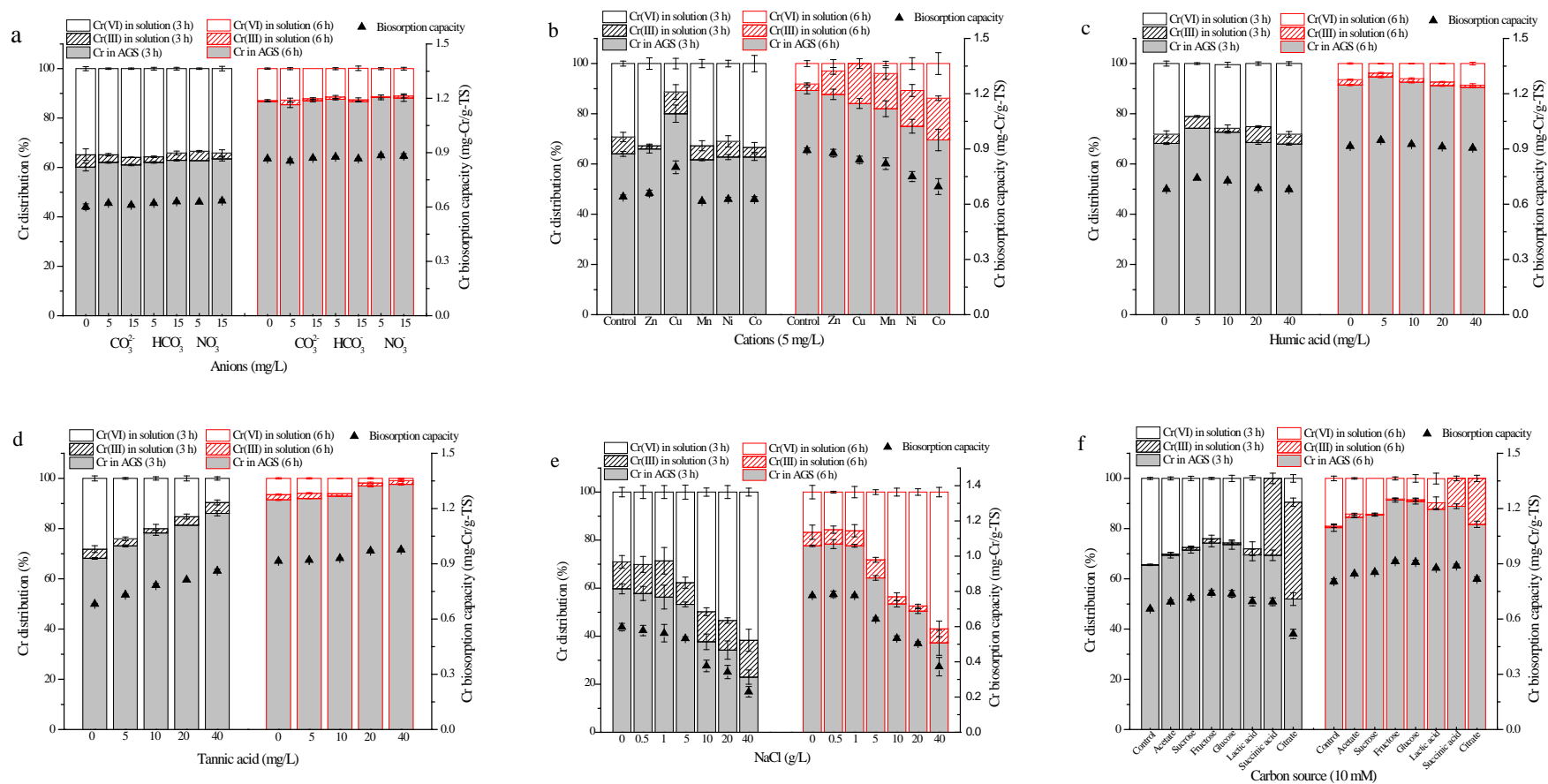


Figure 3-4 Effects of environmental conditions on Cr distribution in solution and algal-bacterial AGS: (a) coexisting anions, (b) coexisting cations, (c) humic acid, (d) tannic acid, (e) salinity, and (f) different carbon sources.

## Chapter 4 Mechanisms of Cr(VI) removal by algal-bacterial AGS

### 4.1 Background

According to the results from Chapters 2 and 3, algal-bacterial AGS has been proven to be an efficient biosorbent for Cr(VI) removal under a wide range of environmental conditions. However, the potential mechanisms involved in the Cr(VI) removal process by algal-bacterial AGS are still unclear. As reported, the mechanisms of biosorption process can be classified into metabolism dependent and non-metabolism dependent ones according to the usage of active or inactive biomass, respectively (Saravanan et al., 2017). When inactive biomass consisting of dead or inactive cells are used for Cr(VI) removal, the process could be described as non-metabolism dependent, in which physio-chemical interaction happens between the solid part of biosorbent and metal ions in the liquid part (Wang et al., 2018). On the other hand, metabolism dependent biosorption process is resulted from active metabolic process of the living cells and strongly supported by microbial viability (Jobby et al., 2018). The physio-chemical interactions still happen when microorganisms are alive, and metal ions could be adhered on the surface of the cells due to the existing of various functional groups. Moreover, Cr(VI) ions could be further reduced to Cr(III) or accumulated in cells through a metabolically active process which is operated by respiration energy in living organisms (Jobby et al., 2018).

Besides, the disposal of HMs containing sludge is problematic due to the characteristic of Cr that it's non-biodegradable and tends to bioaccumulate (Nair et al., 2008). Improper discharge would affect the soil and water quality as well as human and animal health. On the one hand, desorption is an important post adsorption method to recover adsorbates as well as regenerate adsorbents. Considering that the active algal-bacterial AGS could maintain its microbial activity after 6 h Cr(VI) removal process with over 80% total Cr removed from solution at an initial Cr(VI) concentration of 5 mg/L (results from chapter 3), there would be great promise to reuse algal-bacterial AGS after the biosorption processes. On the other hand, when considering the reutilization of Cr-loaded algal-bacterial AGS with Cr loading, either for wastewater treatment or nutrients recovery, it's essential to assess the leaching risk of chromium.

Therefore, the objectives of this chapter are to (1) investigate the effect of cell viability on Cr(VI) removal and (2) analyze the distribution and chemical fraction of the loaded Cr in algal-bacterial AGS. The findings from this study are expected to provide a promising approach for Cr(VI) reduction and total Cr removal by algal-bacterial AGS, which may have great potential in practical application on Cr(VI)-contaminated wastewater or soil remediation.

## **4.2 Materials and methods**

### **4.2.1 Cultivation of bacterial AGS and algal-bacterial AGS**

For AGS cultivation, two cylindrical SBR made of acrylic plastic with working volume of 1.16 L were used with or without illumination (24 h, 3,000 lux) under a constant room temperature ( $25 \pm 2$  °C). 6 cycles per day with each cycle of 4 h ((about 1 min influent feeding, 60 min of non-aeration, 176 min of aeration, 2 min of settling and 1 min of effluent withdrawal). During the aeration stage, air was introduced through air bubble diffusers from the bottom of reactor at an air flow rate of 4 L/min. In both reactors, mature bacterial AGS was used as inoculum and feed with synthetic domestic wastewater with the main characters as following: 300 mg COD/L, 30 mg  $\text{NH}_4^+$ -N/L, and 5 mg  $\text{PO}_4^{3-}$ -P/L. Mature algal-bacterial AGS was obtained after 30 days with illumination supplication and the Chl-a content was detected at around 3.8 mg/g-VS.

### **4.2.2 Cr(VI) biosorption and desorption experiments**

Cr(VI) biosorption experiments were performed in 250 mL shaking flasks containing 100 mL MSM to support the microbe growth and maintain the solution pH. Granules used for biosorption experiments were collected from the reactors at the end of aeration stage with size range from 1.0 to 2.0 mm. The batch experiments were performed to investigate the Cr(VI) removal efficiency by AGS with the initial Cr(VI) concentrations of 5 mg/L and the granule dosage of 5 g-dry weight/L (dry weight) in a rotary shaker at 125 rpm and room temperature of 25 °C. The pH for all the biosorption experiments was 6.

To explore the roles of algae and bacteria in algal-bacterial AGS during Cr(VI) removal process three types of cell treatment were carried out to inhibit cell viability: 1) autoclaving at

121 °C for 15 min, to inactivate both bacteria and algae; 2) addition of antibiotic, 258 mg/L levofloxacin (LVX) to inhibit the activity of bacteria (Hao et al., 2018); 3) addition of metabolic inhibitor, 10 mM sodium azide (NaN<sub>3</sub>) to suppress the respiratory activity (Cabrol et al., 2017). Besides, 10 mM glucose was added as additional electron donor to promote the efficiency of Cr(VI) bioreduction (Das et al., 2014). The Cr(VI) biosorption conditions for each trial were: 5 mg/L Cr(VI), 1 g-wet weight granule/10 ml MSM, pH 6 and contact time of 6 h.

After the biosorption experiments, batch desorption trials were carried out to investigate whether Cr(VI) biosorption by algal-bacterial AGS is reversible or not. Before the desorption trials, Cr-loaded algal-bacterial AGS were obtained after 16 h biosorption with initial Cr(VI) concentration of 5 mg/L, then rinsed gently with DW for 3 times (no Cr was detected in the rinsing water). The desorption efficiencies of 6 desorption agents (0.1 M) including KCl, NaHCO<sub>3</sub>, Na<sub>2</sub>CO<sub>3</sub>, NaOH, HCl and H<sub>2</sub>SO<sub>4</sub> were assessed and compared, and the desorption effect in relation to H<sub>2</sub>SO<sub>4</sub> concentration (ranged from 0.025 to 0.4 M) was further investigated.

#### **4.2.3 Extracellular polymeric substance (EPS) extraction and chemical fractionation**

The extraction of loosely bound EPS (LB-EPS) and tightly bound EPS (TB-EPS) from algal-bacterial AGS was conducted according to a previous study (Zhao et al., 2018) with some modifications. Briefly, algal-bacterial AGS sample was firstly homogenized in a glass homogenizer, then 5 ml mixture was centrifuged at 8000 rpm and 4 °C for 15 min. After the supernatant being collected for LB-EPS fraction measurement, the residue was resuspended with 0.9% (w/v) NaCl to the original volume of 5 mL and then heated at 80 °C for 0.5 h. After cooling, the mixture was centrifuged again at 8000 rpm and 4 °C for 15 min, then the supernatant was collected for TB-EPS fraction measurement. Additionally, supernatant of Cr(VI) removal system was collected for the detection of soluble microbial products (SMP) content. Before determination, all the supernatants were filtrated through 0.22 µm membrane after collection. A detailed schematic diagram is outlined in Figure 4-1.

The distribution and chemical fractionation of Cr in algal-bacterial AGS after 16 h biosorption was analyzed as shown in Figure 4-1. After EPS extraction, Cr distributed in LB-EPS, TB-EPS or residue was quantified by detecting the total Cr content in each part. Intra or



extra cellular Cr was determined by adding 10% HCl to the ground mixture of AGS. After centrifugation, metal content in the supernatant or residual part was termed as extracellular or intracellular metal, respectively (Cai et al., 2018). As for the determination of chemical fractionation, Tessier et al. extraction procedures (Tessier et al., 1979) with some modifications were used in this study. This method was designed to separate the metals in algal-bacterial AGS into six fractions including: (1) F1, water soluble, (2) F2, exchangeable, (3) F3, carbonate bound, (4) F4, Fe/Mn oxides bound, (5) F5, organic bound, and (6) F6, residual fraction. This fractionation method has been proven to be reliable by several previous studies (Asensio et al., 2013; Wu et al., 2020; Yao et al., 2009).

Before chemical fractionation, Cr-loaded algal-bacterial AGS was firstly dried at  $(105\pm 2)$  °C for 24 h, then ground into powder. The metals fractionation was carried out according to the following sequential extraction procedures: (1) F1: 0.1 g (dry weight) sample was used to extract with 4 ml of DW at room temperature ( $25\pm 2$  °C) for 1 h under continuously shaking (water soluble). (2) F2: the residue from F1 was extracted with 4 ml 1 M  $\text{NH}_4\text{OAc}$ , at pH 7 and room temperature for 2 h under continuously shaking (exchangeable). (3) F3: the residue from F2 was leached with 4 ml 1 M  $\text{NH}_4\text{OAc}$  at pH 5 (pH adjusted with acetic acid) and room temperature for 2 h under continuously shaking (carbonate bound). (4) F4: the residue from F3 was extracted with 4 ml of 0.04 M hydroxylamine hydrochloride ( $\text{NH}_2\text{OH}\cdot\text{HCl}$ ) in 25% acetic acid (v/v) at pH 3 and 80 °C for 6 h under occasionally shaking (Fe/Mn oxide bound). (5) F5: The residue from F4 was extracted at 80 °C with 3 ml 30%  $\text{H}_2\text{O}_2$  (pH was adjusted to 2 with  $\text{HNO}_3$ ) for 5.5 h, occasional shaking. 1 ml of 3.2 M  $\text{NH}_4\text{OAc}$  in 20% (v/v)  $\text{HNO}_3$  was added when the sample was cooled down and DW was added to reach a final volume of 4 ml, continuous shaking at room temperature for 0.5 h (organic bound). (6) F6: The residue from the F5 was digested at 120 °C with  $\text{HNO}_3$  and  $\text{H}_2\text{SO}_4$  for 12 h, occasionally shaking (residual).

After each extraction step, the samples were centrifuged at 10000 rpm for 15 min. The resultant supernatants were removed for metal concentration determination, and the residues were washed with 4 mL DW, then centrifuged again. The amount of metals in rinsing water was added to the earlier step before washing. The metal mobility was indicated as mobility factor ( $\text{MF}(\%) = 100 \times (\text{F1} + \text{F2} + \text{F3}) / (\text{F4} + \text{F5} + \text{F6})$ ).

#### **4.2.4 Analytical methods**

Before metal ion detection, all the supernatant samples were filtered through 0.22  $\mu\text{m}$  membrane. The residual samples were digested with  $\text{HNO}_3$  and  $\text{H}_2\text{O}_2$  at 100  $^\circ\text{C}$  until the liquid became colorless and transparent, then filtered through 0.22  $\mu\text{m}$  membrane. The concentration of Cr(VI) was quantified by the spectrophotometric method using a UV–Visible spectrophotometer at 540 nm (UV 1800, Shimadzu, Japan) with 1,5-diphenyl-carbazide complexation in acidic medium. The concentrations of total Cr, Ca, Mg, and Fe in filtrates or those from residue samples were measured using ICPS-8100 (Shimadzu, Japan). Cr(III) concentration was obtained by subtracting Cr(VI) concentration from the total Cr concentration. Cr(VI) in Cr-loaded algal-bacterial AGS was extracted by alkaline extraction without Cr(III) oxidation. The ground granules were mixed with alkaline solution (0.5 M NaOH and 0.28 M  $\text{Na}_2\text{CO}_3$ ) and 1 mol/L  $\text{MgCl}_2$  was added to prevent Cr(III) oxidation (James et al., 1995; Novotnik et al., 2012), then heated at 90  $^\circ\text{C}$  for 60 min.

The contents of polysaccharides (PS) and proteins (PN) in the extracted EPS samples were determined by phenol-sulfuric acid method (glucose as standard) (DuBois et al., 1956) and Lowry-Folin method (bovine serum albumin as standard), respectively (Lowry et al., 1951). Duplicate experiments and triplicate determinations were conducted in this study, and all the results were expressed as mean or mean  $\pm$  SD.

### **4.3 Results and discussion**

#### **4.3.1 Effect of cell viability and additional electron donor on Cr(VI) removal**

Cr(VI) removal capacity by algal-bacterial AGS was evaluated at an initial Cr(VI) concentration of 5 mg/L under pH 6, which has been confirmed as the optimal pH in Chapter 2. As shown in Figure 4-2a, 62.8% or 85.1% of total Cr was removed from solution after 3 or 6 h, respectively, with negligible Cr(III) left in supernatant. Considering that the fresh algal-bacterial AGS discharged from the reactors was used for these Cr(VI) biosorption tests, the change of granular microbial activity during the treatment should be paid more attention. On the other hand, algal-bacterial AGS is a symbiosis system of bacteria and microalgae; up to now,

however, no report could be found to address their specific contribution to the Cr(VI) biosorption process. Therefore, in this study, autoclave sterilization was applied to completely inactivate the microorganisms in algal-bacterial AGS that was then examined whether simple chemical reaction (non-metabolism dependent) or/and metabolism of the cells (metabolism dependent) were involved in the Cr (VI) biosorption process. In addition, partial inactivation was also performed via inhibitors addition. LVX was used in this study, which is a fluoroquinolone antimicrobial agent with rapid bactericidal activity and can directly inhibit bacterial DNA synthesis (Noel et al., 2009). Thus, the contribution of algae to Cr(VI) biosorption by algal-bacterial AGS could be distinguished with specific bacterial inhibition through LVX addition. As known, sodium azide ( $\text{NaN}_3$ ) is widely used as a strong metabolic inhibitor of the respiratory activity (Cabrol et al., 2017). In this study, the involvement of the metal respiratory (Mtr) pathway in Cr(VI) biosorption by algal-bacterial AGS was explored with  $\text{NaN}_3$  addition. Moreover, additional electron donor (glucose) was added to assist the function of chromate reductase in this study.

As shown in Figure 4-2b, a dramatic decline in total Cr(VI) removal was noticed in the control tests with autoclaved algal-bacterial AGS (29.6%) in comparison with the active one (85.1%), which was same as Cr(VI) reduction (44.0% for inactivated vs. 86.7% for active algal-bacterial AGS). The Cr(VI) removal capacity of the inactivated algal-bacterial AGS could be ascribed to the complexation and reduction of Cr(VI) with the denatured organic matter from the granular biomass. With the additional inhibitor of LVX or  $\text{NaN}_3$ , some slight enhancement was observed, probably attributable to the non-viability related promotion effect by these two inhibitors. Clearly seen, the electron donor (glucose) showed no effect on the inactivated AGS, which could significantly promote the total Cr removal efficiency by the active AGS, from 70.6% to 80.9% for bacterial AGS and from 85.1% to 93.8% for algal-bacterial AGS, respectively. This observation suggests the existence of enzyme-mediate Cr(VI) reduction by the AGS (Han et al., 2017a). It could be inferred that in addition to the non-metabolism dependent physiochemical interactions, the metabolism dependent biosorption resulted from active metabolic process in the living cells (Jobby et al., 2018) dominated the Cr(VI) removal by algal-bacterial AGS.

Comparison was conducted between algal-bacterial AGS and bacterial AGS in the batch experiments (Figures 4-2a and c). After 6 h biosorption, 11.2% decrease in total Cr removal by bacterial AGS was detected after LVX addition compared to the control, in which interestingly, less suppression was noted on Cr(VI) reduction with partial Cr ions remaining in the form of Cr(III) in the solution. On the other hand, an opposite effect of LVX was observed on algal-bacterial AGS, increasing by 3.0% total Cr removal and 7.4% Cr(VI) reduction. The decreased total Cr removal efficiency by bacterial AGS was mainly associated with the inhibited microbial activity of bacteria exposed to antibiotic, which showed negligible impact to microalgae. As reported, nutrients removal efficiency and microbial activity of activated sludge can be dramatically inhibited by LVX in the early stage while recovered later (Hao et al., 2018), which seemed to also occur in the case of bacterial AGS in this study: the total Cr removal was inhibited by 15.7% after 3 h, but the inhibition rate decreased to 11.2% after 6 h exposure to LVX (Figure 4-2c). More importantly, the resistance of algal-bacterial AGS to LVX highlighted its pivotal role in the Cr(VI) biosorption process, suggesting the great potential of algal-bacterial AGS in the treatment of antibiotic-contaminated wastewater.

Regarding the effect of  $\text{NaN}_3$ , the total Cr removal by bacterial AGS was firstly inhibited by 5% after 3 h and then by 7% after 6 h exposure to  $\text{NaN}_3$  (Figures 4-2c), with similar or even higher Cr(VI) reduction rate. In contrast, a continuous promotion trend was noted in the case of algal-bacterial AGS. It's deduced that both bacteria and algae could maintain their Cr(VI) removal capacity with the inhibition of Mtr pathway, suggesting that Mtr pathway might not be the main reduction pathway involved in the Cr(VI) biosorption by algal-bacterial AGS. Besides being reduced via Mtr pathway, which mainly occurs extracellularly (Huang et al., 2019), Cr(VI) could also be transported into cells through the sulfate transport protein and reduced by specific reductase intracellularly (Han et al., 2017b). Results from intra-/extra-cellular distribution of the loaded Cr in algal-bacterial AGS showed that around 69.2% of Cr was intracellularly accumulated (Fig. 5c). This observation ascertains the important role of intracellular Cr(VI) reduction for Cr(VI) biosorption by algal-bacterial AGS.

Therefore, it could be implied that bioactivity of microbes and participation of algae are the principal contributors to the efficient Cr(VI) biosorption by algal-bacterial AGS, which was

mainly mediated by intracellular pathways under the test conditions.

#### **4.3.2 Variations in EPS and SMP during Cr(VI) biosorption**

The above results suggested the importance of microbial activity to the Cr(VI) biosorption by algal-bacterial AGS. It's noteworthy that some changes of microbial metabolism may occur in active microorganisms when exposed to the toxic Cr(VI) solution. Thus, the variation in production and composition of the important metabolic products, EPS and SMP, was measured to reveal the response of algal-bacterial AGS to Cr(VI) exposure. As shown in Figure 4-3, a higher total EPS content was detected in algal-bacterial AGS during the Cr(VI) biosorption process than that in the control (no Cr(VI) exposure), mainly attributable to the increased LB-EPS content which was increased by 28.1%, 31.1% and 6.4% respectively after 1, 3 or 16 h exposure to Cr(VI) solution. However, less variations were noticed in TB-EPS content and the PN/PS ratio.

Compared to EPS, the SMP content was noticed to change obviously, reaching the highest value of  $4.8 \pm 0.5$  mg/g-VS after 16 h exposure to Cr(VI), which was 140% higher than that of the control. As for the PN/PS ratio in SMP, it was approximately similar after 1 h contact between the two test groups (with or without Cr(VI) exposure). While a dramatic elevation in PN/PS ratio was observed in the algal-bacterial AGS after 3 h Cr(VI) exposure, which was  $3.8 \pm 0.4$  in comparison to  $1.4 \pm 0.1$  for the control. While the difference in PN/PS ratio became smaller when the contact time extended to 16 h (2.1 vs. 1.3, with or without Cr(VI) exposure), indicating that some cell lysis may occur during the treatment of Cr(VI)-containing wastewater, which released more proteins under a short-time exposure to Cr(VI).

EPS in AGS are believed to play a key role in the maintenance of stable granular structure, pollutants removal and protection of microbial cells from heavy metal stress (Lin et al., 2020). Interactions of heavy metal with EPS in AGS can increase its tolerance to toxicity and capability to adapt to the hostile environments (Wang et al., 2014). As seen from Figure 4-3b, the increased secretion of LB-EPS with almost no variation in PN/PS ratio when espoused to Cr(VI) was mainly due to the protective response of bacteria and algae in algal-bacterial AGS against the stress of Cr(VI), resulting in higher amount of EPS surrounding the cells, which may

contribute to the complexation of chromium ions (Hou et al., 2013; Wang et al., 2014). When the Cr(VI) concentration in solution became lower over time (no Cr(VI) was detectable after 16 h), the difference in LB-EPS content of algal-bacterial AGS between Cr(VI) exposure and no exposure was reduced from 31.1% (3 h) to 6.4% (16 h). On the other hand, the ascending content and elevated PN/PS ratio of SMP over time might also be ascribed to the secretion of soluble extracellular active reductase or reductants by the bacterial or algal cells under the stress of Cr(VI), which was previously accumulated in algal-bacterial AGS (Das et al., 2014; Tan et al., 2020).

The above results are consistent with previous studies. As reported, more EPS were produced by a chromium tolerant strain *E. cloacae* when Cr(VI) concentration was elevated, and the EPS extracted from this strain was able to reduce 31.7% of Cr(VI) at an initial concentration of 10 mg/L (Harish et al., 2012). Results from Das et al. (2014) showed that the proteins released by a chromium tolerant strain *B. amyloliquefaciens* increased over time in the presence of Cr(VI). Wang et al. (2014) claimed that the production of both LB-EPS and TB-EPS by AGS were increased with the increase of Cr(VI) concentration from 0 to 30 mg/L, especially LB-EPS. In the case of Cu(II) removal by *S. meliloti* CCNWSX0020, Hou et al. (2013) also found that LB-EPS was the major component for Cu(II) immobilization and may act as a microbial protective barrier against heavy metal stress.

#### **4.3.3 Desorption of Cr from Cr-loaded algal-bacterial AGS**

Desorption is an important posttreatment step to recover adsorbates as well as regenerate adsorbents. In order to assess the reusability of algal-bacterial AGS, different desorption reagents were adopted as shown in Figure 4-4a. The highest desorption ratio (33.5%) was achieved by 0.1 M H<sub>2</sub>SO<sub>4</sub> solution, followed by HCl, NaOH, NaCO<sub>3</sub>, DW, KCl and NaHCO<sub>3</sub>. It could be concluded that strong acids and alkalis were better desorption reagents than mild alkaline, neutral salt or DW for Cr desorption from Cr-loaded algal-bacterial AGS under the test conditions in this study, in which 0.1 M H<sub>2</sub>SO<sub>4</sub> was found to have the best desorption performance. However, when H<sub>2</sub>SO<sub>4</sub> concentration was further increased, no obvious increment in desorption ratio could be noticed. In fact, this desorption ratio was approximate to its highest

value, because only around 30.8% of loaded Cr was extracellularly distributed in the algal-bacterial AGS, and the other 69.2% loaded Cr was intracellularly accumulated (Figure 4-5c). Considering that microbial cells were well protected in algal-bacterial AGS from the hostile compounds due to the overproduced EPS surrounding the AGS and its compact granular structure, the intracellular Cr was difficult to be released from cells without destroying the cellular structure. This observation suggests that the loaded Cr in algal-bacterial AGS is not able to be desorbed by using the desorption agents tested in this study, indicating the low environmental risk of heavy metal release from algal-bacterial AGS during Cr(VI)-containing wastewater treatment. The possibility of Cr resource recovery from Cr-loaded algal-bacterial AGS needs further in-depth research.

#### **4.3.4 Distribution and chemical fractionation of Cr in Cr-loaded algal-bacterial AGS**

According to the above results, when considering the reutilization of algal-bacterial AGS after Cr(VI) biosorption process, either for wastewater treatment or resources recovery, it's essential to assess the leaching risk of chromium. In this study, the distribution and chemical fractionation of Cr loaded onto the algal-bacterial AGS were analyzed.

As the first barrier for metal ions to attack microbial cells, EPS are regarded to be able to bound heavy metals and protect microorganisms from the harsh environment (Liu et al., 2015; Mohite et al., 2018). As shown in Figure 4-5a, with the progress of Cr(VI) biosorption, the amount of Cr trapped in algal-bacterial AGS gradually increased to the highest Cr content of 0.98 mg/g-TS, meaning that almost 98% of the added Cr(VI) into the system was accumulated in the granules after 16 h contact. As for the distribution of Cr loaded onto the algal-bacterial AGS, 7.5% and 9.8% were LB- or TB-EPS bounded, respectively, suggesting that around 17.3% out of 30.8% extracellularly accumulated Cr in algal-bacterial AGS was trapped by EPS. This result to a great extent confirmed the result in section 3.4 that the highest desorption efficiency was achieved by H<sub>2</sub>SO<sub>4</sub> solution, as the desorption of metal ions from EPS is favorable under acidic conditions (Liu et al., 2015). Additionally, around 79.2% of the loaded Cr was accumulated in the residual part, as approximately 69.2% of total loaded Cr was intracellularly accumulated, which was difficult to be released under the test acid or alkaline conditions.

However, the risk of this part of Cr should be further analyzed to assess the potential environmental impacts.

In this study, the Tessier et al. (1979) scheme which has been widely employed for metal fractionation was adopted for the chemical fractionation of loaded Cr and other main metals contained in algal-bacterial AGS. Among the six fractions, F1-F3 fractions are considered as mobile forms, which are readily available to biota or leached into environment; the F4-F5 fractions are relatively stable and not bioavailable unless extreme situations; and F6, the residual fraction is not expected to be released under natural conditions over a short time (Nair et al., 2008). Figure 4-5b illustrates the distribution and fractionation of the major metals in Cr-loaded algal-bacterial AGS. As seen, around 61.7% and 4.9% of Cr were respectively bound with organic matters (F5) and in residual fraction (F6), and the MF value of Cr (proportion of the sum of F1, F2 and F3 to the sum of F4, F5 and F6) was 9.5%. In the case of Fe, the MF value (5.4%) was even lower even though it had the largest residual fraction of 35.4%. However, the situation for light metals were totally different, with the MF values as high as 91.0% or 72.7% for Mg and Ca, respectively, which might be helpful for maintaining the high bioactivities of algal-bacterial AGS.

#### **4.3.4 Mechanisms hypothesis**

From the results from Chapters 2, 3 and 4, two possible pathways are proposed for the removal of Cr(VI) from wastewater by algal-bacterial AGS: (1) Cr(VI) is firstly reduced to Cr(III) and then transported and interacted with algal-bacterial AGS through electrostatic attraction or surface complexation under the test conditions; and (2) Cr(VI) ions are actively uptaken by microbial cells and then transported and accumulated in the cells (Figure 4-6).

The first pathway can be evidenced by the following results:

(1) No Cr(VI) could be extracted from the Cr-loaded algal-bacterial AGS, indicating the complete reduction of Cr(VI) into Cr(III). Still, where the Cr(VI) reduction occurs, in solution, on granule surface or inside the granule, needs further investigation.

(2) Cr(VI) reduction efficiency was enhanced with the solution pH decreased from 6 to 2 (Figure 3-3a), suggesting acid condition favors Cr(VI) bioreduction. On the other hand, a higher



proportion of Cr(III) remaining in solution could be explained by the stronger competition between  $H^+$  and  $Cr^{3+}$  at a lower solution pH, indicating that Cr(III) cation rather than Cr(VI) anion determines the total Cr removal by algal-bacterial AGS, and to some extent microbial activity may also contribute to its high total Cr removal efficiency.

(3) All the five additional metal ions inhibited the removal of total Cr to a certain extent (Figure 3-4b). More clearly, despite Cu(II) exhibited the strongest promotion effect on Cr(VI) reduction, the total Cr removal was still declined, implying that the coexistence of these cations would compete with Cr(III) ions, which is responsible for the reduction of total Cr removal.

(4) Cr(VI) reduction could be enhanced effectively with the addition of carbon source, but the total Cr removal efficiency didn't increase accordingly when the access of Cr(III) to algal-bacterial AGS is weakened due to the formation of soluble organo-Cr(III) complex (Figure 3-4f). This observation indicates that the existing form of Cr(III) ions is also crucial for its accumulation in the algal-bacterial AGS. Moreover, albeit organic compounds as electron donors have been previously reported to facilitate Cr(VI) reduction, in which the reaction with organic matter alone is very slow (from months to years) and catalyzers like transition metal ions or enzymes are necessary for the acceleration (Li et al., 2014). In this study, the promotion effect of these carbon sources is supposed to be mediated by microbial enzymes, as the active algal-bacterial AGS possessed similar microbial activity before and after Cr(VI) biosorption (Figure 3-2).

The second pathway is mainly evidenced by the results of intra- and extra-cellular Cr distribution in the Cr-loaded algal-bacterial AGS, around 69.2% of Cr being intracellular part. This observation suggests that cell transport and accumulation is an important mechanism for the total Cr removal by algal-bacterial AGS. Based on this hypothesis, cell viability is crucial during this biosorption process. As shown in Figure 3-2, the microbial activity of algal-bacterial AGS indicated by SOUR can be maintained after biosorption for 6 h. On the other hand, the intracellular Cr could be located either on cell membrane or cytoplasm (Li et al., 2019; Ma et al., 2019a; Tan et al., 2020), depending on the different reduction pathways. For example, Cr(VI) anions ( $CrO_4^{2-}$ ), which resemble with sulfate ion ( $SO_4^{2-}$ ), are prone to cross cell membrane via the sulfate pathway and reduced to Cr(III) by either intracellular or membrane-associated

reductase, then localize in the cytoplasm or cell membrane, respectively (Thatoi et al., 2014; Baldiris et al., 2018 ). Besides, Cr(VI) can be also reduced by extracellular reductase or reductants secreted by active cells and form organic-Cr(III) complex, which is unable to permeate cell membranes, thus remaining extracellularly through surface complexation (Zhu et al., 2019).

It's noteworthy that the immobilized Cr in algal-bacterial AGS after a short time contact with Cr(VI) was mainly in the non-mobile forms which would emphasize a promising application for further utilization of Cr-loaded algal-bacterial AGS. However, despite the fact that Fe/Mn oxides or organic bound fractions are relatively stable, transformation into mobile forms may also happen under certain conditions, such strongly acidic or oxidizing conditions (Nair et al., 2008). More efforts are needed to reduce the MF value and promote the alteration of other fractions into the residual part. Besides to the mobility, distribution of metals in different chemical fractions also reflected the different biosorption mechanisms such as ion exchange, chemical precipitation, and complexation process by algal-bacterial AGS (Yao et al., 2009). The largest fraction of organic-bound for Cr indicating that metal complexation was the dominant mechanism underlying Cr(VI) removal. Similar results have been reported by Yao et al. regarding the Cr(III) biosorption by bacterial AGS. Moreover, the extremely low proportions (<2%) of exchangeable and carbonates bound fractions, suggesting that ion exchange and chemical precipitation appeared only to have minor role in the overall biosorption process. Interestingly, exchangeable fraction was the largest for both Mg and Ca, which was in agree with previous reports that Mg and Ca ions were frequently detected to be released from biosorbents during heavy metal adsorption (Gao et al., 2019). Therefore, it can be concluded that algal-bacterial AGS is a promising and safe biomaterial for hazardous HMs immobilization and cell viability was essential for Cr(VI) removal.

#### **4.4 Summary**

In Chapter 4, responses of algal-bacterial AGS to Cr(VI) exposure were intensively studied in both aspects of Cr(VI) elimination and microbial metabolic alteration. On the one hand, 85.1% of the total added Cr could be removed from solution by algal-bacterial AGS after 6 h contact

under pH 6 at an initial Cr(VI) concentration of 5 mg/L. Microbial viability and participation of algae were crucial for Cr(VI) removal by algal-bacterial AGS, which was mainly mediated by intracellular pathways. On the other hand, EPS analysis showed that more soluble protein, S-EPS and LB-EPS were produced by algal-bacterial AGS when exposure to Cr(VI). Results from metal distribution and chemical fractionation revealed that the loaded Cr in algal-bacterial AGS was completely in the form of Cr(III), among which 17.3% was EPS bound, 69.2% was intracellularly immobilized and only 9.5% was in the form of mobile fractions. The findings from this study provided a promising approach for Cr(VI) reduction and total Cr removal by algal-bacterial AGS, which may have great practical application potential for Cr(VI)-contaminated wastewater or soil remediation.

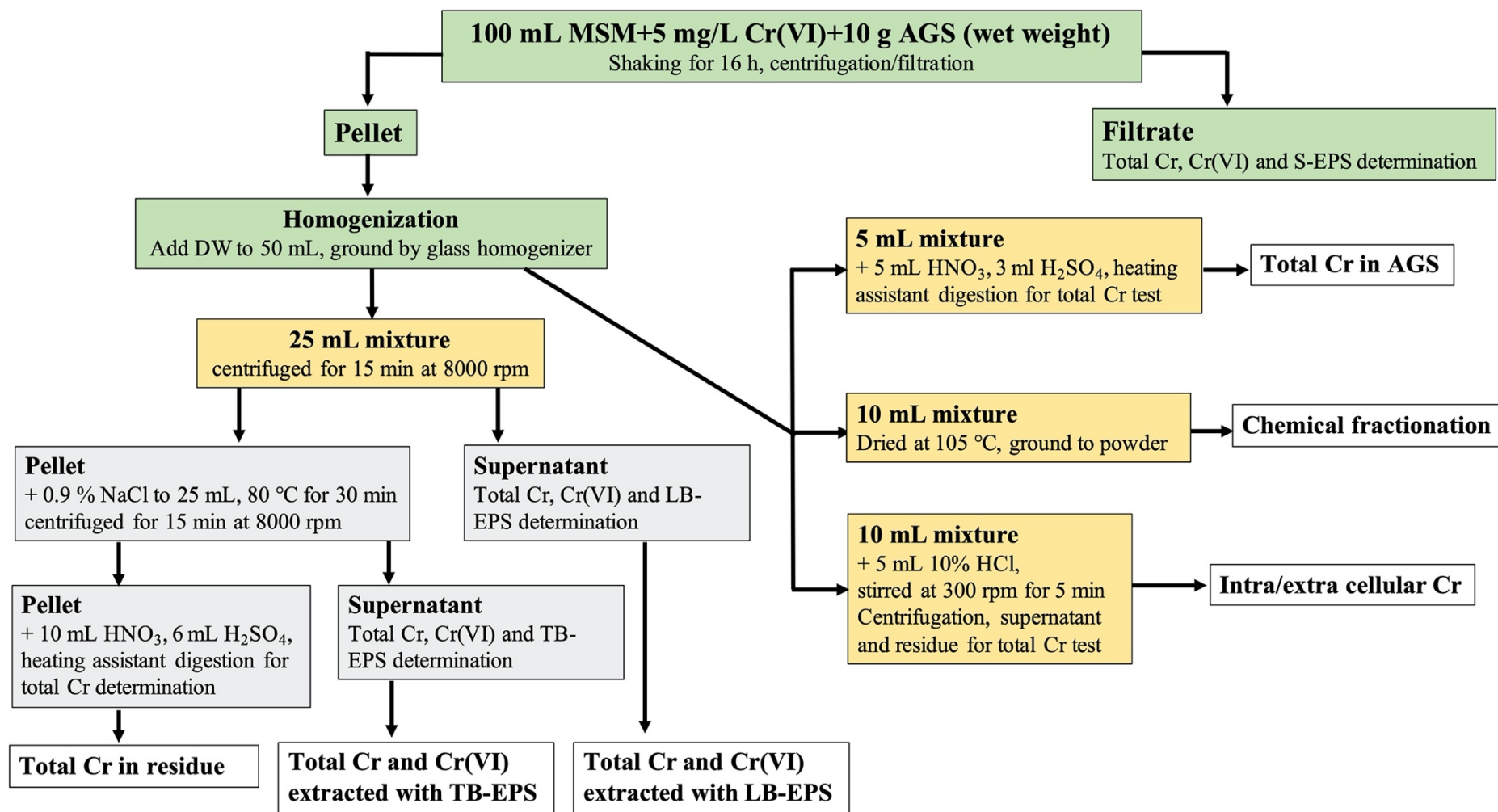


Figure 4-1 Schematic diagram of experiments for EPS extraction and Cr distribution in Cr-loaded algal-bacterial AGS.

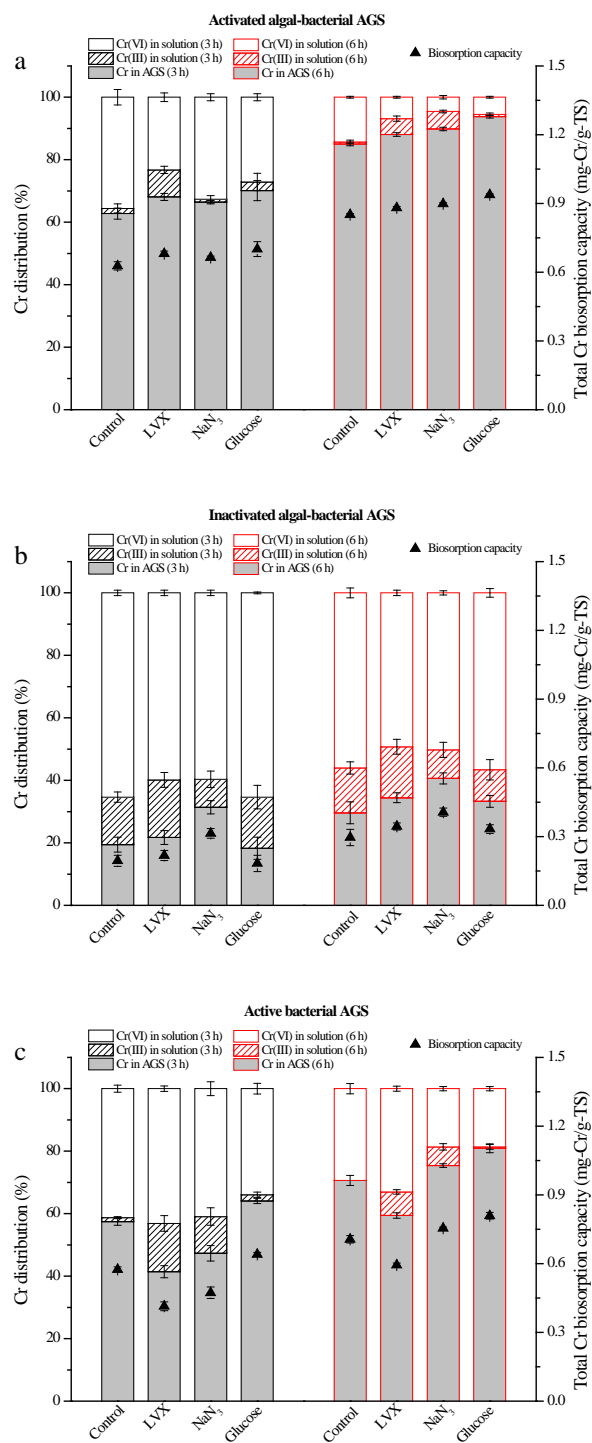


Figure 4-2 Effects of cell viability and electron donors on Cr distribution in solution and algal-bacterial AGS: (a) active algal-bacterial AGS; (b) inactivated algal-bacterial AGS by heating; (c) active bacterial AGS.

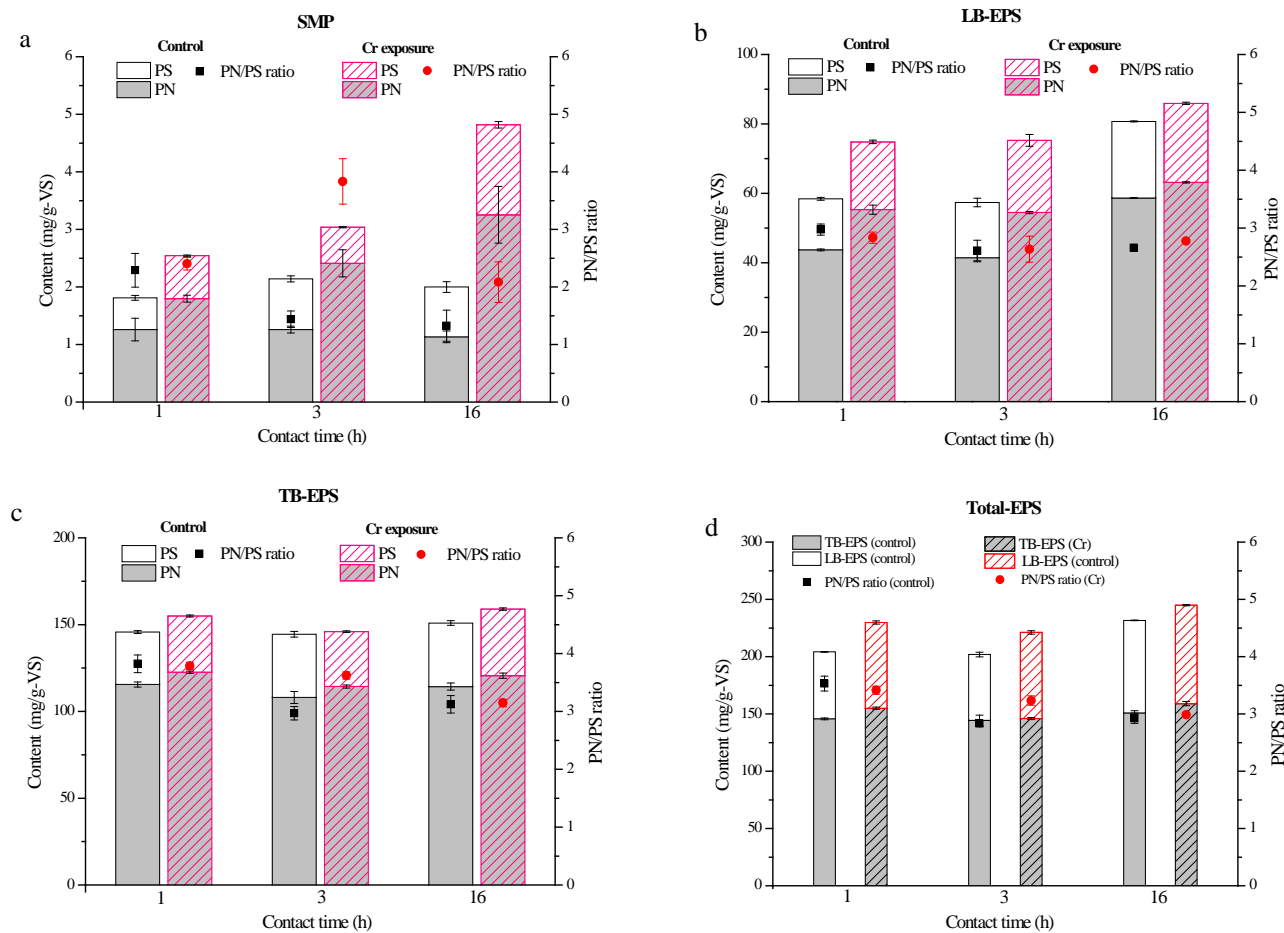


Figure 4-3 Changes of EPS contents and components in algal-bacterial AGS during Cr(VI) removal: (a) soluble EPS (S-EPS); (b) loosely bound EPS (LB-EPS); (c) tightly bound EPS (TB-EPS); (d) total EPS.

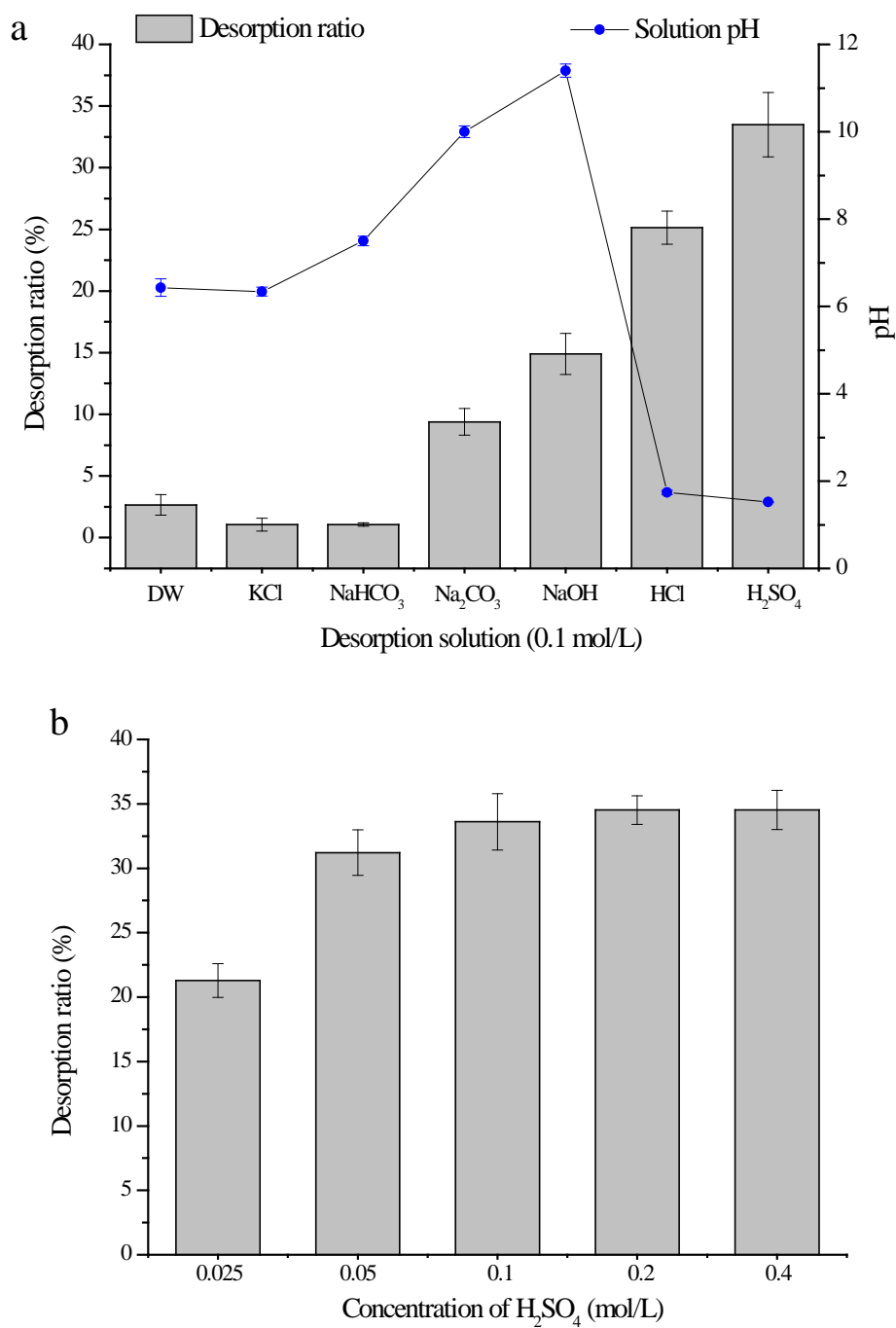


Figure 4-4 Desorption ratio of Cr from Cr-loaded algal-bacterial AGS: (a) effect of different desorption solution; (b) effect of different concentration of H<sub>2</sub>SO<sub>4</sub>. Condition for Cr(VI) removal experiment prior to desorption: contact time, 16 h; initial pH, 6; granule dosage, 5 g-TS/L, Cr(VI), 5 mg/L. Desorption time, 12 h.

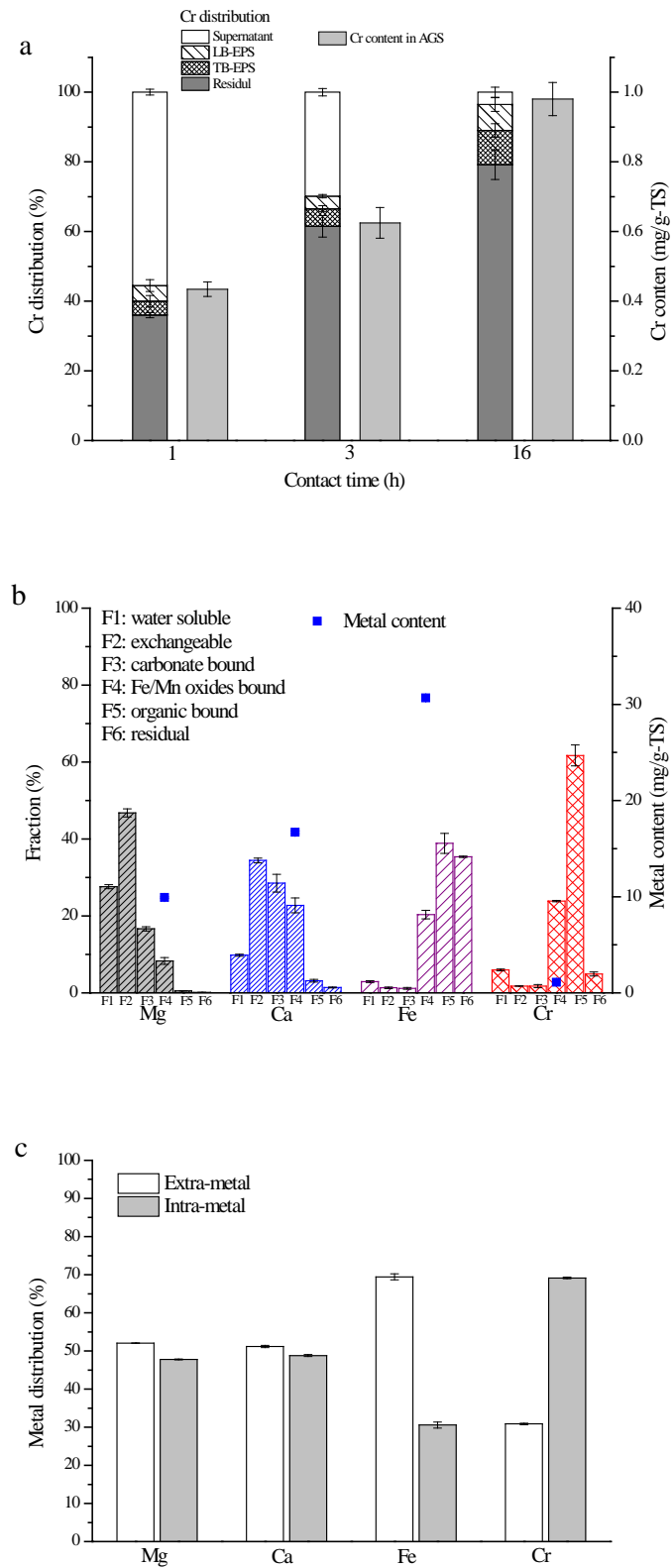


Figure 4-5 The distribution and content of different metal extracted from Cr-loaded algal-bacterial AGS: (a) distribution in EPS; (b) intra/extra cellular distribution; (c) chemical fractionation.



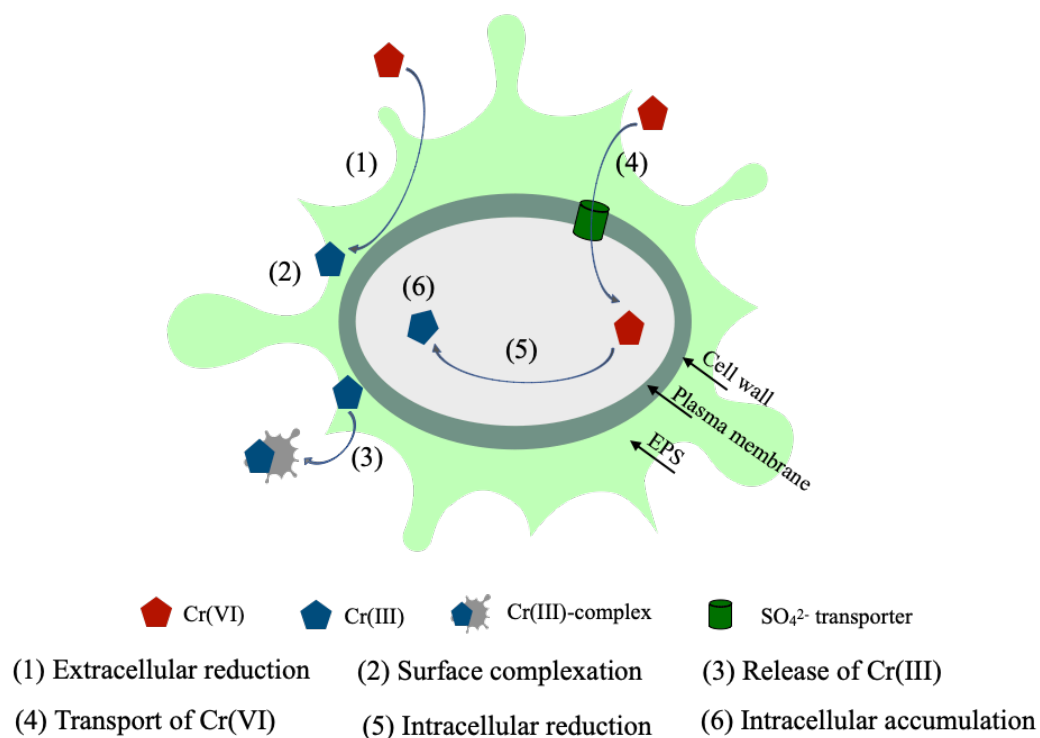


Figure 4-6 Conceptual diagram of Cr(VI) removal mechanism by microbial and microalgae cells in algal-bacterial AGS.

## Chapter 5 Conclusions and future research perspectives

### 5.1 Conclusions

In this study, mature bacterial or algal-bacterial granules were used for Cr(VI) removal from synthetic wastewater in terms of both total Cr removal and Cr(VI) reduction was investigated. The algal-bacterial AGS was cultivated from mature bacterial AGS, and compared with the bacterial AGS regarding Cr(VI) removal capacity, granular stability and metal content. Besides, influences of external environmental factors on Cr(VI) removal and the responses of algal-bacterial AGS were evaluated. Moreover, the underlying mechanisms were also studied by the means of chemical fractionation and microcharacterization. Major results can be concluded as follows.

#### 5.1.1 Comparison between algal-bacterial AGS and bacterial AGS

- 1) Compared to the conventional bacterial AGS, algal-bacterial AGS demonstrated higher biosorption capacity and better granular stability, implying that algal-bacterial AGS can be more potentially utilized as a Cr(VI) removal biomaterial for the treatment of Cr(VI)-containing wastewater.
- 2) The maximum Cr(VI) biosorption capacity of 51.0 mg/g occurred at pH 2 with initial Cr(VI) concentration of 50 mg/L, which was comparable with previous studies using raw or treated AGS, microalgae or other biosorbents.

Results from this section implied that algal-bacterial AGS can be more potentially utilized as a Cr(VI) removal and recovery biomaterial for the treatment of Cr(VI)-containing wastewater.

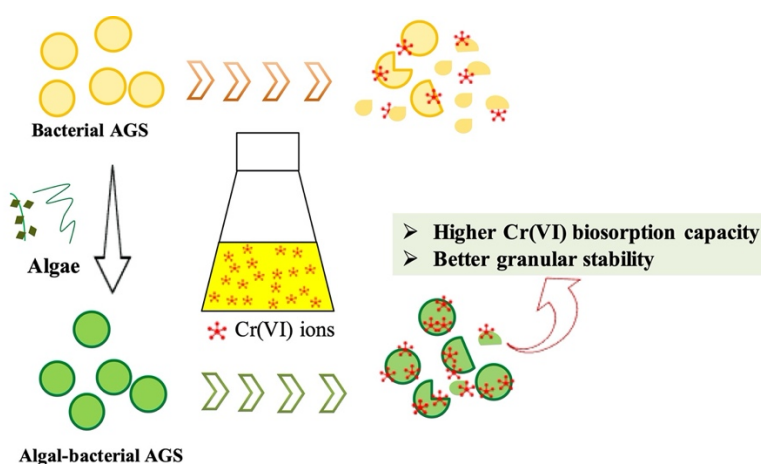


Figure 5-1 Graphical conclusion of Chapter 2.

### 5.1.2 Effects of environmental factors

- 1) Cr(VI) removal by algal-bacterial AGS was investigated in both aspects of Cr(VI) reduction and total Cr immobilization, with the highest reduction rate of 99.3% achieved at the pH 2 after 6 h, but optimum pH for total Cr immobilization (89.1%) was pH 6.
- 2) Co-existing oxyanions exhibited slight effects on Cr(VI) removal, while cations, NOMs and carbon sources all promoted the Cr(VI) reduction rate.
- 3) The removal of total Cr was suppressed at different extents due to the existing of competitive cations or organics. Changes of salinity exhibited significant inhibition to both Cr(VI) reduction and total Cr removal.
- 4) Algal-bacterial AGS was proven to be able to remove Cr(VI) effectively from wastewater under a wide range of conditions with the optimum pH 6.0, through combined enzyme-mediated Cr(VI) reduction and total Cr immobilization.

The results obtained from this section provide useful information on Cr(VI) removal by algal-bacterial AGS under a wide range of environmental conditions, which may find application on the remediation of Cr(VI) contaminated water and soil.

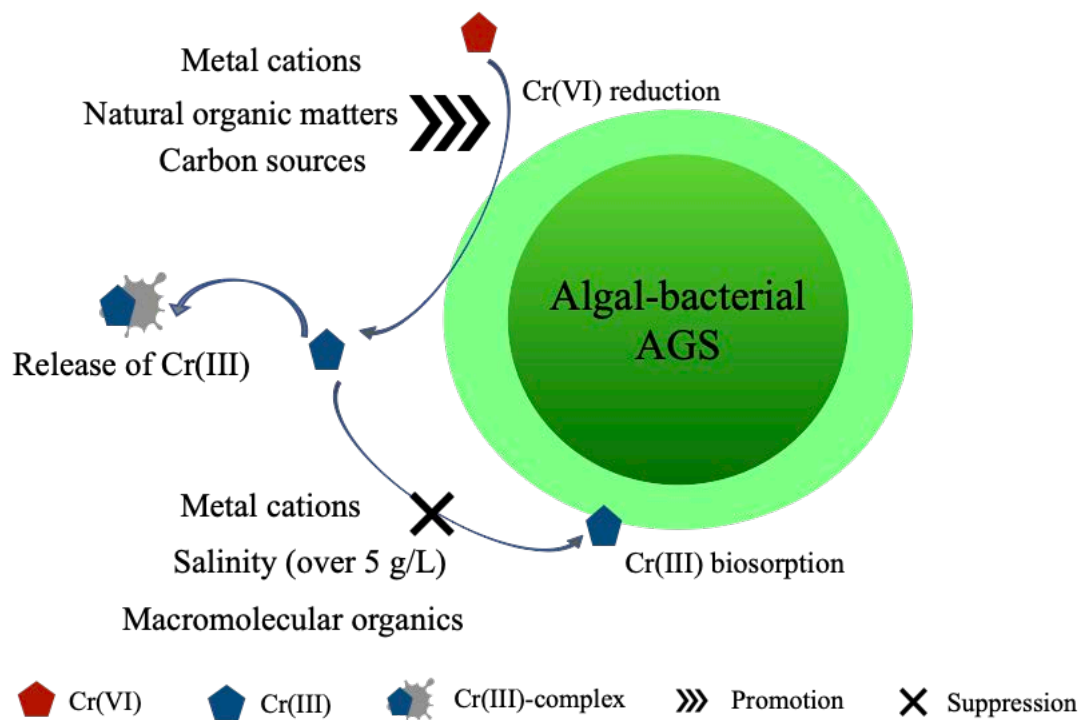


Figure 5-2 Graphical conclusion of Chapter 3.

### 5.1.3 Mechanism analysis

- (1) Total Cr removal rate by algal-bacterial AGS was reduced from 85.1% to 29.3% by sterilization and the addition of electron donor improved Cr(VI) removal efficiency by active AGS but not the inactive group, suggesting the crucial role of microbial viability and participation of algae in Cr(VI) removal by algal-bacterial AGS
- (2) Antibiotic LVX and metabolite inhibitor  $\text{NaN}_3$  inhibited the performance of bacterial AGS but not the algal-bacterial AGS or inactivated one, indicating the importance of algae in maintaining Cr(VI) removal performance of algal-bacterial AGS.
- (3) More soluble protein, S-EPS and LB-EPS were produced by algal-bacterial AGS with Cr(VI) exposure, indicating the production of extracellular enzymes.
- (4) The loaded Cr in algal-bacterial AGS was completely in the form of Cr(III), among which 17.3% was EPS sequestered, 69.2% was intracellularly immobilized and only 9.5% was in the form of mobile fractions.

It's deduced from this section that algal-bacterial AGS is a promising and safe biomaterial for hazardous HMs immobilization and cell viability was essential for Cr(VI) removal.

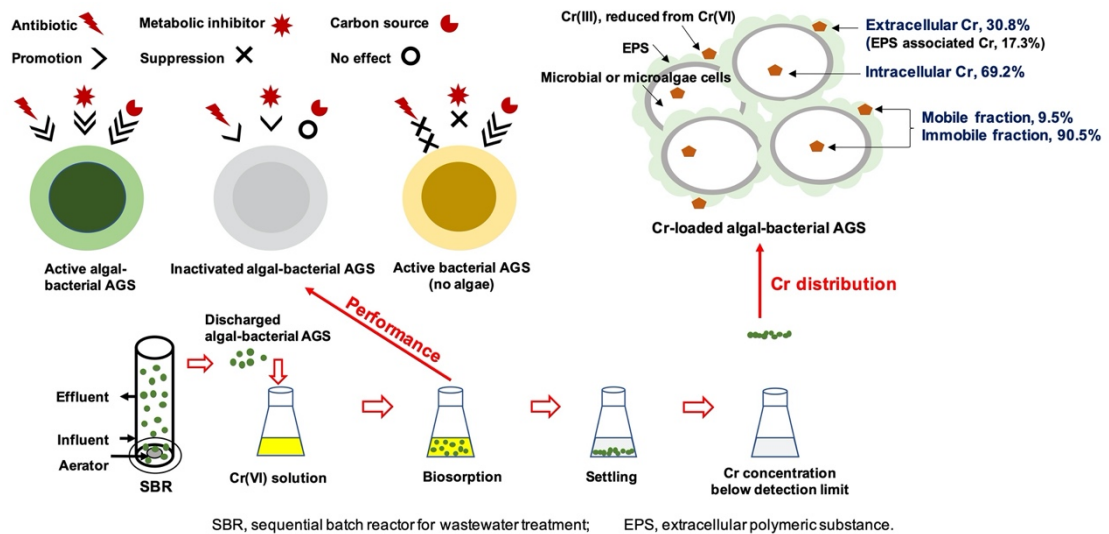


Figure 5-3 Graphical conclusion of Chapter 4.

From above, it can be concluded that algal-bacterial AGS has superiorities than conventional bacterial AGS and the reported biosorbents, can act as a promising biosorbent for Cr(VI) removal. Algal-bacterial AGS can maintain its Cr(VI) removal performance with the co-existing of various environmental factors or even under antibiotic exposure. Cell viability and the existing of algae are crucial for the efficiency of Cr(VI) removal by algal-bacterial AGS.

More importantly, the immobilized Cr in algal-bacterial AGS was existing in a less toxic form of Cr(III) with a low mobility, indicating the safety of using algal-bacterial AGS for hazardous heavy metal remediation. Results from this research are expected to facilitate the utilization of algal-bacterial AGS with high efficiency for heavy metal remediation in the real world of wastewater treatment.

## **5.2 Future research perspectives**

With the aim to achieve more efficient and practical application of algal-bacterial AGS for Cr(VI) remediation, future explorations are still necessary. These results are expected to contribute to a better development of wastewater treatment systems, which can also facilitate the utilization of algal-bacterial AGS with high efficiency in the real world of wastewater treatment. Therefore, the following aspects should be considered in the future research:

- (1) Treating synthetic or real Cr(VI) containing wastewater in a SBR with algal-bacterial AGS. The stability of the reactor in aspects of biomass growth and nutrients removal can be checked to monitor the performance of SBR in treating Cr(VI) containing wastewater. Moreover, variation in microbial community should also be examined to investigate the acclimating ability of microorganisms to Cr(VI) exposure.
- (2) Distinguishing the role of algae and bacteria in Cr(VI) removal by algal-bacterial AGS, which is expected to shed light on the mechanisms involved and the contribution of algae and bacteria to the removal of HMs.
- (3) Re-utilization of Cr-loaded algal-bacterial AGS after Cr(VI) removal processes. As show in chapter 4, Cr loaded in algal-bacterial AGS is difficult to be desorbed with conventional desorption solutions without changing microbial activity. The Cr in algal-bacterial AGS is relatively immobile which suggested the possibility of reutilizing these granules either for nutrients or metal recovery, which could be realized by different post treatments like anaerobic digestion or hydrothermal treatments.

## References

- Abbas, A., Al-Amer, A.M., Laoui, T., Al-Marri, M.J., Nasser, M.S., Khraisheh, M., Atieh, M.A., 2016. Heavy metal removal from aqueous solution by advanced carbon nanotubes: Critical review of adsorption applications. *Sep. Purif. Technol.* 157, 141-161.
- Achary, P.G.R., Ghosh, M.R., Mishra, S.P., 2020. Insights into the modeling and application of some low cost adsorbents towards Cr(VI) adsorption. *Mater. Today Proc.* 30, 267-273.
- Akram, M., Bhatti, H.N., Iqbal, M., Noreen, S., Sadaf, S., 2017. Biocomposite efficiency for Cr(VI) adsorption: Kinetic, equilibrium and thermodynamics studies. *J. Environ. Chem. Eng.* 5, 400-411.
- Aksu, Z., Balibek, E., 2007. Chromium(VI) biosorption by dried *Rhizopus arrhizus*: Effect of salt (NaCl) concentration on equilibrium and kinetic parameters. *J. Hazard. Mater.*, 145, 210-220.
- Arıca, M.Y., Tüzün, İ., Yalçın, E., İnce, Ö., Bayramoğlu, G., 2005. Utilisation of native, heat and acid-treated microalgae *Chlamydomonas reinhardtii* preparations for biosorption of Cr(VI) ions. *Process Biochem.* 40, 2351-2358.
- Asensio, V., Vega, F.A., Singh, B.R., Covelo, E.F., 2013. Effects of tree vegetation and waste amendments on the fractionation of Cr, Cu, Ni, Pb and Zn in polluted mine soils. *Sci. Total Environ.* 443, 446-453.
- Bai, R.S., Abraham, T.E., 2002. Studies on enhancement of Cr(VI) biosorption by chemically modified biomass of *Rhizopus nigricans*. *Water Res.* 36, 1224-1236.
- Baldiris, R., Acosta-Tapia, N., Montes, A., Hernández, J., Vivas-Reyes, R., 2018. Reduction of hexavalent chromium and detection of chromate reductase (ChrR) in *Stenotrophomonas maltophilia*. *Molecules* 23, 406.
- Bardestani, R., Roy, C., Kaliaguine, S., 2019. The effect of biochar mild air oxidation on the optimization of lead(II) adsorption from wastewater. *J. Environ. Manage.* 240, 404-420.
- Cabrol, L., Quemeneur, M., Misson, B., 2017. Inhibitory effects of sodium azide on microbial growth in experimental resuspension of marine sediment. *J. Microbiol. Methods* 133, 62-65.
- Cai, W., Jin, M., Zhao, Z., Lei, Z., Zhang, Z., Adachi, Y., Lee, D.-J., 2018. Influence of ferrous iron dosing strategy on aerobic granulation of activated sludge and bioavailability of phosphorus accumulated in granules. *Bioresour. Technol. Rep.* 2, 7-14.
- Chen, K., Zhao, Z., Yang, X., Lei, Z., Zhang, Z., Zhang, S., 2018. Desorption trials and granular

- stability of chromium loaded aerobic granular sludge from synthetic domestic wastewater treatment. *Bioresour. Technol. Rep.* 1, 9-15.
- Cherdchoo, W., Nithettham, S., Charoenpanich, J., 2019. Removal of Cr(VI) from synthetic wastewater by adsorption onto coffee ground and mixed waste tea. *Chemosphere* 221, 758-767.
- Cid, H.A., Flores, M.I., Pizarro, J.F., Castillo, X.A., Barros, D.E., Moreno-Piraján, J.C., Ortiz, C.A., 2018. Mechanisms of Cu<sup>2+</sup> biosorption on *Lessonia nigrescens* dead biomass: Functional groups interactions and morphological characterization. *J. Environ. Chem. Eng.* 6, 2696-2704.
- Coursolle, D., Baron, D.B., Bond, D.R., Gralnick, J.A., 2010. The Mtr respiratory pathway is essential for reducing flavins and electrodes in *Shewanella oneidensis*. *J. Bacteriol.* 192, 467-474.
- Das, A.P., Mishra, S., 2010. Biodegradation of the metallic carcinogen hexavalent chromium Cr(VI) by an indigenously isolated bacterial strain. *J. Carcinog.* 9, 6.
- Das, S., Mishra, J., Das, S.K., Pandey, S., Rao, D.S., Chakraborty, A., Sudarshan, M., Das, N., Thatoi, H., 2014. Investigation on mechanism of Cr(VI) reduction and removal by *Bacillus amyloliquefaciens*, a novel chromate tolerant bacterium isolated from chromite mine soil. *Chemosphere* 96, 112-121.
- Ding, D., Ma, X., Shi, W., Lei, Z., Zhang, Z., 2016. Insights into mechanisms of hexavalent chromium removal from aqueous solution by using rice husk pretreated using hydrothermal carbonization technology. *RSC Adv.* 6, 74675-74682.
- Dubois, M., Gilles, K. A., Hamilton, J.K., Rebers, P.T., Smith, F., 1956. Colorimetric method for determination of sugars and related substances. *Anal. Chem.* 28, 350-356
- Feng, Q., Wen, S., Zhao, W., Chen, Y., 2018. Effect of calcium ions on adsorption of sodium oleate onto cassiterite and quartz surfaces and implications for their flotation separation. *Sep. Purif. Technol.* 200, 300-306.
- Fomina, M., Gadd, G.M., 2014. Biosorption: Current perspectives on concept, definition and application. *Bioresour. Technol.* 160, 3-14.
- Franca, R.D.G, Pinheiro, H.M., van Loosdrecht, M.C.M, Lourenço, N.D., 2018. Stability of aerobic granules during long-term bioreactor operation. *Biotechnol. Adv.* 36, 228-246.
- Fu, F., Wang, Q., 2011. Removal of heavy metal ions from wastewaters: A review. *J. Environ. Manage.* 92, 407-418.
- Ghangrekar, M.M., Asolekar, S.R., Joshi, S.G., 2005. Characteristics of sludge developed under

- different loading conditions during UASB reactor start-up and granulation. *Water Res.* 39, 1123-1133
- Han, H., Ling, Z., Zhou, T., Xu, R., He, Y., Liu, P., Li, X., 2017a. Copper(II) binding of NAD (P) H-flavin oxidoreductase (NfoR) enhances its Cr(VI)-reducing ability. *Sci. Rep.* 7, 1-12.
- Han, J.C., Chen, G.J., Qin, L.P., Mu, Y., 2017b. Metal respiratory pathway-independent Cr isotope fractionation during Cr(VI) reduction by *shewanella oneidensis* MR-1. *Environ. Sci. Technol. Lett.* 4, 500-504.
- Han, X., Wong, Y.S., Wong, M.H., Tam, N.F.Y., 2007. Biosorption and bioreduction of Cr(VI) by a microalgal isolate, *Chlorella miniata*. *J. Hazard. Mater.* 146, 65-72.
- Harish, R., Samuel, J., Mishra, R., Chandrasekaran, N., Mukherjee, A., 2012. Bio-reduction of Cr(VI) by exopolysaccharides (EPS) from indigenous bacterial species of Sukinda chromite mine, India. *Biodegradation* 23, 487-496.
- Hausladen, D.M., Alexander-Ozinskas, A., McClain, C., Fendorf, S., 2018. Hexavalent chromium sources and distribution in California groundwater. *Environ. Sci. Technol.* 52, 8242-8251.
- Hou, W., Ma, Z., Sun, L., Han, M., Lu, J., Li, Z., Abdalla, M.O.A, Wei, G., 2013. Extracellular polymeric substances from copper-tolerance *Sinorhizobium meliloti* immobilize  $\text{Cu}^{2+}$ . *J. Hazard. Mater.* 261, 614-620.
- Huang, X.N., Min, D., Liu, D.F., Cheng, L., Qian, C., Li, W.W., Yu, H., 2019b. Formation mechanism of organo-chromium (III) complexes from bioreduction of chromium (VI) by *Aeromonas hydrophila*. *Environ. Int.* 129, 86-94.
- Huang, Y., Zhou, B., Li, N., Li, Y., Han, R., Qi, J., Lu, X., Li, S., Feng, C., Liang, S., 2019a. Spatial-temporal analysis of selected industrial aquatic heavy metal pollution in China. *J. Clean. Prod.* 238, 117944.
- James, B.R., Petura, J.C., Vitale, R.J., Mussoline, G.R., 1995. Hexavalent chromium extraction from soils: A comparison of five methods. *Environ. Sci. Technol.* 29, 2377-2381.
- Jang, E.H., Pack, S.P., Kim, I. and Chung, S., 2020. A systematic study of hexavalent chromium adsorption and removal from aqueous environments using chemically functionalized amorphous and mesoporous silica nanoparticles. *Sci. Rep.* 10, 1-20.
- Jiang, Y., Liu, Y., Zhang, H., Yang, K., Li, J., Shao, S., 2020. Aerobic granular sludge shows enhanced resistances to the long-term toxicity of Cu(II). *Chemosphere* 253, 126664.
- Jobby, R., Jha, P., Yadav, A.K., Desai, N., 2018. Biosorption and biotransformation of



- hexavalent chromium [Cr(VI)]: A comprehensive review. *Chemosphere* 207, 255-266.
- Karthik, C., Barathi, S., Pugazhendhi, A., Ramkumar, V.S., Thi, N.B.D., Arulselvi, P.I., 2017. Evaluation of Cr(VI) reduction mechanism and removal by *Cellulosimicrobium funkei* strain AR8, a novel haloalkaliphilic bacterium. *J. Hazard. Mater.* 333, 42-53.
- Khadhar, S., Sdiri, A., Chekirben, A., Azouzi, R., Charef, A., 2020. Integration of sequential extraction, chemical analysis and statistical tools for the availability risk assessment of heavy metals in sludge amended soil. *Environ. Pollut.* 263, 114543.
- Kotaś, J., Stasicka, Z., 2000. Chromium occurrence in the environment and methods of its speciation. *Environ. Pollut.* 107, 263-283.
- Kumar, K.S., Dahms, H.U., Won, E.J., Lee, J.S., Shin, K.H., 2015. Microalgae-A promising tool for heavy metal remediation. *Ecotox. Environ. Safe.* 113, 329-352.
- Lai, C.Y., Zhong, L., Zhang, Y., Chen, J.X., Wen, L.L., Shi, L.D., Sun, Y.P., Ma, F., Rittmann, B.E., Zhou, C. Tang, Y., Zheng, P., Zhao H.P., 2016. Bioreduction of chromate in a methane-based membrane biofilm reactor. *Environ. Sci. Technol.* 50, 5832-5839.
- Li, C. B., Hein, S., Wang, K., 2008. Biosorption of chitin and chitosan. *Mater. Sci. Technol.* 24, 1088-1099.
- Li, M., He, Z., Hu, Y., Hu, L., Zhong, H., 2019. Both cell envelope and cytoplasm were the locations for chromium(VI) reduction by *Bacillus* sp. M6. *Bioresour. Technol.* 273, 130-135.
- Li, Y., Qin, C., Zhang, J., Lan, Y., Zhou, L., 2014. Cu(II) catalytic reduction of Cr(VI) by tartaric acid under the irradiation of simulated solar light. *Environ. Eng. Sci.* 31, 447-452.
- Lilli, M.A., Moraetis, D., Nikolaidis, N.P., Karatzas, G.P., Kalogerakis, N., 2015. Characterization and mobility of geogenic chromium in soils and river bed sediments of Asopos basin. *J. Hazard. Mater.* 281, 12-19.
- Lin, H., Ma, R., Hu, Y., Lin, J., Sun, S., Jiang, J., Li, T., Liao, Q., Luo, J., 2020. Reviewing bottlenecks in aerobic granular sludge technology: Slow granulation and low granular stability. *Environ. Pollut.* 263, 114638.
- Liu, W., Zhang, J., Jin, Y., Zhao, X., Cai, Z., 2015. Adsorption of Pb(II), Cd(II) and Zn(II) by extracellular polymeric substances extracted from aerobic granular sludge: Efficiency of protein. *J. Environ. Chem. Eng.* 3, 1223-1232.
- Liu, W., Zhao, X., Wang, T., Zhao, D., Ni, J., 2016. Adsorption of U(VI) by multilayer titanate nanotubes: Effects of inorganic cations, carbonate and natural organic matter. *Chem. Eng. J.* 286, 427-435.

- Liu, Y., Yang, S.-F., Xu, H., Woon, K.-H., Lin, Y.-M., Tay, J.-H., 2003. Biosorption kinetics of cadmium(II) on aerobic granular sludge. *Process Biochem.* 38, 997-1001.
- Lowry, O.H., Rosebrough, N.J., Farr, A.L., Randall, R.J., 1951. Protein measurement with the Folin phenol reagent. *J. Biol. Chem.* 193, 265-275.
- Lv, X., Hu, Y., Tang, J., Sheng, T., Jiang, G., Xu, X., 2013. Effects of co-existing ions and natural organic matter on removal of chromium(VI) from aqueous solution by nanoscale zero valent iron (nZVI)-Fe<sub>3</sub>O<sub>4</sub> nanocomposites. *Chem. Eng. J.* 218, 55-64.
- Ma, H.L., Zhang, Y., Hu, Q.H., Yan, D., Yu, Z.Z., Zhai, M., 2012. Chemical reduction and removal of Cr(VI) from acidic aqueous solution by ethylenediamine-reduced graphene oxide. *J. Mater. Chem.* 22, 5914-5916.
- Ma, L., Xu, J., Chen, N., Li, M., Feng, C., 2019a. Microbial reduction fate of chromium (Cr) in aqueous solution by mixed bacterial consortium. *Ecotoxicol. Environ. Saf.* 170, 763-770.
- Ma, S., Song, C.S., Chen, Y., Wang, F., Chen, H.L., 2018. Hematite enhances the removal of Cr(VI) by *Bacillus subtilis* BSn5 from aquatic environment. *Chemosphere* 208, 579-585.
- Ma, Y., Zhong, H., He, Z., 2019b. Cr(VI) reductase activity locates in the cytoplasm of *Aeribacillus pallidus* BK1, a novel Cr(VI)-reducing thermophile isolated from Tengchong geothermal region, China. *Chem. Eng. J.* 371, 524-534.
- Machado, M.D., Soares, E.V., Soares, H.M., 2010. Removal of heavy metals using a brewer's yeast strain of *Saccharomyces cerevisiae*: Chemical speciation as a tool in the prediction and improving of treatment efficiency of real electroplating effluents. *J. Hazard. Mater.* 180, 347-353.
- Mala, J.G.S., Sujatha, D., Rose, C., 2015. Inducible chromate reductase exhibiting extracellular activity in *Bacillus methylotrophicus* for chromium bioremediation. *Microbiol. Res.* 170, 235-241.
- Markiewicz, B., Komorowicz, I., Sajnóg, A., Belter, M., Barańkiewicz, D., 2015. Chromium and its speciation in water samples by HPLC/ICP-MS-technique establishing metrological traceability: A review since 2000. *Talanta* 132, 814-828.
- Micheletti, E., Colica, G., Viti, C., Tamagnini, P., De Philippis, R., 2008. Selectivity in the heavy metal removal by exopolysaccharide-producing cyanobacteria. *J. Appl. Microbiol.* 105, 88-94.
- Mishra, R.R., Dhal, B., Dutta, S.K., Dangar, T.K., Das, N.N., Thatoi, H.N., 2012. Optimization and characterization of chromium(VI) reduction in saline condition by moderately halophilic *Vigribacillus* sp. isolated from mangrove soil of Bhitarkanika, India. *J. Hazard.*

- Mater. 227, 219-226.
- Mitra, S., Sarkar, A., Sen, S., 2017. Removal of chromium from industrial effluents using nanotechnology: A review. *Nanotechnol. Environ. Eng.* 2, 11.
- Mohite, B.V., Koli, S.H., Patil, S.V., 2018. Heavy metal stress and its consequences on exopolysaccharide (EPS)-producing *Pantoea agglomerans*. *Appl. Biochem. Biotechnol.* 186, 199-216.
- Moussavi, G., Barikbin, B., 2010. Biosorption of chromium (VI) from industrial wastewater onto pistachio hull waste biomass. *Chem. Eng. J.* 162, 893-900.
- Nair, A., Juwarkar, A.A., Devotta, S., 2008. Study of speciation of metals in an industrial sludge and evaluation of metal chelators for their removal. *J. Hazard. Mater.* 152, 545-553.
- Nanchaiah, Y.V., Reddy, G.K.K., 2018. Aerobic granular sludge technology: Mechanisms of granulation and biotechnological applications. *Bioresour. Technol.* 247, 1128-1143.
- Němeček, J., Lhotský, O., Cajthaml, T., 2014. Nanoscale zero-valent iron application for in situ reduction of hexavalent chromium and its effects on indigenous microorganism populations. *Sci. Total Environ.* 485, 739-747.
- Noel, G.J., 2009. A review of levofloxacin for the treatment of bacterial infections. *Clin. Med. Ther.* 1, CMT-S28.
- Novotnik, B., Zuliani, T., Ščančar, J., Milačič, R., 2012. The determination of Cr(VI) in corrosion protection coatings by speciated isotope dilution ICP-MS. *J. Anal. At. Spectrom.* 27, 1484-1493.
- OCHEMOnline, Infrared Spectroscopy Absorption Table, OCHEMOnline (2020). [https://chem.libretexts.org/Ancillary\\_Materials/Reference/Reference\\_Tables/Spectroscopic\\_Parameters/Infrared\\_Spectroscopy\\_Absorption\\_Table](https://chem.libretexts.org/Ancillary_Materials/Reference/Reference_Tables/Spectroscopic_Parameters/Infrared_Spectroscopy_Absorption_Table) (accessed on 22<sup>nd</sup> March 2020)
- Olguin, M.T., López-González, H., Serrano-Gomez, J., 2013. Hexavalent chromium removal from aqueous solutions by Fe-modified peanut husk. *Water Air Soil Pollut.* 224, 1654.
- Peng, H., Guo, J., 2020. Removal of chromium from wastewater by membrane filtration, chemical precipitation, ion exchange, adsorption electrocoagulation, electrochemical reduction, electrodialysis, electrodeionization, photocatalysis and nanotechnology: A review. *Environ. Chem. Lett.* 18, 1-14.
- Pradhan, D., Sukla, L.B., Mishra, B.B., Devi, N., 2019. Biosorption for removal of hexavalent chromium using microalgae *Scenedesmus* sp.. *J. Clean Prod.* 209, 617-629.
- Quan, X., Cen, Y., Lu, F., Gu, L., Ma, J., 2015. Response of aerobic granular sludge to the long-term presence to nanosilver in sequencing batch reactors: Reactor performance, sludge

- property, microbial activity and community. *Sci. Total Environ.* 506, 226-233.
- Rahman, Z., Singh, V.P., 2019. The relative impact of toxic heavy metals (THMs) (arsenic (As), cadmium (Cd), chromium (Cr)(VI), mercury (Hg), and lead (Pb)) on the total environment: an overview. *Environ. Monit. Assess.* 191, 419.
- Ranasinghe, S.H., Navaratne, A.N., Priyantha, N., 2018. Enhancement of adsorption characteristics of Cr(III) and Ni(II) by surface modification of jackfruit peel biosorbent. *J. Environ. Chem. Eng.* 6, 5670-5682.
- Reizabal, A., Costa, C.M., Saiz, P.G., Gonzalez, B., Pérez-Álvarez, L., de Luis, R.F., Garcia, A., Vilas-Vilela, J.L., Lanceros-Méndez, S., 2020. Processing strategies to obtain highly porous silk fibroin structures with tailored microstructure and molecular characteristics and their applicability in water remediation. *J. Hazard. Mater.* 403, 123675.
- Rozada, F., Otero, M., Morán, A., García, A.I., 2008. Adsorption of heavy metals onto sewage sludge-derived materials. *Bioresour. Technol.* 99, 6332-6338.
- Saravanan, A., Kumar, P.S., Yashwanthraj, M., 2017. Sequestration of toxic Cr(VI) ions from industrial wastewater using waste biomass: A review. *Desalination Water Treat.* 68, 245-266.
- Shahid, M., Shamshad, S., Rafiq, M., Khalid, S., Bibi, I., Niazi, N.K., Dumat, C., Rashid, M.I., 2017. Chromium speciation, bioavailability, uptake, toxicity and detoxification in soil-plant system: A review. *Chemosphere* 178, 513-533.
- Shi, L., Deng, X., Yang, Y., Jia, Q., Wang, C., Shen, Z., Chen, Y., 2019. A Cr(VI)-tolerant strain, *Pisolithus* sp1, with a high accumulation capacity of Cr in mycelium and highly efficient assisting *Pinus thunbergii* for phytoremediation. *Chemosphere* 224, 862-872.
- Son, E.B., Poo, K.M., Chang, J.S., Chae, K.J., 2018. Heavy metal removal from aqueous solutions using engineered magnetic biochars derived from waste marine macro-algal biomass. *Sci. Total Environ.* 615, 161-168.
- Srinath, T., Verma, T., Ramteke, P.W., Garg, S.K., 2002. Chromium (VI) biosorption and bioaccumulation by chromate resistant bacteria. *Chemosphere* 48, 427-435.
- Suksabye, P., Nakajima, A., Thiravetyan, P., Baba, Y., Nakbanpote, W., 2009. Mechanism of Cr(VI) adsorption by coir pith studied by ESR and adsorption kinetic. *J. Hazard. Mater.* 161, 1103-1108.
- Sun, F., Sun, W.-L., Sun, H.-M., Ni, J.-R., 2011a. Biosorption behavior and mechanism of beryllium from aqueous solution by aerobic granule. *Chem. Eng. J.* 172, 783-791.
- Sun, X.-F., Liu, C., Ma, Y., Wang, S.-G., Gao, B.-Y., Li, X.-M., 2011b. Enhanced Cu(II) and

- Cr(VI) biosorption capacity on poly (ethylenimine) grafted aerobic granular sludge. *Colloid Surf. B* 82, 456-462.
- Sun, X.-F., Ma, Y., Liu, X.-W., Wang, S.-G., Gao, B.-Y., Li, X.-M., 2010. Sorption and detoxification of chromium (VI) by aerobic granules functionalized with polyethylenimine. *Water Res.* 44, 2517-2524.
- Tan, H., Wang, C., Zeng, G., Luo, Y., Li, H., Xu, H., 2020. Bioreduction and biosorption of Cr(VI) by a novel *Bacillus* sp. CRB-B1 strain. *J. Hazard. Mater.* 386,121628.
- Tessier, A., Campbell, P.G., Bisson, M.J.A.C., 1979. Sequential extraction procedure for the speciation of particulate trace metals. *Anal. Chem.* 51, 844-851.
- Thatoi, H., Das, S., Mishra, J., Rath, B.P., Das, N., 2014. Bacterial chromate reductase, a potential enzyme for bioremediation of hexavalent chromium: A review. *J. Environ. Manage.* 146, 383-399.
- US EPA, 2009. National Primary Drinking Water Regulations, EPA 816-F-09-004. U.S. Environmental Protection Agency: Washington, DC. <https://www.nrc.gov/docs/ML1307/ML13078A040.pdf> (accessed on 22 March 2020)
- Viti, C., Marchi, E., Decorosi, F., Giovannetti, L., 2014. Molecular mechanisms of Cr(VI) resistance in bacteria and fungi. *FEMS Microbiol. Rev.* 38, 633-659.
- Wang, J., Chen, C., 2009. Biosorbents for heavy metals removal and their future. *Biotechnol. Adv.* 27, 195-226.
- Wang, J., Lei, Z., Tian, C., Liu, S., Wang, Q., Shimizu, K., Zhang, Z., Adachi, Y., Lee, D.-J., 2020a. Ionic response of algal-bacterial granular sludge system during biological phosphorus removal from wastewater. *Chemosphere* 264, 128534.
- Wang, L., Liu, X., Lee, D.-J., Tay, J.H., Zhang, Y., Wan, C.L., Chen, X.F., 2018. Recent advances on biosorption by aerobic granular sludge. *J. Hazard. Mater.* 357, 253-270.
- Wang, P., Sun, D., Zhang, S., Huang, X., Bi, Y., Qian, M., Zhao, W., Huang, F., 2020b. Constructing mesoporous phosphated titanium oxide for efficient Cr(III) removal. *J. Hazard. Mater.* 384, 121278.
- Wang, X.H., Song, R.H., Teng, S.X., Gao, M.M., Ni, J.Y., Liu, F.F., Wang, S., Gao, B.Y., 2010. Characteristics and mechanisms of Cu(II) biosorption by disintegrated aerobic granules. *J. Hazard. Mater.* 179, 431-437.
- Wang, Y., Li, Y., Zhang, Y., Wei, W., 2019. Effects of macromolecular humic/fulvic acid on Cd(II) adsorption onto reed-derived biochar as compared with tannic acid. *International J. Biol. Macromol.* 134, 43-55.

- Wang, Z., Gao, M., Wang, S., Xin, Y., Ma, D., She, Z., Wang, Z., Chang, Q., Ren, Y., 2014. Effect of hexavalent chromium on extracellular polymeric substances of granular sludge from an aerobic granular sequencing batch reactor. *Chem. Eng. J.* 251,165-174.
- Wilén, B.M., Liébana, R., Persson, F., Modin, O. and Hermansson, M., 2018. The mechanisms of granulation of activated sludge in wastewater treatment, its optimization, and impact on effluent quality. *Appl. Microbiol. Biotechnol.* 102, 5005-5020.
- Wu, J., Li, Q., Lv, Z., 2020. Regulating and intervening act of Cr chemical speciation effect on the electrokinetic removal in Cr contaminated soil in arid area. *Sep. Purif. Technol.* 250, 117167.
- Wu, J., Zhang, H., He, P.J., Yao, Q., Shao, L.M., 2010. Cr(VI) removal from aqueous solution by dried activated sludge biomass. *J. Hazard. Mater.* 176, 697-703.
- Xia, S., Song, Z., Jeyakumar, P., Shaheen, S.M., Rinklebe, J., Ok, Y.S., Bolan, N., Wang, H., 2019. A critical review on bioremediation technologies for Cr(VI)-contaminated soils and wastewater. *Crit. Rev. Environ. Sci. Technol.* 49, 1027-1078.
- Xu, H., Liu, Y., 2008. Mechanisms of  $\text{Cd}^{2+}$ ,  $\text{Cu}^{2+}$  and  $\text{Ni}^{2+}$  biosorption by aerobic granules. *Sep. Purif. Technol.* 58, 400-411.
- Yao, L., Ye, Z.F., Tong, M.P., Lai, P., Ni, J.R., 2009. Removal of  $\text{Cr}^{3+}$  from aqueous solution by biosorption with aerobic granules. *J. Hazard. Mater.* 165, 250-255.
- Zhang, B., Lens, P.N.L., Shi, W., Zhang, R., Zhang, Z., Guo, Y., Bao, X., Cui, F., 2018. Enhancement of aerobic granulation and nutrient removal by an algal-bacterial consortium in a lab-scale photobioreactor. *Chem. Eng. J.* 334, 2373-2382.
- Zhang, J., Chen, S., Zhang, H., Wang, X., 2017. Removal behaviors and mechanisms of hexavalent chromium from aqueous solution by cephalosporin residue and derived chars. *Bioresour. Technol.* 238, 484-491.
- Zhang, Y., Dong, X., Liu, S., Lei, Z., Shimizu, K., Zhang, Z., Adachi, Y., Lee, D.-J., 2020. Rapid establishment and stable performance of a new algal-bacterial granule system from conventional bacterial aerobic granular sludge and preliminary analysis of mechanisms involved. *J. Water Process Eng.* 34, 101073.
- Zhang, Y., Zhu, C., Liu, F., Yuan, Y., Wu, H., Li, A., 2019. Effects of ionic strength on removal of toxic pollutants from aqueous media with multifarious adsorbents: A review. *Sci. Total Environ.* 646, 265-279.
- Zhao, X., Liu, W., Cai, Z., Han, B., Qian, T., Zhao, D., 2016. An overview of preparation and applications of stabilized zero-valent iron nanoparticles for soil and groundwater

- remediation. *Water Res.* 100, 245-266.
- Zhao, Z., Yang, X., Cai, W., Lei, Z., Shimizu, K., Zhang, Z., Utsumi, M., Lee, D.-J., 2018. Response of algal-bacterial granular system to low carbon wastewater: Focus on granular stability, nutrients removal and accumulation. *Bioresour. Technol.* 268, 221-229.
- Zhao, Z., Liu, S., Yang, X., Lei, Z., Shimizu, K., Zhang, Z., Lee, D.-J., Adachi, Y., 2019. Stability and performance of algal-bacterial granular sludge in shaking photo-sequencing batch reactors with special focus on phosphorus accumulation. *Bioresour. Technol.* 280, 497-501.
- Zhou, Y., Zhang, Z., Zhang, J., Xia, S., 2016. Understanding key constituents and feature of the biopolymer in activated sludge responsible for binding heavy metals. *Chem. Eng. J.* 304, 527-532.
- Zhu, Y., Yan, J., Xia, L., Zhang, X., Luo, L., 2019. Mechanisms of Cr (VI) reduction by *Bacillus* sp. CRB-1, a novel Cr (VI)-reducing bacterium isolated from tannery activated sludge. *Ecotoxicol. Environ. Saf.* 186, 109792.
- Zhuo, N., Lan, Y., Yang, W., Yang, Z., Li, X., Zhou, X., Liu, Y., Shen, J., Zhang, X., 2017. Adsorption of three selected pharmaceuticals and personal care products (PPCPs) onto MIL-101 (Cr)/natural polymer composite beads. *Sep. Purif. Technol.* 177, 272-280.
- Zia, Q., Tabassum, M., Lu, Z., Khawar, M.T., Song, J., Gong, H., Meng, J., Li, Z., Li, J., 2020. Porous poly (L-lactic acid)/chitosan nanofibres for copper ion adsorption. *Carbohydr. Polym.* 227, 115343.
- Zou, H., Huang, J.C., Zhou, C., He, S., Zhou, W., 2020. Mutual effects of selenium and chromium on their removal by *Chlorella vulgaris* and associated toxicity. *Sci. Total Environ.* 724, 138219.

## Acknowledgements

First of all, I wish to express my greatest appreciation towards my supervisors, Prof. Zhenya Zhang, Prof. Zhongfang Lei and Prof. Kazuya Shimizu for providing me the opportunity to undertake this research, and for their encouragement, determination and depth of knowledge. The thesis would not have been written successfully without their continuous supervision and guidance.

Special thanks should go to my thesis committee members, Prof. Zhenya Zhang, Prof. Zhongfang Lei, Prof. Kazuya Shimizu and Prof. Keiko Yamaji for their patient reading and listening, valuable suggestions and comments.

My special appreciation to my labmates and friends' enthusiasm and support in providing relevant assistance and help to complete this study. Thanks to Mr. Jingmin Nie, Ms. Yu Wei, Mrs. Thi Hang Ho, Mr. Guanghao Zhang, Mr. Shota Hirayama, Mr. Bach Van Nguyen and other friends for their countless assistance and encouragement during the three years of my research.

The deepest gratitude goes to my family for their priceless love and support. Special thanks to my husband (Ziwen Zhao), little princess (Nian Nian) for their endless love and care, make me the luckiest wife and mother in the world. Finally, I would like to thank my parents Mr. Yuping Yang and Mrs. Sanxiu Liu, for giving birth to me at the first place and supporting me spiritually throughout my life. Unable to share this achievement with my father is my greatest regret, but he is always in my heart and supporting me. This dissertation would not have been completed without their love, care, and unselfish support.



## Publications

1. **Yang, X.**, Zhao, Z., Yu, Y., Shimizu, K., Zhang, Z., Lei, Z., Lee, D.-J., 2020. Enhanced biosorption of Cr(VI) from synthetic wastewater using algal-bacterial aerobic granular sludge: Batch experiments, kinetics and mechanisms. *Sep. Purif. Technol.* 251, 117323.
2. **Yang, X.**, Nie, J., Wang, D., Zhao, Z., Kobayashi, M., Adachi, Y., Shimizu, K., Lei, Z., Zhang, Z., 2019. Enhanced hydrolysis of waste activated sludge for methane production via anaerobic digestion under N<sub>2</sub>-nanobubble water addition. *Sci. Total Environ.* 693, 133524.
3. **Yang, X.**, Nie, J., Wei, Y., Zhao, Z., Shimizu, K., Lei, Z., Zhang, Z., 2020. Simultaneous enhancement on lignin degradation and methane production from anaerobic co-digestion of waste activated sludge and alkaline lignin supplemented with N<sub>2</sub>-nanobubble water. *Bioresour. Technol. Rep.* 11, 100470.
4. Ho, T.H.<sup>#</sup>, **Yang, X.**<sup>#</sup> (**These two authors contributed equally to this work**), Nie, J., Zhao, Z., Wei, Y., Shimizu, K., Zhang, Z., Lei, Z., 2020. Effect of nanobubble water on anaerobic methane production from lignin. *Res. Chem. Intermed.* 46, 4767-4780.
5. Wang, D., **Yang, X.**, Tian, C., Lei, Z., Kobayashi, N., Kobayashi, M., Adachi, Y., Shimizu, K., Zhang, Z., 2019. Characteristics of ultra-fine bubble water and its trials on enhanced methane production from waste activated sludge. *Bioresour. Technol.* 273, 63-69.
6. Zhao, Z., **Yang, X.**, Cai, W., Lei, Z., Shimizu, K., Zhang, Z., Utsumi, M., Lee, D.-J., 2018. Response of algal-bacterial granular system to low carbon wastewater: Focus on granular stability, nutrients removal and accumulation. *Bioresour. Technol.* 268, 221-229.
7. Fan, Y., **Yang, X.**, Lei, Z., Adachi, Y., Kobayashi, M., Zhang, Z., Shimizu, K., 2021. Novel insight into enhanced recoverability of acidic inhibition to anaerobic digestion with nanobubble water supplementation. *Bioresour. Technol.* 124782.
8. Chen, K., Zhao, Z., **Yang, X.**, Lei, Z., Zhang, Z., Zhang, S., 2018. Desorption trials and granular stability of chromium loaded aerobic granular sludge from synthetic domestic wastewater treatment. *Bioresour. Technol. Rep.* 1, 9-15.
9. Dong, X., Zhao, Z., **Yang, X.**, Lei, Z., Shimizu, K., Zhang, Z., Lee, D.-J., 2020. Response and recovery of mature algal-bacterial aerobic granular sludge to sudden salinity disturbance in influent wastewater: Granule characteristics and nutrients removal/accumulation. *Bioresour. Technol.* 321, 124492.
10. Fan, Y., Lei, Z., **Yang, X.**, Kobayashi, M., Adachi, Y., Zhang, Z., Shimizu, K., 2020. Effect of nano-bubble water on high solid anaerobic digestion of pig manure: Focus on digestion

stability, methanogenesis performance and related mechanisms. *Bioresour. Technol.* 315, 123793.

11. Zhao, Z., Liu, S., **Yang, X.**, Lei, Z., Shimizu, K., Zhang, Z., Lee, D.-J., Adachi, Y., 2019. Stability and performance of algal-bacterial granular sludge in shaking photo-sequencing batch reactors with special focus on phosphorus accumulation. *Bioresour. Technol.* 280, 497-501.